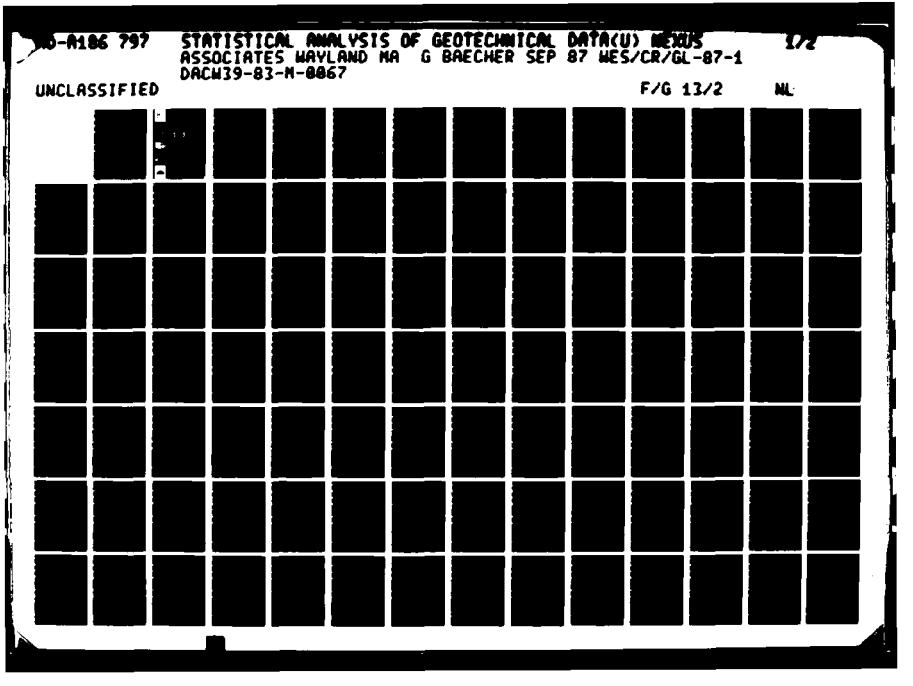
AD-A186 797
STATISTICAL ANALYSIS OF GEOTECHNICAL DATA(U) NEXUS
ASSOCIATES WAYLAND MA G BAECHER SEP 87 WES/CR/GL-87-1
DACW39-83-M-0067
1/2
UNCLASSIFIED
F/G 13/2
NL

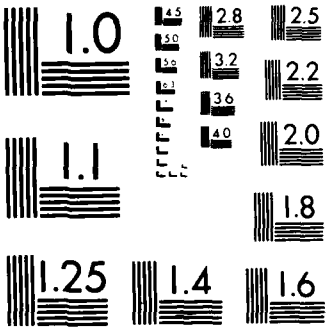

MICROCOPY RESOLUTION TEST CHART
NATIONAL BUREAU OF STANDARDS-1963-A

US Army Corps of Engineers

COPY

GEOTECHNICAL LABORATORY

CONTRACT REPORT GL-87-1

STATISTICAL ANALYSIS OF GEOTECHNICAL DATA

by

Gregory Baecher

NEXUS Associates
Wayland, Massachusetts 01778-1401

September 1987
Final Report

Prepared for DEPARTMENT OF THE ARMY
US Army Corps of Engineers
Washington, DC 20314-1000

Under Contract No. DACW39-83-M-0067

Monitored by Geotechnical Laboratory
US Army Engineer Waterways Experiment Station
PO Box 631, Vicksburg, Mississippi 39180-0631

Destroy this report when no longer needed. Do not return it to the originator.

The findings in this report are not to be construed as an official Department of the Army position unless so designated by other authorized documents.

The contents of this report are not to be used for advertising, publication, or promotional purposes. Citation of trade names does not constitute an official endorsement or approval of the use of such commercial products.

AD-A186797

Unclassified

SECURITY CLASSIFICATION OF THIS PAGE

REPORT DOCUMENTATION PAGE

Form Approved OMB No. 0704-0188

1a REPORT SECURITY CLASSIFICATION: Unclassified	1b RESTRICTIVE MARKINGS
2a SECURITY CLASSIFICATION AUTHORITY	3 DISTRIBUTION/AVAILABILITY OF REPORT: Approved for public release; distribution unlimited
2b DECLASSIFICATION/DOWNGRADING SCHEDULE	
4 PERFORMING ORGANIZATION REPORT NUMBER(S)	5 MONITORING ORGANIZATION REPORT NUMBER(S): Contract Report GL-87-1
6a NAME OF PERFORMING ORGANIZATION: NEXUS Associates; 6b OFFICE SYMBOL (If applicable)	7a NAME OF MONITORING ORGANIZATION: USAEWES Geotechnical Laboratory
6c ADDRESS (City, State, and ZIP Code): Wayland, MA 01778-1401	7b ADDRESS (City, State, and ZIP Code): PO Box 631, Vicksburg, Mississippi 39180-0631
8a NAME OF FUNDING/SPONSORING ORGANIZATION: US Army Corps of Engineers; 8b OFFICE SYMBOL (If applicable)	9 PROCUREMENT INSTRUMENT IDENTIFICATION NUMBER: DACW39-83-M-0067
8c ADDRESS (City, State, and ZIP Code): Washington, DC 20314-1000	10 SOURCE OF FUNDING NUMBERS: PROGRAM ELEMENT NO; PROJECT NO; TASK NO; WORK UNIT ACCESSION NO 32221

11 TITLE (Include Security Classification): Statistical Analysis of Geotechnical Data

12 PERSONAL AUTHOR(S): Baecher, Gregory

13a TYPE OF REPORT	13b TIME COVERED	14 DATE OF REPORT (Year, Month, Day)	15 PAGE COUNT
Final report	FROM ____ TO ____	September 1987	[illegible]

16 SUPPLEMENTARY NOTATION: Available from National Technical Information Service, 5285 Port Royal Road, Springfield, VA 22161

17 COSATI CODES			18 SUBJECT TERMS (Continue on reverse if necessary and identify by block number)
FIELD	GROUP	SUB-GROUP	Embankment dams; Risk assessment; Statistics

19 ABSTRACT (Continue on reverse if necessary and identify by block number)

A tutorial introduction to practical techniques of statistical data analysis for geotechnical engineering--the intended audience is the practicing geotechnical engineer with little background in statistics. The approach summarizes soil parameters by two numbers: a best estimate and a measure of uncertainty. Uncertainties in soil parameter estimates of four types are considered--(a) variability in the soil deposit; (b) random measurement error; (c) measurement bias; and (d) limited numbers of tests. The first two cause data scatter. The second two cause systematic error. A procedure is developed to [illegible]

20 DISTRIBUTION/AVAILABILITY OF ABSTRACT: ☒ UNCLASSIFIED/UNLIMITED ☐ SAME AS RPT ☐ DTIC USERS

21 ABSTRACT SECURITY CLASSIFICATION: [illegible]

22a NAME OF RESPONSIBLE INDIVIDUAL | 22b TELEPHONE (Include Area Code) | 22c OFFICE SYMBOL

DD Form 1473, JUN 86 — Previous editions are obsolete. SECURITY CLASSIFICATION OF THIS PAGE [illegible]

PREFACE

This report, prepared by Gregory B. Baecher of NEXUS Associates, Wayland, Massachusetts, with assistance from D. DeGroot, and C. Erikson, under Contract DACW39-83-M-0067, provides details for the statistical analysis of geotechnical engineering aspects of new dam projects. It was part of work done by the US Army Engineer Waterways Experiment Station (WES) in the Civil Works Investigation Study (CWIS) sponsored by the Office, Chief of Engineers, US Army. This study was conducted during the period October 1983 to September 1985 under CWIS Work Unit 32221, entitled "Probabilistic Methods in Soil Mechanics." Mr. Richard Davidson was the OCE Technical Monitor.

The report is an introduction to practical techniques of statistical data analysis for use in geotechnical engineering. The intended audience is the practicing geotechnical engineer with little or no background in statistics. Readers with a developed background in statistics may find the methodological presentation rudimentary, but may still find interest in the numerical examples which come from actual construction projects. Two other reports were prepared under the same contract, "Statistical Quality Control for Engineered Embankments," (Contract Report GL-87-2), and "Error Analysis for Geotechnical Engineering," (Contract Report GL-87-3), in addition to a final report.

Ms. Mary Ellen Hynes-Griffin, Earthquake Engineering and Geophysics Division (EEGD), Geotechnical Laboratory (GL), WES was the Contracting Officer's Representative and WES Principal Investigator for CWIS Work Unit 32221. General supervision was provided by Dr. A. G. Franklin, Chief, EEGD, and Dr. W. F. Marcuson III, Chief, GL.

Commander and Director of WES during the publication of this report was COL Dwayne G. Lee, CE. Dr. Robert W. Whalin was Technical Director.

CONTENTS

	Page
PREFACE	1
LIST OF FIGURES	4
LIST OF TABLES	8
LIST OF PLATES	9
PART I: INTRODUCTION	10
Background	10
Purpose	10
General Description of Statistical Data Analysis	11
Organization of This Report	12
PART II: DESCRIBING SOILS DATA	13
Histograms and Frequency Functions	13
Histograms	13
Frequency Distributions	15
Probability Paper	16
Mean and Standard Deviation	16
Mean	17
Standard Deviation	17
Coefficient of Variation	19
Correlation	19
Means and Standard Deviations of Calculated Parameters	22
Regression Analysis	25
Shortcut Estimates	28
Shortcuts for Estimating the Mean	28
Shortcuts for Estimating the Standard Deviation	29
Shortcuts for Estimating the Correlation Coefficient	29
PART III: SPATIAL VARIATION AND DATA SCATTER	43
Trends and Variations About Trends	43
Estimating Trends	44
Residuals About Trends	45
Trends vs. Residuals	47
Autocorrelation and Autocovariance	48
Estimating Autocovariance and Autocorrelation	51
Measurement Noise	53
Sources and Character of Measurement Noise	53

Page

Models for Measurement Noise 55
Direct Estimation of Measurement Noise 56
Indirect Estimation of Measurement Noise 56
Rejecting Outlier Data 60
Size Effect Factor 63
Spatial Averaging 64
Spatial Extremes 69

PART IV: SYSTEMATIC ERRORS 107

Sources and Importance of Systematic Error 107

Measurement and Model Bias 108
Causes of Measurement and Model Bias 109
Assessing Magnitude of Bias 109
Statistical Error 110
Sampling Variations 110
Error in the Mean 111
Error in the Standard Deviations 113
Error in Regression Coefficients 114

PART V: CONSTRUCTING A STATISTICAL SOIL ENGINEERING PROFILE 121

Decomposition of Uncertainty 121
Simple Soil Profile: Field Vane Data 123
Site Conditions 124
Systematic Error 124
Statistical Soil Engineering Profile 125
Simple Soil Profile: SPT Data 126
Site Conditions and Data Scatter 126
Systematic Error 126
Statistical Soil Engineering Profile 127
Derived Soil Profiles 127
Site Conditions 127
Normalized Soil Properties (SHANSEP) 128
Soil Data 129
Systematic Errors 130
Statistical Soil Engineering Profile 130
Error Analysis 131

REFERENCES 144

APPENDIX A: Statistical Considerations in Estimating Autocovariance . . A1

APPENDIX B: Symbol List B1

LIST OF FIGURES

		Page
Figure 1.	Sources of Error in Soil Property Estimates.	34
Figure 2.	Histograms of Soil Property Data: (a) Symmetric Distribution of Variability; (b) Skewed Distribution of Variability.	35
Figure 3.	Frequency Distribution for The Data of Fig. 2a.	36
Figure 4.	Probability Paper Plot of Compaction Data.	37
Figure 5.	Scatter Plot of Compaction Control Data Showing Water Content vs. Dry Density	38
Figure 6.	Various Scatter Plots Showing Different Levels of Correlation	39
Figure 7.	First-Order Propagation of Error Through The Model $y = g(x)$.	40
Figure 8.	Cone Penetration Resistance in a Copper Porphyry Tailings Pile.	41
Figure 9.	Ballon Shortcut Method for Estimating Correlation Coefficient.	42
Figure 10a.	Data Displaying Trend With Location.	73
Figure 10b.	Data Displaying Erratic Variation With Location.	73
Figure 11.	Maximum Past Pressure Data as a Function of Depth.	74
Figure 12a.	Artificially Generated Statistically Independent Residuals off Regression Line	75
Figure 12b.	Dependent Residuals Typical of Actual Soil Data.	76
Figure 13.	Standard Penetration Test Blow Counts as Function of Depth.	77
Figure 14a.	Scatter Plot of Residuals At Close Spacings.	78
Figure 14b.	Scatter Plot of Residuals At Medium Spacings.	79
Figure 14c.	Scatter Plot of Residuals At Far Spacings.	80

Page

Figure 15. Autocorrelation Function of SPT Data in Figure 13. 81

Figure 16. Effect of Variance and Correlation on Variability of Soils Data. 82

Figure 17. Site Plan for Hydraulic Bay Fill Data. 83

Figure 18. Scatter Plot of SPT Data. 84

Figure 19. Horizontal Autocovariance Function of SPT Data in Figures 17 and 18. 85

Figure 20. Study Area on SF Bay Mud Analyzed by Javette (1983). 86

Figure 21. Autocorrelation Function of Water Content Over Small Interval of San Francisco Bay Mud. 87

Figure 22. Autocorrelation Function of Water Content Over Large Interval of San Francisco Bay Mud. 88

Figure 23. Effect of Scale on Autocorrelation Function. 89

Figure 24. Autocorrelation Function of Rock Joint Density in A Copper Porphyry. 90

Figure 25. Autocorrelation Function of Compacted Water Content in Clay Core of an Embankment Dam. 91

Figure 26. Autocorrelation Function of Cone Penetration Resistance in North Sea Clay. 92

Figure 27. Estimation Procedure for Nonuniformly Spaced Data. 93

Figure 28. Schematic Representation of Measurement Error. 94

Figure 29. Histogram of Strike and Dip Measurements Made by Different Operators on the Same Rock Joint. 95

Figure 30. Autocovariance Function is Composed of Spatial Variability and Random Measurement Noise Signatures. 96

Figure 31a. SPT Blow Count Data in a Dune Sand (after Hilldale, 1971). 97

Figure 31b. Autocorrelation of SPT Data in Figure 31a. 98

Figure 32. Field Vane Data in a Soft Marine Clay. 99

Page

Figure 33a. Horizontal Autocovariance Function for the FV Data of Figure 32. 100

Figure 33b. Vertical Autocovariance Function for the FV Data of Figure 32. 101

Figure 34. Vertical Autocovariance Function of Cone Penetration Data in a Copper Porphyry Deposit. 102

Figure 35. SPT Blow Count Data in a Silty Sand. 103

Figure 36. Size Effect Factor for Spatial Averaging Along A Line. 104

Figure 37. Size Effect Factor for Spatial Averaging Over a Plane. 105

Figure 38. Size Effect Factor for Spatial Averaging Within A 3D Volume. 106

Figure 39. Bjerrum's Correction Factor for Field Vane Strength Measurements in Soft Clay. 116

Figure 40. Average Field Vane Strength With Depth for the Data of Figure 32. 117

Figure 41. Averaging of Blow Count Data. 118

Figure 42. Maximum Past Pressure Data in an Overconsolidated Clay. 119

Figure 43. Statistical Error in Maximum Past Pressure For the Data of Figure 41. 120

Figure 44. Sources of Error or Uncertainty in Soil Property Estimates 135

Figure 45. Design Profile for Undrained Strength From the Data of Figure 32. 136

Figure 46. Design Profile for Undrained Strength Showing the Effect of Spatial Averaging on Standard Deviation Envelopes. 137

Figure 47. SPT Blow Count Data Showing Typical Measurements for One Section of Embankment Foundation. 138

Figure 48. Horizontal Autocorrelation Function for the SPT data of Fig. 47. 139

Figure 49. Statistical Soil Engineering Profile Showing Typical Results for One Section of Embankment. 140

Page

Figure 50. In Situ Undrained Strength Data for a Site on Gulf of Mexico Clay. 141

Figure 51. Laboratory Test Results to Determine SHANSEP Strength Parameters. 142

Figure 52. Statistical Soil Engineering Profile for Derived Soil Properties Using SHANSEP Procedure. 143

LIST OF TABLES

		Page
Table 1.	Multiplication Factors for Estimating Standard Deviation from The Range of Sample Data (After Snedecor and Cochran, 1980).	31
Table 2.	Frequency Distribution of Test Statistic for Outliers Based on Range (after Dixon, 1953).	70
Table 3.	Summary of Parameter Estimates for Error Analysis of End-of-Construction Stability Analyses for An Embankment on Soft Clay.	132
Table 4.	Soil Profile Uncertainties for Error Analysis	132

LIST OF PLATES

		Page
Plate 1.	Error analysis of modulus calculation from laboratory data.	32
Plate 2.	Shortcut estimates of summary parameters.	33
Plate 3.	Analysis of Noise in SPT Blow Count Data	71
Plate 4.	Spatial Averaging of SPT Blow Count Data	72
Plate 5.	Statistical Soil Engineering Profile for SPT Data	133

STATISTICAL ANALYSIS FOR GEOTECHNICAL DATA

PART I: INTRODUCTION

Background

Traditionally, the planning of geotechnical site characterization and the analysis of data which result have been accomplished by ad hoc procedures. These rest primarily on intuition and visual inspection of data. Advances in geotechnical testing and modeling combined with stricter regulatory oversight have led to changes with important implications for site characterization and data analysis. Principal among these are: (a) increased numbers and quality of geotechnical data, (b) increased concern with quality assurance in engineering, and (c) increased regulatory interest in the connection between performance assessments, parameter estimates, and supporting data.

At the same time, growing experience with the use of simple statistical methods in geotechnical engineering has provided techniques tailored to the special needs of geotechnical practice. These methods provide means for accomodating recent changes, and for improving the practice of geotechnical engineering. Such statistical methods are well suited to automatic data processing; they provide an explicit, repeatable procedure for obtaining parameter values; and they allow quantified levels of confidence to be assigned to parameter estimates.

Purpose

The purpose of this report is provide potential users of statistical methods for geotechnical data analysis with an introduction to practical concepts, definitions, and techniques. The report is not exhaustive; it intends to present simple, useful techniques in sufficient detail that a reader not already conversant with statistical theory may undertake practical analyses

of geotechnical data. These analyses should make better, more powerful use of data than has been possible with ad hoc procedures, and should provide estimates of uncertainty in engineering parameters to serve as the basis for error analysis of engineering calculations. This report complements materials presented in "Error analysis for geotechnical engineering," (Contract Report GL-87-3), in which the use of quantified estimates of uncertainty and error in geotechnical modeling is discussed.

General Description of Statistical Analysis

The approach to statistical analysis of geotechnical data developed in this report is based on summarizing a parameter value by two numbers: a best estimate and a measure of uncertainty. The 'mean' or arithmetical average is used for the first; the 'standard deviation' or root-mean-square variation is used for the second. These and other statistical terms are defined as they appear in later sections. Importantly, the methods used in the report do not require restrictive assumptions on the shape of probability distributions (e.g., the assumption of Normal distributions), and as a result the report considers probability distributions with only passing interest. The main concept behind the approach of this report is that uncertainty or error in geotechnical parameter estimates can be divided into four types, and the importance of each can be analyzed individually. The ability to separately consider each principal source of uncertainty greatly simplifies the task of analyzing data. Once each source of uncertainty has been considered individually, explicit rules based on probability theory are used to calculate the overall uncertainty in a parameter estimate.

The four types of uncertainty in a geotechnical parameter estimate are, (a) actual variability in the soil deposit, (b) random measurement error, (c) measurement bias, and (d) limited numbers of tests (Fig. 1). The first two cause the scatter so common in geotechnical measurements. The last two cause systematic errors which are unrelated to location. Each of these sources of uncertainty affects engineering calculations in its own way and as a result should be analyzed individually. At the end, the four uncertainties are combined to construct a statistical soil profile. The statistical profile shows the best estimate profile of soil properties with depth, and provides uncertainty envelopes about that profile. The statistical design profile is the first step in error analysis, as described in the accompanying report, "Error analysis for geotechnical engineering," (Contract Report GL-87-3).

Organization of This Report

This report is organized in five parts. After the Introduction, Part II summarizes common techniques for summarizing data using statistical descriptions. Part III introduces techniques for modeling and summarizing the spatial character of soil property data and the means for establishing the amount of measurement error in observed data scatter. Part IV addresses systematic or bias errors in measurements and in models. Finally, part V puts the techniques for Parts II, III, and IV together to summarize a soil profile statistically.

PART II: DESCRIBING SOILS DATA

Engineering data on soils properties are usually scattered. Graphical and simple mathematical techniques are useful in summarizing this scatter so that a better understanding of the data can be developed. For the present purposes, such graphical and mathematical techniques are used to obtain, (a) best estimates of soil engineering properties, and (b) quantitative assessments of the uncertainty or error in such estimates.

Histograms and Frequency Distributions

Histograms and frequency distributions are graphical descriptions of the variability or scatter of data. Plotting a histogram or frequency distribution is usually the first step in data analysis.

Histograms

A histogram is a diagrammatic representation of the frequency with which measurements lie within specified intervals of magnitude. For example, Fig. 2a shows a histogram of standard penetration test (SPT) blow count data within a single stratum of silty alluvial sand. The intervals along the horizontal axis of the histogram are each of the same width, and the height of the bars shows the frequeny of data lying within each interval. Since the intervals are all of the same width, the area of each bar is also proportional to the frequency of data within that interval.

A histogram is a convenient way of displaying data since many important features are immediately apparent in diagrammatic form. For example, the data of Fig. 2a are seen to vary about a central peak at about 9 blows/ft. The data are more or less symmetric about this peak, and data which vary substantially from the peak are infrequent. The bulk of the data lies within an interval

approximately between 3 to 15 blows/ft, with extreme values ranging from 0 to 24 blows/ft. A symmetric distribution of data like Fig. 2a is often described as bell-shaped.

A histogram of another set of cone pentration test data is shown in Fig. 2b. These data are not symmetric about their peak frequency. The largest frequency occurs near the lower end of the scale, and while the frequencies decline on both sides of the peak, they do so more slowly on the upper side, that is, as penetration resistance increases. Such distributions are said to be skewed.

To construct a histogram the following procedure is used:

1. Divide the horizontal axis of the graph into about 5 to 10 intervals of constant width.
2. Count the number of data having values within each interval.
3. Plot this number as a vertical bar above the appropriate interval.

About 5 to 10 intervals are used because this number typically allows a sufficient number of data in each interval for the observed frequencies to vary smoothly, and yet provides adequate definition of the shape of the distribution of data. For small numbers of data a convenient rule-of-thumb for choosing the number of intervals is

$$k = 1 + 3.3 \log_{10} n \quad , \tag{1}$$

in which n = the number of data values and k (rounded to the next higher integer) = the number of intervals (Sturges, 1926). The choice of number of intervals can affect the visual interpretation of data scatter. Thus, it is

sometimes useful to construct more than one histogram, using a different number of intervals on each plot in order to obtain an intuitive feel for the data scatter. This problem is circumvented by using a frequency distribution, as described below.

Usually, it is convenient to specify interval boundaries to one fewer decimal places than that to which the data are measured, avoiding the problem of where to place values falling directly on an interval boundary. When this is not possible some consistent procedure should be adopted for deciding how to count data which fall directly on an interval boundary. For example, any value lying on a boundary might be automatically counted in the lower interval. Some people prefer to allocate 1/2 unit to each adjacent interval. This is an acceptable procedure but it leads to noninteger frequencies which may be awkward.

Frequency Distributions

A frequency distribution is obtained by changing the vertical axis from the frequency of data within class intervals to the cumulative fraction of data less than a particular value. The frequency distribution is a fraction-less-than (or percent-less-than) curve. Fig. 3 shows the frequency distribution for the SPT data of Fig. 2a.

To construct a frequency distribution the following procedure is used:

1. Arrange the data in ascending order, $x_1, x_2, \ldots, x_i, \ldots, x_n$.

2. For each value x_i, calculate the frequency f_i of data less than or equal to that value, $f_i = i/n$. For the largest value, assign the frequency $f_n = n/n+1$.

3. Plot the value of the data x_i along the horizontal axis and its corresponding cumulative frequency f_i along the vertical axis.

The advantages of the frequency distribution are that it does not require data to be grouped into arbitrary numbers of intervals and the fraction of data less-than or greater-than any value can be immediately read from the graph. The disadvantage is that the shape of the distribution of data is not as clearly apparent in a frequency distribution as in a histogram.

Probability Paper

Probability paper is graph paper with special grids designed such that the cumulative frequencies of particular types of frequency distributions plot as straight lines. Fig. 4 shows the data of Fig. 2a plotted on Normal probability paper. Normal probability paper causes bell-shaped distributions (more precisely, Normal distributions) to plot as straight lines. Other types of probability paper are also available. In this report little use is made of the *mathematical shape of the frequency distributions of data*. Nevertheless, probability papers are commonly encountered in practice and in statistical software, and are often a convenient way to plot data.

Mean and Standard Deviation

Graphical descriptions of the variability among data are useful for obtaining a feeling for the scatter in a particular data set, but for engineering applications a mathematical description of data scatter is usually needed. This is conveniently provided by the mean and standard deviation. The mean is a quantitative measure of the central location of the scatter of measurements along the x-axis. The standard deviation is a quantitative measure of the dispersion of the measurements. Together, the mean and standard

deviation summarize important information about the distribution of measured values, and provide a useful description of data scatter for use in analysis.

Mean

The mean of a set of measurements x_i, i=1,...,n, is the arithmetic average,

$$m_x = \frac{1}{n} \sum_{i=1}^{n} x_i = \text{"mean"} \quad . \tag{2}$$

The mean is the center of gravity of the data along the X-axis. In this report, the mean is used as the best estimate of a soil parameter because it is neither conservative nor unconservative. In some references the mean is called the expected value of x and denoted E[x], but this expression is not used here. In Fig. 2a the mean of the histogram of the SPT data is 8.9 blows/ft.

Standard Deviation

The standard deviation measures the variability of data about their mean. Mathematically, the standard deviation is the square root of the sum of squares of the difference between each measurement and the mean,

$$s_x = \sqrt{\frac{1}{n-1} \sum (x_i - m_x)^2} = \text{"standard deviation"} \quad . \tag{3}$$

For the histogram of SPT data in Fig. 2a, the standard deviation is 4.4 blows per ft. The standard deviation can be thought of as the square root of the moment of inertia of the data about the mean. Whereas, the mean describes the center of the data along the X-axis, the standard deviation describes the spread. The mean and standard deviation are measured in the same units as the data themselves. The denominator (n-1) is used in Eqn. 3 rather than n because

the mean m_x that appears in the Eqn. 3 is itself also estimated from the data. Thus, to the extent that m_x differs slightly from the real mean of x in a soil deposit, the variations $(x_i-m_x)^2$ are on average slightly smaller than the corresponding variations about the real mean. Mathematically, the squared variations are on average too small by the factor $(n-1)/n$, and thus the denominator in Eqn. 3 corrects for this bias.

For a bell-shaped, or Normal, distribution of data the mean occurs at the 0.5 fractile. The 0.5 fractile, denoted $x_{0.5}$, is that value of x which splits the data into two sets, half smaller and half larger. 50% of the data are smaller than $x_{0.5}$. The value $x_{0.5}$ is commonly called the median. Again, for a Normal distribution the mean plus one standard deviation occurs at the 0.84 fractile; the mean minus one standard deviation occurs at the 0.16 fractile. This can be determined from tables of the Normal distribution which are found in most statistics textbooks (e.g., Benjamin and Cornell, 1969). When data plot as a line on Normal probability paper, the mean and standard deviation can be readily estimated by fitting a line to the data and determining the values of x which correspond to the 0.16, 0.5, and 0.84 fractiles. Denoting these $x_{0.16}$, $x_{0.5}$, and $x_{0.84}$,

$$m_x \approx x_{0.5} \quad , \tag{4}$$

$$s_x \approx \frac{x_{0.84} - x_{0.16}}{2} \quad . \tag{5}$$

In calculations it is sometimes convenient to deal with s_x^2 rather than s_x, just as in mechanics it is convenient to deal with the moment of inertia

rather than its square root. The square of the standard deviation is called the variance, and is exacatly equivalent to the moment of inertia in mechanics. The variance in the moment of inertial of the data about the mean m_x,

$$V_x = s_x^2 = \text{"variance"} \quad . \tag{6}$$

The variance of the data in Fig. 2a is (4.4 blows/ft)^2 = 19.4 (blows/ft)^2. The variance is measured in the square of the units of the data. If the data are measured in blows/ft, the variance is measured (blows/ft)^2. Given their similarity to mechanical moments, the mean and variance are often called (statistical) moments of the data. The mean is the first moment about x=0. The variance is the second moment about $x=m_x$. A description of soil properties using only means and standard deviations is said to be a second-moment description.

Coefficient of Variation

The ratio of the standard deviation to the mean, or the proportional variability, is called the coefficient of variation,

$$\Omega_x = s_x/m_x = \text{"coefficient of variation"} \quad . \tag{7}$$

The coefficient of variation of the data in Fig. 2a is Ω_x = (4.4 blows/ft/8.9 blows/ft) = 0.49, and could be expressed as a percentage (i.e., 49%).

Correlation

For two or more soil properties, variations in different properties may be associated with one another. That is, variations may not be independent. For example, the water content and undrained strength of clays are known to be associated with one another. Thus, variations in water content and undrained

strength are not independent, they depend on one another through causal mechanical factors.

Soil properties or engineering parameters may also be associated with one another not by a causal mechanical factor but by the way they are measured or estimated. For example, triaxial compression tests might be performed to estimate the effective strength parameters (c',ϕ') of the Mohr-Coulomb strength criterion. If c' and ϕ' are estimated by fitting a line to the resulting Mohr circles, error can be introduced by the way the envelope is fit. An envelope drawn too flat, leads to a ϕ' which is too small. An envelope drawn too steep leads to a ϕ' which is too large. However, if an envelope is drawn too flat, then for the envelope to still fit the data, the cohesion intercept c' must be made larger than it should be. Conversely, if the envelope is drawn too steep, the cohesion intercept must be made smaller than it should be to still fit the data. Errors in the estimates of ϕ' and c' are associated with one another.

The strength of association between soil parameters is expressed by the correlation coefficient,

$$r_{xy} = \frac{1}{n} \Sigma \left(\frac{x_i - m_x}{s_x}\right)\left(\frac{y_i - m_y}{s_y}\right) = \text{"correlation coefficient"} \quad , \qquad (8)$$

in which m_x and my = the means of x and y, respectively; s_x and s_y = the respective standard deviations of x and y. The two terms within the summation are the deviations of x and y measured in units of their respective standard deviations. That is, they are standardized dimensionless deviates. Thus the correlation coefficient is a non-dimensional measure of the degree to which two parameters vary together.

The range of r_{xy} is $-1 \leq r_{xy} \leq +1$: $r_{xy} = +1$ indicates a perfect linear relation between x and y having positive slope, $r_{xy} = -1$ indicates a perfect linear relation between x and y having negative slope, $r_{xy} = 0$ indicates no relation between x and y. When $r_{xy} = 0$, x and y are said to be independent and the scatter diagram of y plotted against x shows no trend.

If the variations of x and y are not normalized by their respective standard deviations, the covariance is obtained,

$$C_{x,y} = \frac{1}{n} \Sigma (x_i - m_x)(y_i - m_y) = \text{"covariance"} \quad . \tag{9}$$

The covariance is not dimensionless. From Eqns. 8 and 9,

$$C_{x,y} = (s_x s_y) r_{xy} \quad . \tag{10}$$

Fig. 5 shows a scatter plot of compaction control data collected during the construction of an engineered fill. Compaction water content is plotted along the X-axis; compacted dry density is plotted along the Y-axis. Each point corresponds to one test in which both water content and dry density were measured. As should be expected, water content and dry density are, on average, inversely related to one another. The correlation coefficient for the data of Fig. 5 calculated using Eqn. 8 is $r_{xy} = -0.7$.

For comparison, Fig. 6 shows scatter plots of x,y having various coefficients of correlation. When $r_{xy} > 0$ the data cloud slopes upward to the right. An intuitive feel can be obtained by thinking of a vertical line through m_x and a horizontal line through m_y dividing the scatter diagram into four quadrants. In the upper right quadrant both $(x_i - m_x)$ and $(y_i - m_y)$ are positive, thus their product is positive. In the lower left quadrant both

(x_i-m_x) and (y_i-m_y) are negative, thus again their product is positive. In the other two quadrants the products are negative. Therefore any cloud of data which has most of its points in the upper right and lower left quadrants has an $r_{xy}>0$. Conversely, any cloud with most of its points in the lower right and upper left quadrants has an $r_{xy}<0$. If the points fall equally in all four quadrants, $r_{xy} \approx 0$. It is important to note that the correlation coefficient is a measure of linear association. Two parameters may be deterministically related, but non-linearly, and have an r_{xy} other than ±1.

Means and Standard Deviations of Calculated Parameters

Means and standard deviations are used above to describe best estimates and uncertainties about measured properties. Correlation coefficients are used to describe association among properties or among uncertainties in properties. For engineering analysis, measured properties are sometimes transformed mathematically to obtain desired input parameters for engineering models. Deformation might be used to calculate elastic moduli, or in situ stresses and measured strengths might be used to calculate normalized soil properties.

The mathematics needed for relating a second-moment description of soil properties, loads or other measurements to a corresponding second-moment description of calculated results are relatively uncomplicated. Some equation is chosen for calculating the results of interest. For example, to calculate elastic modulus from stress and strain measurements the equation would be $E = \sigma/\epsilon$, in which σ = stress and ϵ = strain. Next, means, standard deviations, and correlation coefficients are evaluated for all the input parameters. In the example, the input parameters would be stress and strain, and the

corresponding statistical moments would be m_σ, m_ε, s_σ, s_ε, and $r_{\sigma\varepsilon}$. Then these means, standard deviations and correlation coefficients are used in conjunction with the equation to determine resulting means, standard deviations, and correlation coefficients (if applicable) on the calculated result(s). In the example, the result is the scalar value E.

Mean of a Calculated Parameter

Operationally, mean soil properties are propagated through an equation using a first-order approximation. This is a linear approximation in the vicinity of the best estimates of the soil properties. Mathematically, the calculation of some result y based on a soil parameter x can be expressed as a function,

$$y = g(x) \quad . \tag{11}$$

By taking a Taylor's series expansion of g(x) at the point m_x and then truncated all but the first two (i.e., linear) terms, the tangent at m_x is obtained (Fig. 7). For most geotechnical purposes this linearization is sufficiently accurate. For strongly nonlinear cases, other methods are available. These are discussed in the report, "Error analysis for geotechnical engineering," (Contract Report GL-87-3). Applying rudimentary probability theory leads to the convenient result,

$$m_y \doteq g(m_x) \quad , \tag{12}$$

in which $\doteq$ indicates first-order approximation. In words, the mean or best estimate of the result y is the function of the mean or best estimate of the parameter x. This is the common deterministic solution, using the

best-estimate or mean soil property as input. In the example above $m_E \doteq m_\sigma/m_\varepsilon$ (see Plate 1).

Standard Deviation of a Calculated Parameter

By similar reasoning, standard deviatons on input soil properties x may also be propagated through an equation y=g(x) to find a corresponding standard deviation on the calculated parameter y. The first-order approximation leads to the relation

$$s_y \doteq \left(\frac{dy}{dx}\right) s_x \quad , \tag{13}$$

in which the derivative dy/dx can be thought of as an influence factor. In words, the standard deviation of the prediction y is the product of the standard deviaton of the parameter x and an influence factor equal to the derivative of y with respect to x. For modulus calculated from an uncertain stress but known strain, $s_E \doteq (dE/d_\sigma)s_\sigma$. The relation is exact when g(x) is linear.

When the prediction y depends on a set of parameters, $\underline{x} = \{x_1,\ldots,x_n\}$, the equivalent forms of Eqn. 12 and 13 are,

$$m_y \doteq g(m_{x_1},\ldots,m_{x_n}) \quad , \tag{14}$$

$$s_y^2 \doteq \sum \sum \frac{dy}{dx_i}\frac{dy}{dx_j} C_{x_i,x_j} \tag{15}$$

Note, when the x_i, x_j are independent, $C_{x_i,x_j}=0$ for $i\neq j$ and $C_{x_i,x_j}=s_{x_i}^2=V_{x_i}$ for $i=j$, thus,

$$V_y \doteq \Sigma \left[\frac{dy}{dx_i}\right]^2 V_x \ . \qquad (16)$$

The example calculation of modulus from both an uncertain stress and an uncertain strain is carried out in Plate 1. Two special cases deserve note because they are common in practice and lead to simple results. For the case in which y is a linear combination of a set of independent parameters $y = \Sigma a_i x_i$ the variance of y is exactly,

$$V_y = \Sigma a_i^2 V_{xi} \qquad (17)$$

For the case in which y is a power function (product) of a set of independent parameters, $y = \prod_{i=1}^{n} x_i^{a_i}$, the coefficient of variation of y is approximately,

$$1+\Omega_y^2 = \Sigma (1+a_i^2 \Omega_{x_i}^2) \qquad (18)$$

which for small coefficients of variation (e.g., less than 30%) reduces to,

$$\Omega^2_y = \Sigma a_i^2 \Omega^2_{xi}. \qquad (19)$$

Regression Analysis

When two soil properties or parameters are associated with one another, their correlation coefficient can be used to predict one property or parameter from the other. This is done with regression analysis. Regression analysis is used to fit lines or curves to data. For example, regression analysis can be used to estimate undrained strength of a saturated clay from water content.

The common criterion for fitting trend lines or curves to data is by minimizing the sum of squared residuals off the trend. This is called the

least-squares fit. The cone penetration resistance data shown in Fig. 8 appear to increase more or less linearly with depth. Mathematically, this trend in the data can be expressed as,

$$y = a + bx \tag{20}$$

in which y = undrained strength, x = log water content, and a and b are constants. The constant a is the intercept at x = 0; b is the slope.

The problem of trend fitting is to estimate the coefficients a and b from a set of n data pairs (y_i, x_i) such that the resulting trend line is 'best.' Under the least-squares criterion a and b are estimated such that the sum of the squared residuals in the y-direction, $u_i=[y_i-(a+bx_i)]^2$, is minimized. The values of a and b which minimize the sum of squared residuals provide the best prediction of y for a given x, and can be shown to be (Benjamin and Cornell, 1979),

$$\hat{a} = \frac{(\Sigma x_j^2)(\Sigma y_i) - (\Sigma x_i)(\Sigma x_i y_i)}{n\,(\Sigma x_i^2) - (\Sigma x_i)^2} \quad , \tag{21}$$

$$\hat{b} = \frac{n(\Sigma x_j y_i) - (\Sigma x_i)(\Sigma x_i y_i)}{n(\Sigma x_i^2) - (\Sigma x_i)^2} \quad . \tag{22}$$

The variance of the residuals is

$$V_u = \frac{1}{n-2} \Sigma\, [y_i - (\hat{a}+b\hat{x}_i)]^2 \tag{23}$$

This best fitting line to the data of Fig. 8 is shown in the Fig. The two

envelopes about the line are +/- one standard deviation $s_u = \sqrt{v_u}$,

$$\text{upper envelope:} \quad y = \hat{a} + \hat{b}x + s_u \tag{24}$$

$$\text{lower envelope:} \quad y = \hat{a} + \hat{b}x - s_u \tag{25}$$

In regression analysis the best fitting line is chosen to be that which minimizes squared deviations of data in the y-direction (i.e., vertically). This is the line which gives the best estimate of y for a known value of x. If the reverse prediction were desired, that is the best estimate of x for a known value of y, then a different regression line would give the best result. To predict x from y the best line is that which minimizes squared deviations of data in the x-direction. This is found by interchanging x's and y's in Eqns. 20 through 23.

Non-linear trends are fit to data in much the same way as lines are, Typically, a direct least squares fit is used, sometimes after a transformation of the data to fit a linear model. For example, exponential or power functions can be transformed through the logarithm,

$$y = a\, x^b \tag{26}$$

$$\ln y = \ln a + b \ln x \tag{27}$$

and then a linear regression fit to lny:lnx. This is a common approach, although statisticians usually warn that a transformation of data such as this implicitly alters some statistical assumptions underlying regression analysis (Snedecor and Cochran, 1980). For example, with linear regression analysis the scatter of the data about the best fitting line is assumed to be the same all along the line. If regression analysis is applied to the logarithm of the data

and the same equations 21 and 22 are used to estimate regression coefficients, then the scatter of the logarithm of the data, not the data themselves, is implicitly assumed to be the same all along the line. In many--but not all--cases the transformation of a non-linear relation to a linear one causes few difficulties.

Shortcut Estimates

In a number of situations faced in the field, quick but only approximate estimates of means, standard deviation, or correlation coefficients are desired from limited numbers of data. Shortcut techniques are available for this purpose. These provide savings of time and effort while often causing only minor losses of precision.

Shortcuts for Estimating the Mean

An easy, quick, and often good estimate of the mean can be obtained from the median. The median is the middle value of a data set. It is that value which is larger than half the measurements and smaller than the other half. For example, if, say, five data are listed in ascending order 6,9,10,12,15, the median is 10. For an even number of data, say 6,9,10,12,15,16 the difference between the two middle data is halved to give the median, that is (10+12)/2=11. For data scatter which is symmetric about its central value and for small numbers of data, the sample median is actually a good estimate of the mean. On the other hand, if the data scatter is asymmetric--for example, if there are many small values and a few large values--the sample median is not a good estimator of the mean.

A second shortcut for estimating the mean is by taking one-half the sum of the largest and smallest measured values, $(1/2)(x_{max} + x_{min})$. This

estimator is sensitive to the extreme values in a set of measurements, and thus fluctuates considerably. It is not a good shortcut estimator and should only be used with caution.

Shortcuts for Estimating the Standard Deviation

A useful estimator of the standard deviation from small numbers of tests is the sample range $w_x=|x_{max}-x_{min}|$. The range is the span of data from largest to smallest. Like the standard deviation, the range is a measure of dispersion in a set of data. However, the relationship between the standard deviation and the sample range, on average, depends on how many tests are made. To obtain a best estimate of s_x from the range of data w_x a multiplier N_n is used which depends on sample size (Table 1). The best estimate of the standard deviation is $s_x \approx N_n w_x$ (see Plate 2).

As for the sample median, the range is a good estimator of the standard deviation for small n and symmetric data scatter. Even for modest n it remains fairly good. However, for asymmetric data scatter the range, which is strongly affected by outliers, is not a good estimator of the standard deviation. Fortunately, with the notable exception of hydraulic parameters such as permeability, most geotechnical data display symmetric scatter. In the case of hydraulic permeability data a logarithmic transformation usually makes the data scatter symmetric, and again the median and range become convenient estimators.

Shortcuts for Estimating the Correlation Coefficient

Calculation of correlation coefficients by Eqn. 8 can be tedious. A simple and quick approximation is obtained graphically from the shape of the scatter plot of y vs. x. The method works well whenever the outline of the scatter plot is approximately elliptical, and works even with small numbers of

data. Using Chatillon's (1984) term and procedure, this is called the balloon method:

STEP 1: Plot a scatter diagram of y vs. x.
STEP 2: Draw an ellipse (balloon) surrounding all or most of the points on the plot.
STEP 3: Measure the vertical height of the ellipse at its center, h, and the vertical height of the ellipse at its extremes, H.
STEP 4: Approximate the correlation coefficient as: $r_{xy} \approx \sqrt{1 - (h/H)^2}$.

An example of the method is shown in Fig. 9. For these data the balloon method gives a correlation coefficient of 0.81, whereas the correlation coefficient calculated by Eqn. 8 is 0.83. Empirically, the method works well for $r_{xy}>0.5$.

Shilling (1984) has suggested a similar method for approximately estimating the correlation coefficient. The principal difference from Chatillon's method is that the data are normalized by their standard deviation before being plotted:

STEP 1: Plot a scatter diagram of $(y-m_y)/s_x$ vs. $(x-m_x)/s_y$.
STEP 2: Draw an ellipse surrounding all or most of the points on the plot.
STEP 3: Measure the length of the principal axis of the ellipse having positive slope, D, and the length of the principal axis of the ellipse having negative slope, d.
STEP 4: Approximate the correlation coefficient as $r_{xy} \approx (D^2-d^2)/(D^2+d^2)$.

This methods works about as well as Chatillon's. For the data of Fig. 9 Shilling's method gives $r_{xy} \approx 0.80$.

Table 1
Multiplier for Estimating Standard Deviation from Sample Range
(from Snedecor and Cochran, 1980)

$$s_x \approx N_n (x_{max} - x_{min})$$

n	Multiplier N_n	n	Multiplier N_n
2	0.886	12	0.815
3	0.591	13	0.300
4	0.486	14	0.294
5	0.430	15	0.288
6	0.395	16	0.283
7	0.370	17	0.279
8	0.351	18	0.275
9	0.337	19	0.271
10	0.325	20	0.268
11	0.315		

Table 1. Multiplication Factors for Estimating Standard Deviation from The Range of Sample Data (After Snedecor and Cochran, 1980).

PLATE 1

SUBJECT: Error analysis of modulus calculation from laboratory data.

PROBLEM: Calculate constrained modulus from laboratory measurements of stress and strain

SOLUTION:

DATA:

Initial stress	$\sigma_o = 60$ psi	$s_{\sigma o} = 2$ psi
Stress increment	$\Delta\sigma = 5$ psi	$s_{\Delta\sigma} = 0.5$ psi
Measured strain	$\varepsilon = 0.096$	$s_\varepsilon = 0.01$

BEST ESTIMATE OF CONSTRAINED MODULUS:

$$E = \sigma/\varepsilon$$

$$m_E = m_\sigma / m_\varepsilon$$

$$= 5 \text{ psi} / 0.096 = 52 \text{ psi.}$$

UNCERTAINTY (STATNDARD DEVIATION) OF MODULUS:

$$sE \doteq (dE/d\sigma)^2 \, s_{\Delta\sigma}{}^2 + (dE/d\varepsilon)^2 \, s_\varepsilon{}^2$$

$$= (1/\varepsilon)^2 \, s_{\Delta\sigma}{}^2 + (-\sigma/\varepsilon^2)^2 \, s_\varepsilon{}^2$$

$$= (1/0.096)^2 \, (0.5 \text{ psi})^2 + (-5 \text{ psi}/0.096^2)^2 \, (0.01)^2$$

$$= (7.5 \text{ psi})^2$$

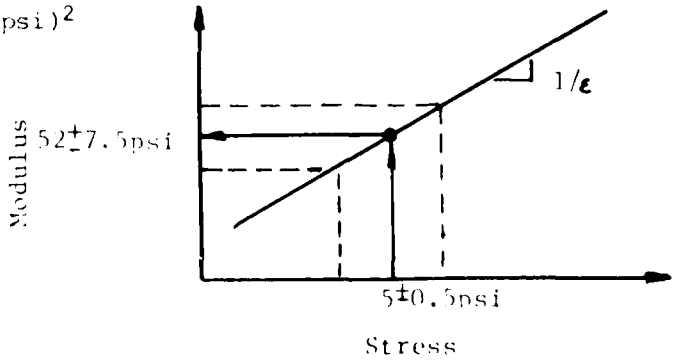

PLATE 2

SUBJECT: Shortcut estimates of summary parameters.

A] DATA:

Test Number	Measured Strength (kPa)
1	38
2	51
3	43
4	39
5	48
6	45
7	42
8	45
9	49

B] ESTIMATE MEAN:

By Equation 2

$$m_x = \frac{1}{n} \Sigma x_i$$

$$= \frac{1}{9} (400 \text{ kPa})$$

$$= \underline{44.4 \text{ kPa}}$$

Shortcut Method Using Median

$m_x \approx$ median of x_i

$= \underline{45 \text{ kPa}}$

C] ESTIMATE STANDARD DEVIATION:

By Equation 3

$$s_x = \frac{1}{n-1} \Sigma (x_i - m_x)^2$$

$$= \underline{4.2 \text{ kPa}}$$

Shortcut Method Using Range

$w = (x_{max} - x_{min})$

$= 51 - 38$ kPa

$= 13$ kPa

$s_x \approx N_n w_n$

From Table 1, $N_9 = 0.337$

$= (0.337)(13)$

$= \underline{4.4 \text{ kPa}}$

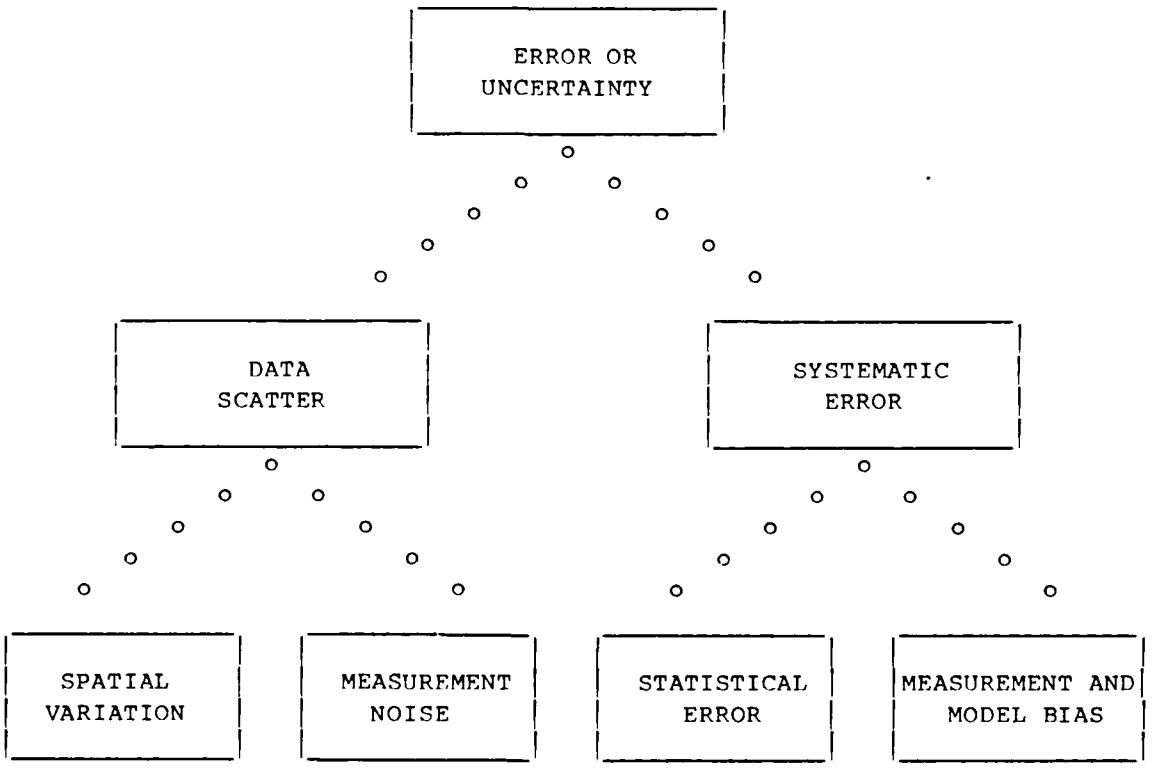

Figure 1. Sources of Error or Uncertainty in Soil Property Estimates.

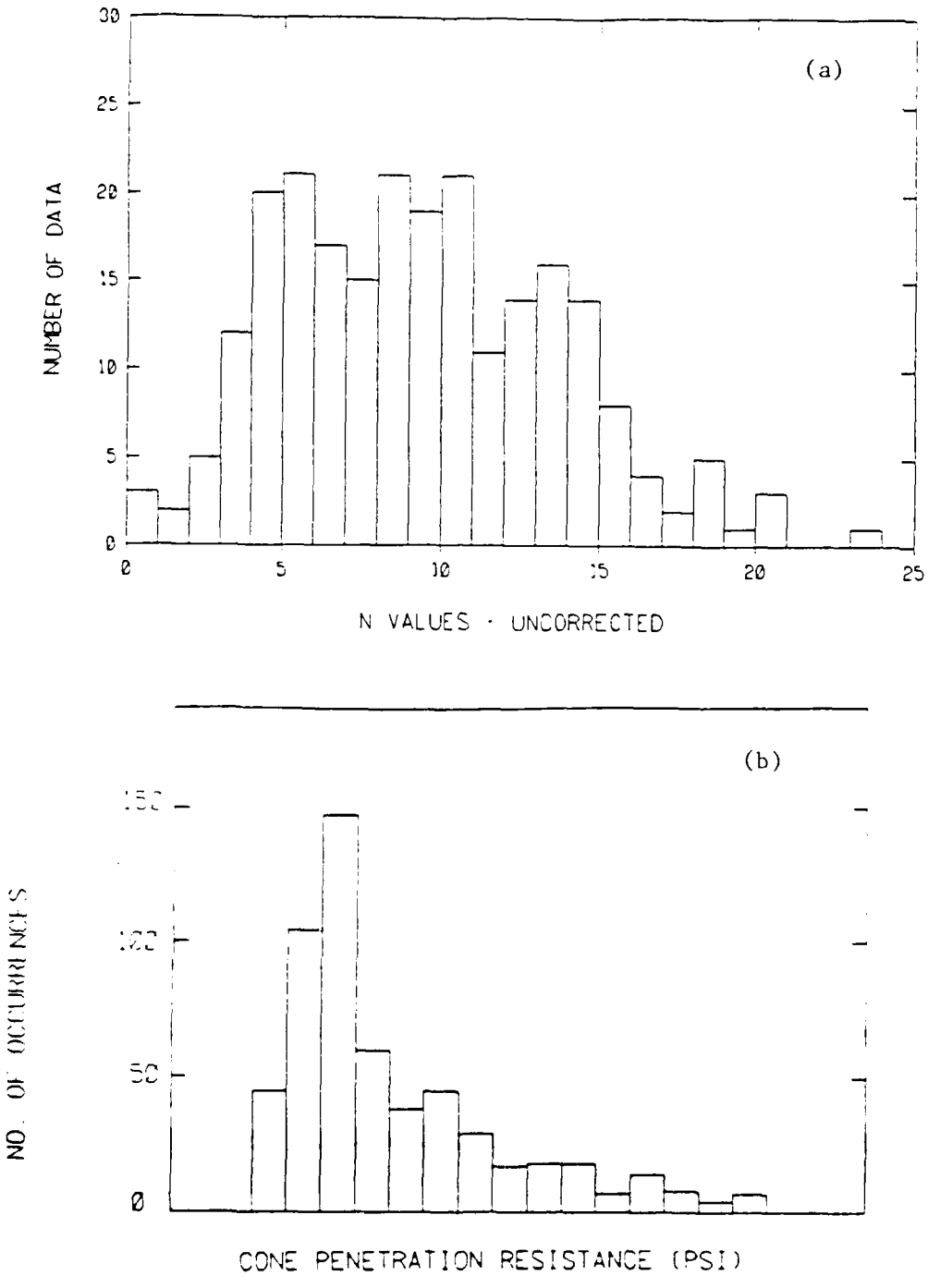

Figure 2. Histograms of Soil Property Data: (a) Symmetric Distribution of Variability; (b) Skewed Distribution of Variability.

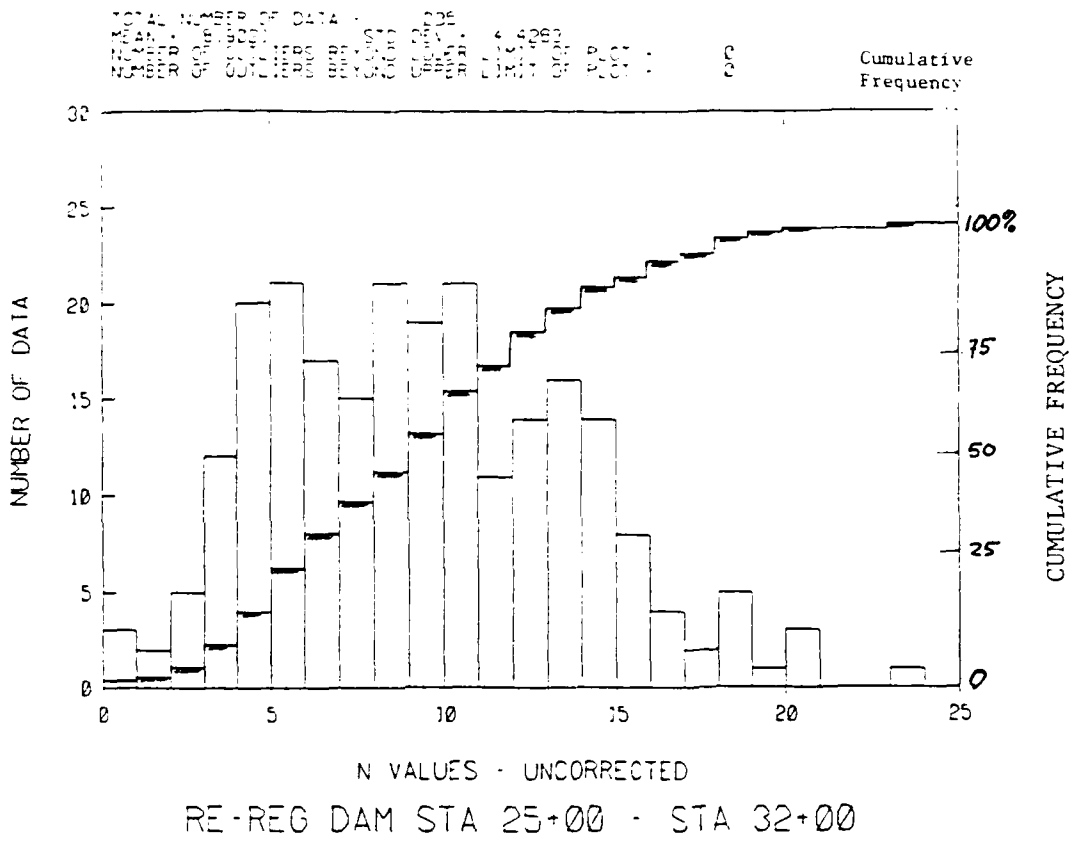

Figure 3. Frequency Distribution of SPT Data From Fig. 2a.

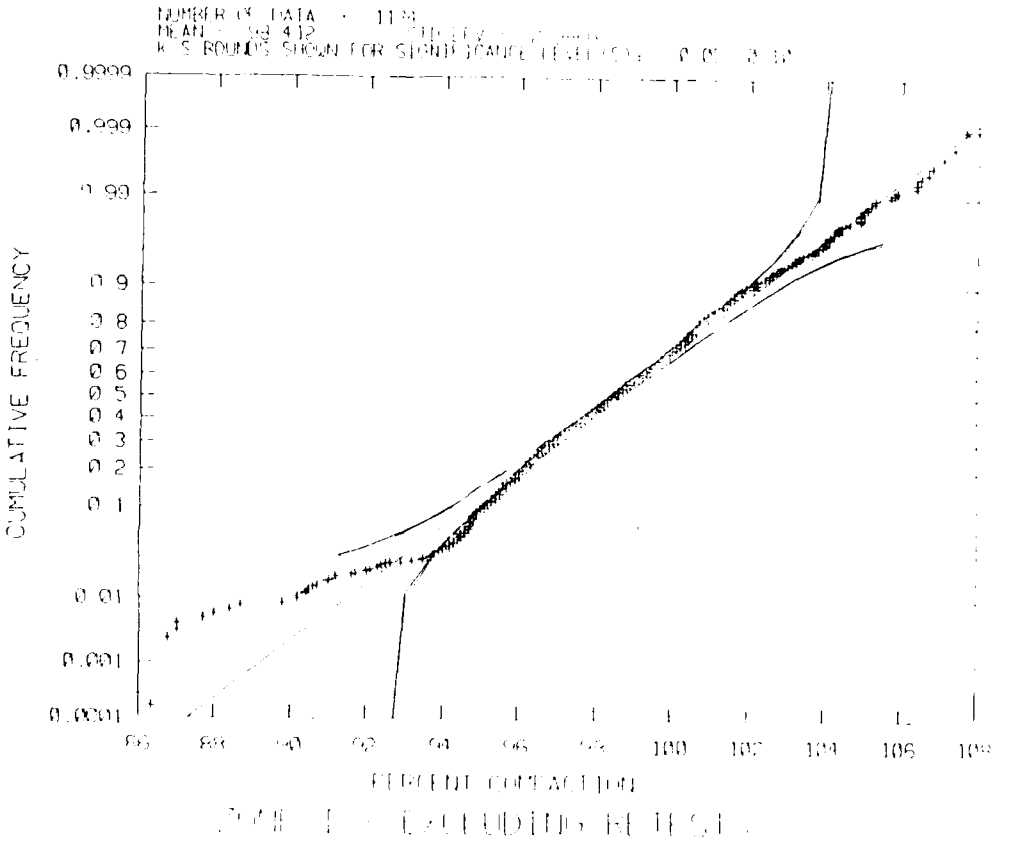

Figure 4. Probability Paper Plot of Compaction Control Data. Middle line shows best fit to data; outside lines show statistical goodness of fit (Kolmogorov) bounds.

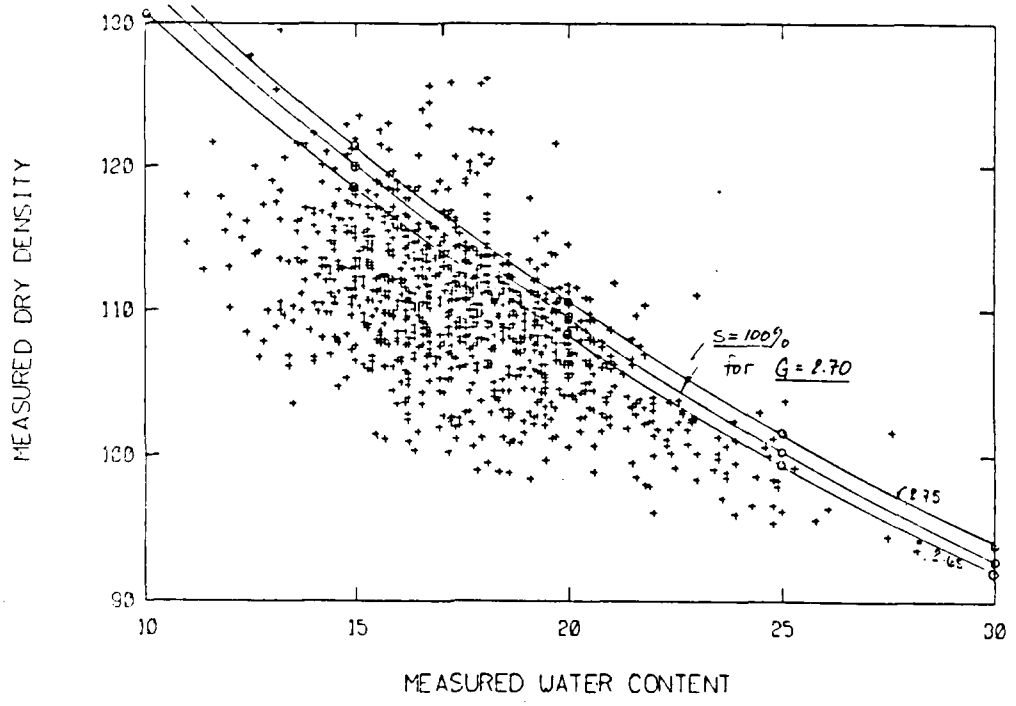

Figure 5. Scatter Plot of Compaction Control Data Showing Water Content vs. Dry Density.

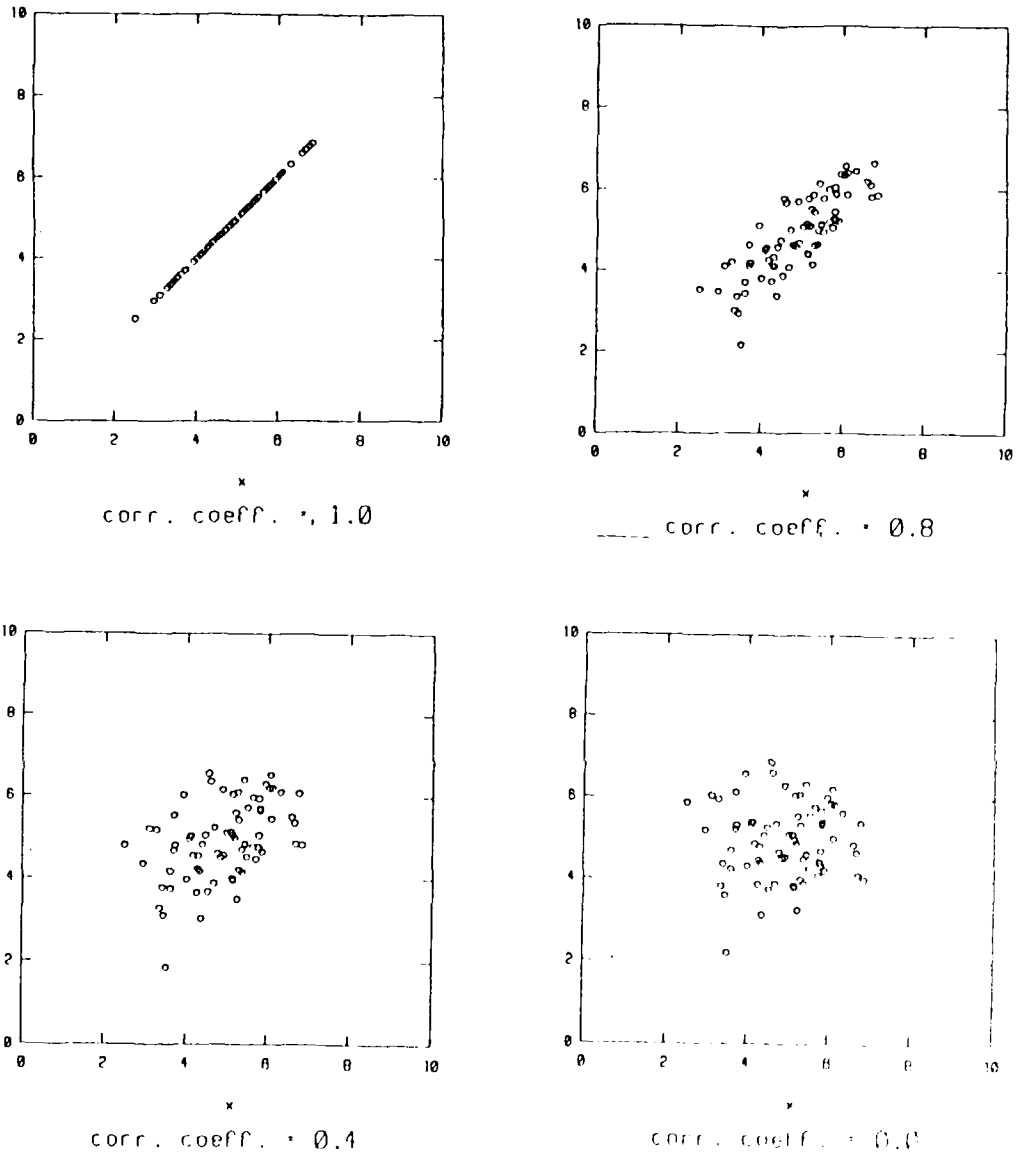

Figure 6. Various Scatter Plots Showing Different Levels of Correlation.

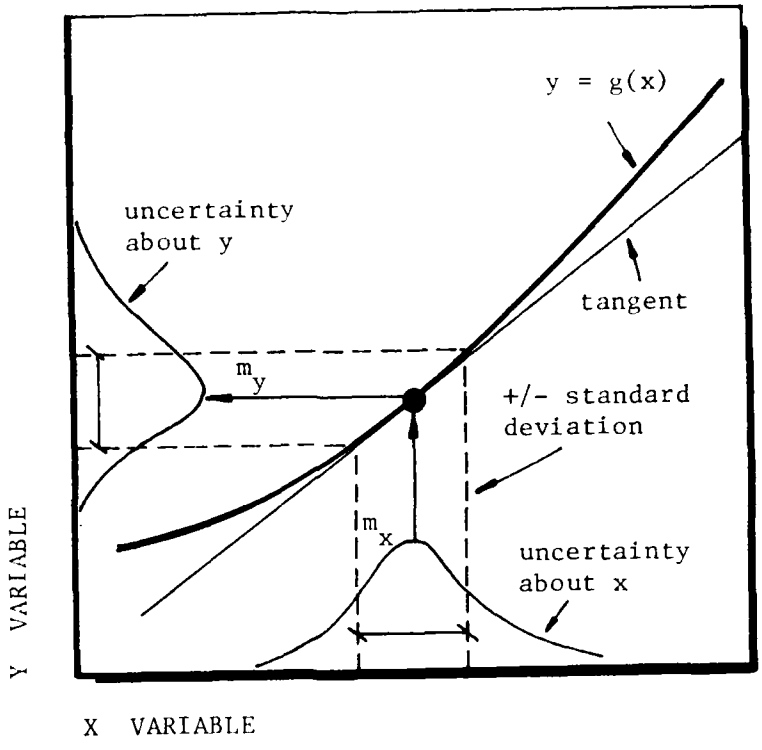

Figure 7. First-Order Propagation of Error Through The Model y = g(x).

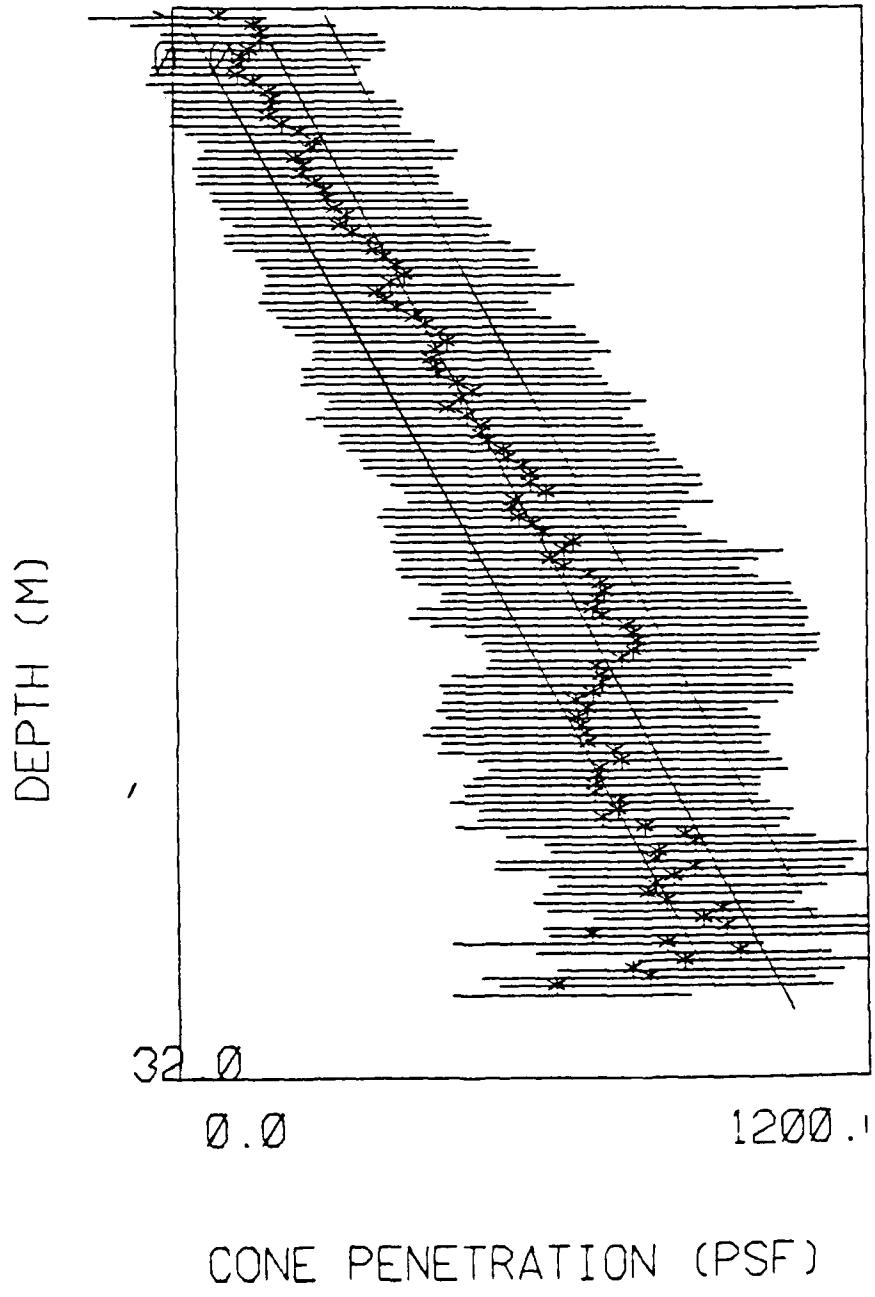

Figure 8. Cone Penetration Resistance in a Copper Porphyry Tailings Pile. Star shows depth interval mean; bars indicate range of data. Envelopes show +/-standard deviation.

SHILLING'S METHOD:

$r_{x,y} = (12.0^2 - 4.0^2)/(12.0^2 + 4.0^2)$

$= 0.80$

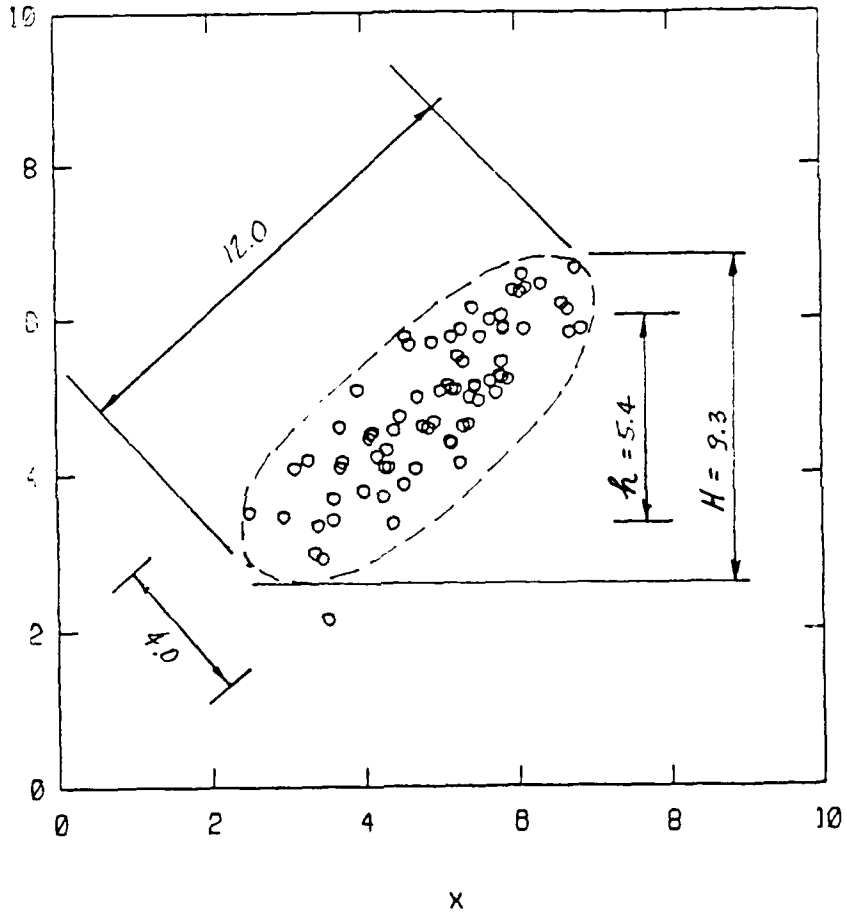

CHITILLON'S:

$r_{x,y} = \sqrt{1 - (5.4/9.3)}$

$= 0.81$

Figure 9. Ballon Shortcut Method for Estimating Correlation Coefficient.

PART III: SPATIAL VARIATION AND DATA SCATTER

Soils are geological materials formed by weathering processes and, except for residual soils, are transported by physical means to their present locations. They have been subject to various stresses, pore fluids, and physical and chemical changes. Thus, it is hardly surprising that the physical properties of soils vary from place to place within resulting deposits.

The scatter observed in soil data comes both from this spatial variability and from errors in testing. Each of these exhibits a distinct statistical signature which can be used to draw conclusions about the character of a soil deposit and about the quality of testing.

Part III presents the tools required to interpret the structure of spatial variation, and to draw conclusions about the impact of spatial variation on engineering calculations.

Trends and Variations About Trends

In Part II, means and standard deviations were used to describe the variability in a set of soil property data. These are useful measures, but they combine data in such a way that spatial information is lost. To describe the variation of soil properties in space, additional tools are needed.

Consider the two sequences of hypothetical measurements shown in Figs. 10a and 10b. Presume that each measurement was made at the same elevation, one in each of nine consecutive borings along a line. These two sets of data have the same mean and standard deviation, but clearly reflect different soil conditions. The first data exhibit a distinct horizontal trend, the second are erratic. This difference cannot be inferred from the mean and standard deviation alone, for they are the same in both cases.

In principle, the spatial variation of a soil deposit can be characterized

in detail, but only if a large number of tests is made. In reality, the number of tests required far exceeds that which would be practical. Thus, for engineering purposes a simplification is introduced--that is, a model--within which spatial variability is separated into two parts: (i) a known deterministic trend, and (ii) residual variability about that trend. This model is written,

$$x_i = t_i + u_i, \tag{28}$$

in which x_i is the soil property at location i, t_i is the value of the trend at i, and u_i is the residual variation. The trend is characterized deterministically by an equation. The residuals are characterized statistically, by a mean, standard deviation, and something statisticians call an autocorrelation function. Rather than characterize soil properties at every point, data are used to estimate a smooth trend, and remaining variations are described statistically.

The residuals are characterized statistically because there are too few data to do otherwise. This does not assume soil properties are random; they are not. While statistical techniques provide a convenient way to describe what is known about spatial variation, one has always to be wary that grouping data together does not mask a real and crutial "geological detail."

Estimating Trends

Trends are estimated by fitting well-defined mathematical functions (i.e., lines, curves, or surfaces) to data points in space. The easiest way to do this is by regression analysis as outline in Part II. For example, Fig. 11 shows maximum past pressure measurements as a function of depth in a deposit

of Gulf of Mexico clay. For geological reasons the increase of maximum past pressure with depth is expected to be linear within this homogeneous stratum. Data from an overlying dessicated crust are not shown.

The equation for the trend of maximum past pressure σ'_{vm}, with depth z is

$$\sigma'_{vm} = a + bz + u \tag{29}$$

in which a and b are regression coefficients (intercept and slope), and u = residual variation about the trend. Applying Eqns. 21 and 22 to the data leads to

$$a \approx 3 \text{ sf} \tag{30}$$

$$b \approx 0.06 \text{ ksf/ft} \tag{31}$$

for which the corresponding trend line is shown on Fig. 11. For data analysis purposes, the regression line $m_{\sigma'_{vm}} = 3 + 0.06z$ is the best estimate or mean of the maximum past pressure as a function of depth.

Residuals About Trends

Residual variation not accounted for by the trend is characterized by a standard deviation or variance. By the procedure through which the trend is fit, the residuals must have zero mean. The variance of the residuals is calculated by Eqn. 23 to be $V_u = 1 \text{ksf}^2$. This is the variability of σ_{vm}' unexplained by the trend line. Plus and minus one standard deviation bounds with depth are shown in Fig. 11. The standard deviation s_u is the uncertainty in maximum past pressure at any elevation. This is the uncertainty in σ'_{vm} at a point in the soil deposit caused by modeling spatial variation with a smoothly varying trend, here the line of Eqn. 29. Presumably,

the standard deviation of the residuals is the same everywhere along the line. This is an assumption of the least squares fitting procedure. Usually this assumption is good, but it can be relaxed if necessary (Johnson, 1960).

Another assumption in fitting trends is that residual variations are unrelated (i.e., independent) from one place to another. In fact, this is seldom the case for geotechnical data. Fig. 12a shows residuals which have been artificially generated to be independent from one to another. Fig. 12b shows residuals typical of most soil data. Inspection shows a difference in character. The first set appears 'erratic;' the second, 'wavy.'

The waviness of residual soil data reflects spatial structure that is ignored in the regression analysis. If a measurement at depth i in the profile lies above the average trend with depth, as a general rule measurements at adjacent depths also lie above the trend, and vice versa. This is called 'autocorrelation.' The longer the apparent 'wave length' of the residuals the farther autocorrelation extends.

More formally, autocorrelation is the property that residuals off the mean trend are not statistically independent, and that the degree of association among them as measured by the correlation coefficient depends on their relative separation in space.

Correlation was introduced in Part II. Correlation is the property that, on average, two variables are associated with one another. Knowing the value of one provides information on the value of the other. The strength of such association is measured by a correlation coefficient, ranging between plus and minus one.

In the same way that two variables of different types can be related (e.g., water content and undrained strength), so too can values of the same

variable at different locations. For example, Fig. 13, shows standard penetration test (SPT) blow counts as a function of depth. In the horizontal direction these blow counts have an approximately constant mean, therefore detrending is not needed. In Figs. 14a,b,c the blow count data are plotted against one another. The horizontal axis records the blow count at location i; the vertical axis records the corresponding blow count at a location separated by δ from location i. When δ is large as in Fig. 14c, the correlation between u_i and $u_{i+\delta}$ is slight. However, as δ becomes smaller, as in Fig. 14a, the correlation increases. As $\delta \to 0$, naturally, the correlation approaches +1. Plotting the correlation coefficient so obtained as a function of separation distance δ gives the autocorrelation function, denoted $R_x(\delta)$. Plotting the correlation coefficient multiplied by the data variance (i.e., the covariance of Equation 9) gives the autocovariance function, denoted $C_x(\delta)$. The autocovariance is shown in Fig. 15a.

The effect of correlation structure on residual variation can be seen in Fig. 16 in which four cases are sketched schematically. Spatial variability about a trend is characterized by variance and autocorrelation. Large variance implies that the absolute magnitude of the residuals is large; large autocorrelation implies that the 'wave length' of variation is long.

Trends vs. Residuals

As can be seen from the preceding section, the division of spatial variation into a trend and residuals about the trend is an artifact of analysis. By changing the trend model fit to data, for example, by replacing a linear trend with a polynomial, the variance and autocorrelation function of the residuals can be changed almost arbitrarily. From a practical view the selection of a trend line or curve is in effect a decision on how much of the

data scatter to model as a deterministic function of space, and how much to treat statistically. Dividing spatial variability into a deterministic part and a statistical part is a matter of practicality. Prudence requires that each datum be judged for what it might say about a soil deposit, but engineering analysis requires models of soil properties for making predictions.

As a rule of thumb, trend surfaces should be kept as simple as possible without doing injustice to a set of data or ignoring the geologic setting. The problem with using trend surfaces that are very flexible, as for example high order polynomials, is that the number of data from which the parameters of those equations are estimated is limited. The more parameter estimates that a trend surface requires, the more uncertainty there is in the numerical values of those estimates. Uncertainty in regression coefficient estimates increases rapidly as the flexibility of the trend increases. Uncertainty in regression coefficients is discussed in more detail in Part IV.

Autocorrelation and Autocovariance

This section presents a more mathematical treatment of autocorrelation and autocovariance. If $x_i = t_i + u_i$ is a continuous variable and the soil deposit is zonally homogeneous, then at locations i and j, which are close together, the residuals u_i and u_j should be expected to be similar. That is, the variations reflected in u_i and u_j are associated with one another. When the locations are close together, the association is usually strong. As the locations become more widely separated, the association usually decreases. As the separation between two locations i and j approaches zero, u_i and u_j become the same, the association becomes perfect. Conversely, as the separation becomes large, u_i and u_j become independent, the association becomes zero. This spatial association of residuals off the trend t_i is summarized by a

mathematical function describing the correlation of u_i and u_j as the separation δ increases. This description is called the autocorrelation function. In concept, the autocorrelation function is a mathematical way of summarizing the correlations shown in the scatterplots of Figs. 14a,b,c. Mathematically, the autocorrelation function $R_x(\delta)$ is

$$R_x(\delta) = \left(\frac{1}{n_\delta - k}\right) \Sigma \left(\frac{x_i - t_i}{s_x}\right)\left(\frac{x_j - t_j}{s_x}\right) = \text{"autocorrelation function"} \quad , \qquad (32)$$

in which n_δ = the number of data pairs having separation distance δ, and k = the number of coefficients needed to define the trend model (e.g., the parameters a and b in Eq. 29). $R_x(\delta)$ expresses the correlation of two residuals off the trend surface as a function of their separation distance. By definition, the autocorrelation at zero separation distances is $R_x(0)=1.0$. Empirically, for most soils, autocorrelation decreases monotonically to zero as δ increases.

If $R_x(\delta)$ is multiplied by the variance of the residuals V_u, the autocovariance function is obtained, as shown in Fig. 15,

$$C_x(\delta) = R_x(\delta)V_u = \text{"autocovariance function"} \quad . \qquad (33)$$

The relationship between the autocorrelation function of Eqn. 32 and the autocovariance function of Eqn. 33 is the same as that between the correlation coefficient of Eqn. 8 and the covariance of Eqn. 9.

Consider the site shown in Fig. 17 which overlies an hydraulic bay fill. SPT data taken in the silty fine sand between elevations +3 and -7m show little if any trend horizontally, and so a constant trend at the mean of the data is assumed. Fig. 18 shows the histogram of SPT data. Fig. 19 shows autocovariance functions in the horizontal direction estimated for three intervals of elevation. At short separation distances the data show distinct

association, i.e., correlation. At large separation distances the data exhibit essentially no correlation.

In natural deposits, correlations in the vertical direction extend to much shorter distances than in the horizontal direction. A ratio of about one to ten for these correlation distances is common. Horizontally, autocorrelation may be isotropic (e.g., $R_x(\delta)$ in the north-south direction is the same as $R_x(\delta)$in the east-west direction) or anisotropic, depending on geologic history; however, in practice, isotropy is often assumed. Also, autocorrelation is typically assumed to be the same everywhere within a deposit. This assumption, called stationarity, is equivalent to assuming that the deposit is statistically homogeneous.

It is important to emphasize that the autocorrelation function is an artifact of the way soil variability is separated between a 'trend' and 'residuals.' Since there is nothing innate about the chosen trend t_i, and since changing the trend changes $R_x(\delta)$, the autocorrelation function reflects a modeling decision. The influence of changing trends on $C_x(\delta)$ is illustrated in Figs. 20, 21 and 22, showing data analyzed by Javette (1983). Fig. 21 shows autocorrelations of water content in San Francisco Bay Mud within an interval of 3 ft. Fig. 22 shows the same autocorrelation function when the entire site is considered. The difference comes from the fact that in Fig. 21 the mean trend is taken locally within the 3 ft. interval. In Fig. 22 the mean trend is taken globally across the site. The schematic drawing in Fig. 23 suggests why the autocorrelations should differ.

Autocorrelation can be found in almost all spatial data which are analyzed using a model of the form of Eqn. 28. For example, Fig. 24 shows the autocorrelation of joint (i.e., rock fracture) density in a copper porphyry

deposit; Fig. 25 shows the autocorrelation of water content in the compacted clay core of a rock fill dam; Fig. 26 shows the autocorrelation of cone penetration resistance in North Sea Clay. In mining, the importance of autocorrelation to ore reserve estimates has been recognized for many years. In mining "geostatistics" a complimentary function to the autocorrelation function, called the variogram (Matheron, 1971), is more commonly used to express the spatial structure of data. The variogram requires a less restrictive statistical assumption on stationarity than the autocorrelation function requires and is therefore often preferred for estimation problems. On the other hand, the variogram is sometimes more difficult to use in engineering analyses, and thus for geotechnical purposes the autocorrelation is more commonly used. In practice, the two ways of characterizing spatial structure are quite similar.

Estimating Autocovariance and Autocorrelation

This section considers only a straightforward and often used approach to estimating autocovariance and autocorrelation, the 'moment estimate.' For more detailed discussion of statistical aspects of estimating $C_x(\tau)$, including more efficient estimators, see Appendix A.

Consider the simple case of measurements made at equally spaced intervals along a line, as for example in a boring. Presume that the measurements $\underline{x} = (x_1,\ldots,x_n)$ are unaffected by measurement error. The autocovariance of the measurements at separation τ is,

$$\hat{C}_x(\tau) = \frac{1}{n-j} \sum (x_i - t_i)(x_{i+j} - t_{i+j}) \qquad (34)$$

$$= \frac{1}{n-2} \sum (u_i)(u_{i+\delta}) \tag{35}$$

This autocovariance is called the 'sample autocovariance,' and it is used as an estimator of the real autocovariance at separation distance δ. The real autocovariance is that which would be obtained if the true values of soil properties at every point in space were known. The general expression of the sample autocovariance for any arbitrary distance δ is,

$$\hat{C}_x(\delta) = \frac{1}{n_\delta - k} \sum (x_i - t_i)(x_{i+\delta} - t_{i+\delta}) \tag{36}$$

$$= \frac{1}{n_\delta - k} \sum (u_i)(u_{i+\delta}) \tag{37}$$

in which n_δ = the number of pairs of data at separation distance δ, and k = the number of parameter estimates required for the trend. For n uniformly spaced data on a line with constant-mean trend, $n_\delta = n-\delta$ (because there are $n-\delta$ pairs of data with separation distance δ) and k=1 (because only one coefficient is needed to define a constant mean).

In the general case, measurements are seldom uniformly spaced and, at least in the horizontal plane, seldom lie on a line. For such situations the sample autocovariance can still be used as an estimator, but with some alteration. The most common way to accomodate non-uniformly placed measurements is by dividing separation distances into bands, and then taking the averages of Eqn. 36 within those bands (Fig. 27). This introduces some bias to the estimate but for most engineering purposes it is sufficiently accurate.

Measurement Noise

Random measurement error is that part of data scatter attributable to instrument or operator induced variations from one test to another. This variability may sometimes increase a measurement and sometimes decrease it, but its effect on any one, specific measurement is unknown. As a first approximation, instrument and operator effects on measured properties of soils can be represented by a frequency diagram as shown schematically in Fig. 28. In repeated testing--presuming that repeated testing were possible on the same specimen--measured values differ. Sometimes the measurement is higher than the real value of the property, sometimes it is lower, and on average it may systematically differ from the real value. The systematic difference between the real value and the average of the measurements is said to be measurement bias, while the variability of the measurements about their mean is said to be random measurement error.

Sources and Character of Random Measurement Error or Noise

Random errors enter measurements of soil properties through a variety of sources related to the personnel and instruments used in soil investigations or laboratory testing.

Operator or personnel errors arise in many types of measurements where reading scales is necessary, personal judgement is needed, or operators affect the mechanical operation of a piece of testing equipment (e.g., SPT hammers). In each of these cases operator differences have systematic and random components. One person, for example, may consistently read a gage too high, another too low. If required to make a series of replicate measurements, a single individual may report numbers which vary one from the other over the

series. Figure 29 shows histograms of strike and dip measurements made by many people on the same rock joint, using the same Brunton compass.

Such variability is common and widely recognized, and as soil testing moves to more and more automated procedures, this operator variability will decrease. With hand operated field vane devices an operator may unconsciously vary the rate of torque from one test to another, thereby influencing measured undrained strengths. With an automated vane such variability is lessened. Naturally, operators also sometimes make mistakes. If these mistakes are small and not easily identified by inspection, they too become random measurement errors.

Instrumental error arises from variations in the way tests are set up, loads are delivered, or soil response is sensed. The separation of measurement errors between operator and instrumental causes is not only indistinct, but also unimportant for most purposes. In triaxial tests soil samples may be positioned differently with respect to loading plattens in succeeding tests. Handling and trimming may cause differing amounts of disturbance from one specimen to the next. Piston friction may vary slightly from one movement to another, or temperature changes may affect fluids and solids. The aggregate result of all these variables is differences between measurements that are unrelated to the soil properties of interest.

Assignable causes of minor variation are always present because a very large number of variables affect any measurement. One attempts to control those which have important effects, but this leaves uncontrolled a large number which individually have only small effects on a measurement. These assignable causes of variation if not identified may influence the precision and possibly the accuracy of measurements by biasing the results.

For example, hammer efficiency in the SPT test strongly affects measured blow counts. Efficiency with the same hammer can vary by 50% or more from one blow to the next (Kavazanjian, 1983). Hammer efficiency can be controlled, but only at some cost. If uncontrolled, it becomes a source of random measurement error and increases the scatter in SPT data.

Models for Measurement Error

Random measurement errors are ones whose sign and magnitude cannot be predicted, they may be plus or minus. Typically, random errors tend to be small and they tend to distribute themselves equally on both sides of zero. Measurement error is the cumulative effect of an indefinite number of small 'elementary' errors simultaneously affecting a measurement.

The common model of measurement error is,

$$z = x + e \quad , \tag{38}$$

in which z is the measurement, x is the soil property being measured, and e is a random error of zero mean. Were systematic errors present, the mean of e would differ from zero.

An important property of e in Eqn. 38 is that it is assumed statistically independent from one measurement to another and to have the same mean (i.e., 0) and variance V_e for each measurement. The value e takes on at one measurement is assumed to be unrelated to the value it takes on at any other. This has important practical implications; for example, it means that if many measurements are averaged together to estimate a property, measurement noise averages out.

Random measurement error can be estimated in a variety of ways, some direct and some indirect. As a general rule, the direct techniques are

difficult to apply to the soil measurements of interest to geotechnical engineers. Nevertheless, direct techniques provide insight into the nature of random errors. Indirect methods, on the other hand, are generally more practical.

Direct Estimation of Measurement Noise

The traditional way of estimating random measurement error is by replicate testing. The same property is measured repeatedly on the same specimen and the results compared. An example was shown in Fig. 29 with replicate measurements of joint strike and dip. Presumably, the property being measured does not change from test to test, so the variability observed in test results comes from random errors.

Replicate testing is a simple, direct, and accurate way of establishing random measurement error. Unfortunately, it is seldom of use because the properties engineers are most interested in are measured destructively. Performing the same test on different specimens, no matter how closely together they were sampled in the field, always leaves unanswered how much of the variability is due to measurement and how much to real differences in the soil.

Indirect Estimation of Measurement Noise

Indirect methods for estimating V_e usually involve correlations of the property in question either with other properties such as index tests, or with itself through the autocorrelation function. The easiest and most powerful methods involve the autocorrelation function. Combining Eqns. 28 and 38, data are represented as

$$z_i = t_i + u_i + e_i \quad . \tag{39}$$

The autocovariance of z in Eqn. 39, after the trend has been removed, becomes

$$C_z(\delta) = C_x(\delta) + C_e(\delta) \tag{40}$$

in which $C_x(\delta)$ is from Eqn. 33, and $C_e(\delta)$ is the autocovariance function of e. Eqn. 40 can be verified by substituting z_i for $x_i - t_i$ in Eqn. 32 and algebraically rearranging. Since e_i and e_j are independent except for i=j, the autocovariance function of e is a spike at $\delta=0$ and zero elsewhere. Thus, $C_z(\delta)$ is composed of two functions as shown in Fig. 30. By extrapolating the observed autocovariance function to the origin, an estimate is obtained of the fraction of data scatter that comes from random error. For the data of Fig. 31, $V_e \approx 0.5V_z$. In the "geostatistics" literature this is called the nugget effect.

For the field vane data of Fig. 32, the random measurement error contribution to data scatter is about 20 kPa^2, or 40% of the variance. Fig. 33a shows the horizontal autocovariance function of the data in a Fig. 32a. Fig. 33b shows the vertical autocovariance function. These data are analyzed by a different and more powerful procedure in Appendix A to yield approximately the same estimate. Fig. 34 shows the vertical autocorrelation of cone penetration resistance data in a copper porphyry tailings embankment. Here the measurement error is very small.

The importance of random measurement errors is well illustrated by a case involving a large number of shallow footings placed on approximately ten meters of uniform sand. The site was characterized by Standard Penetration blow count measurements, predictions were made of settlement, and settlements were subsequently measured (Hilldale-Cunningham, 1971).

Inspection of the SPT data and subsequent settlements reveals an interesting discrepancy. Since footing settlements on sand tend to be proportional to the inverse of average blow count beneath the footing, it would be expected from Eqn. 19 that the coefficient of variation of the settlements equaled approximately that of the vertically averaged blow counts. Mathematically, settlement is predicted by a formula of the form,

$$\rho \propto \frac{\Delta q}{N} q(b) \quad , \tag{41}$$

in which ρ=settlement, Δq=net applied stress at the base of the footing, N=average corrected blow count, and g(b)=a function of footing width (see, Lambe and Whitman, 1969). Therefore, by Eqn. 19 the coefficient of variation of ρ should be,

$$\Omega_\rho \doteq \Omega_N \quad . \tag{42}$$

In fact, the coefficient of variation of the vertically averaged blow counts is about Ω_N=0.44. The observed values of total settlements for 268 footings have mean 0.35 inches and standard deviation 0.12 inches; so, Ω_ρ=(0.12/0.35)=0.34. Why the difference?

The explanation is found in estimates of the measurement noise in the blow count data. Plate 3 shows the horizontal autocorrelation function for the blow count data. By extrapolating this function to the origin, the noise (or high frequency) content of the data is estimated to be about 50% of the data scatter variance. This means that,

$$(\Omega_{soil})^2 = (\Omega_{data})^2 \, (0.5) \qquad (43)$$
$$= (0.35)^2$$

which is close to the observed variability of the settlements. Measurement noise of 50% or even more of the observed scatter of in situ test data, particularly the SPT, has been noted on several projects (e.g., Baecher, Marr, Lin, and Consla, 1980; Schmertmann, personal communication, 1986).

In fact, while random measurement error exhibits itself in the autocorrelation or autocovariance function as a spike at r=0, real variability of the soil at a scale smaller than the minimum boring spacing cannot be distinguished from measurement error when using the extrapolation technique. Thus, it need not be that the 'noise' component estimated from the horizontal autocovariance function in the horizontal direction is the same as that estimated from the vertical.

For many, but not all, applications the distinction between measurement error and small scale variability is unimportant. For any engineering application in which average properties within some volume of soil are important, the small scale variability averages quickly and therefore has little effect on predicted performance. Thus, for practical purposes it can be treated as if it were a measurement error. On the other hand, if performance depends on extreme properties--no matter their geometric scale--this unimportance no longer obtains. Some engineers think that piping (internal erosion) in dams is such a mode of performance. However, few physical mechanisms of performance easily come to mind which are strongly affected by small scale spatial variabilities, unless those anomalous features are continuous over a large extent in at least one dimension.

Rejecting Outlier Data

It is often the case with geotechnical measurements that one or more data differ strikingly from the bulk of the measurements made. This presents the often difficult question of whether to reject the data as anomalous, or to decide that they reflect real and important variations in soil or rock mass properties. The decision that data are anomalous could mean one of at least two things, (a) that they are thought erroneous, or (b) that they are thought to be real but unimportant.

The profile of Fig. 35 shows SPT blow count data with depth in a silty sand deposit. Near elevation 73 in boring SS-56-66 one of the measurements appears very high (N=12bpf), at least compared to the apparent trend of the FV strengths with depth. It is certainly the case that this high value may reflect local variation in soil properties or may reflect an interstratified layer of much stronger material. However, given that the high value does not appear in the nearby borings, the likelihood of this high value reflecting real and important variation in sand strength seems improbable. More likely, the high value has been caused by a rock fragment or small sand lens, or possibly by an error. A decision must be made either to treat the measurement as part of the data set and to include it in the statistical analysis, or to reject it and remove it from the analysis.

In principle, it may be possible to retrace steps through the documentation of a testing program to see whether an explanataion for the unusually large measurement can be found. Yet, unless an extraordinary quality assurance program has been followed, this tracing often leads to no clear answer. In such case, the decision to accept or reject the measurement has to

be made on the basis of the set of data alone, and on the relation of a particular measurement to the general characteristics of the bulk of the data. The decision is ultimately subjective. By throwing out an 'outlier' one may in fact be throwing out the most interesting piece of information about the soil or rock formation.

In judging whether an extreme value is real and important or simply an outlier which can be rejected, statisticians prefer to follow some formal policy whereby the probability of accepting or rejecting the measurement erroneously can be calculated. A suitable value for this probability is decided upon, and then an explicit rule for rejecting data is derived.

To decide whether to accept or reject an extreme individual measurement, a common procedure is to use the quantity

$$t = \frac{z_i - m_z}{s_z} \tag{44}$$

in which m_x and s_x are the mean and standard deviation of the set of measurements $z_1,\ldots,z_n$, which includes the suspect value z_i. If the z are Normally distributed, the quantity t should have a student's t distributional form with $\nu=n-1$ degrees-of-freedom. Thus, the probability of an individual measurement deviating as much from the mean as z_i does can be evaluated from tables of the Student's t distribution (e.g., Benjamin and Cornell, 1970). Some critical probability level α is chosen, usually $\alpha=0.05$ or $\alpha=0.01$, and if the probability of a deviation at least as large as observed with z_i is less than α, the measurement is rejected. Using this rule, the probability of rejecting a measurement z_i which truly is appropriately part of the data set is α.

Considering the outlying measurement in Fig. 35, the test value t equals.

$$t = \frac{12bpf - 3.8bpf}{2.56bpf} = 3.2 \qquad (45)$$

in which m=3.8bpf and s=2.56bpf. Comparing this value to tables of the Student's t for n=35 data (=n-1=34 degrees of freedom), the probability of a deviation as large as observed is about 0.001. Since this value is smaller than either common criterion =0.05 or =0.01, the measurement is rejected from the data set. While the outlier test based on Eqn. 44 is exact only for data that are Normally distributed, it remains approximately correct as long as the data are not highly skewed. Therefore, for geotechnical applications it is usually satisfactory.

A shortcut outlier test, that does not require computing the mean and standard deviation uses the test value,

$$= \frac{z_n - z_{n-1}}{z_n - z_1} , \qquad (46)$$

in which the measurements z_1, z_2, ..., z_n are listed in ascending order. The quantity $(z_n - z_{n-1})$ is the interval separating the largest from the second largest measurement, and $(z_n - z_1)$ is the range of the data. Dixon (1953) has worked out values of corresponding to probabilities =0.05 and =0.01 (Table 2). For a specific outlier to be tested, the value is computed and compared to the tabulated value for the chosen level.

The test using , however, only works well with small n (e.g., <10). Were we to compare the 12 bpf measurement only with other measurements in the upper stratum of the same boring, of which there are 4, then,

$$= \frac{z_n - z_{n-1}}{z_n - z_1} = \frac{12 - 5}{12 - 3} = 0.77 \qquad (47)$$

which is slightly greater than the critical value for =0.05 and therefore the measurement is again rejected from the data set.

The critical values of Table 2 also apply to the test of outlier values to the low end of the data set, using the test value

$$= \frac{z_2 - z_1}{z_n - z_1} , \qquad (48)$$

in which z_2 is the second lowest measured value. As with the t-test-value of Eqn. 44, the r-value assumes the data set to be Normally distributed.

A problem when evaluating outliers on the low and presumablly unconservative side of a data set is that the risk associated with incorrectly rejecting an anomalous measurement must be carefully considered. The decision to include or reject such a measurement often rests more on geological judgement than on engineering analysis.

Size Effect Factor

The volume of soil influenced by an in situ test, or contained in a laboratory specimen, is small compared with that influenced by a prototype structure. To make predictions of how the prototype will perform, one needs to estimate the properties within this larger, representative volume of soil, and the variability among such representative volumes.

This is done by assuming the representative volume to be composed of a large number of small elements, for example, each the size of a test specimen. The mean and standard deviation of the properties of small elements are

evaluated, and then the spatial structure described by the autocorrelation function is used to calculate corresponding means and standard deviations for the larger volumes. These calculations are summarized in a size-effect factor, R, which in many cases can be expressed by simple formulas or can be graphed.

Spatial Averaging

Empirically, the variability of soil properties among small volumes of soil, say test specimens, is larger than that among large volumes, say the soil under a footing. Within a small volume, physical properties tend to be more or less the same throughout. Some individual specimens may have greater than average properties throughout while some may have less than average, but within each specimen there is less variability than there is among the average properties of different specimens. Within large volumes the opposite is true, there tends to be a mixture of high and low properties in any one volume. Thus, with small volumes the properties of individual volumes may vary sharply from the mean across the site, but with large volumes internal variations balance out such that the average property from one large volume to another differs very little. The mean of large volumes remains the same as the mean of small volumes, but the standard deviation of the average property from one large volume to the next is smaller than the standard deviation of the average property from one small volume to the next.

The extent of averaging of properties within a large volume of soil depends on the structure of the spatial variation. More precisely, the extent of averaging depends on the standard deviation of properties from point to point and on the autocorrelation function.

The influence of spatial averaging on the variability among average element properties can be illustrated by vertically averaging SPT blow counts in boring logs. Plate 4 shows a set of six SPT boring logs. First, one N value from each boring is randomly chosen and the mean and standard deviation of the 6 values are calculated. The mean is 3.3bpf and the standard deviation is 2.5bpf. The mean is about the same as before, but the standard deviation has gone down. Continuing, the greater the number of N-values for each boring included in the average, the smaller the standard deviation of the 6 boring averages. The decrease of the standard deviation of average blow count as the number of N values included in each average increases is a manifestation of spatial averaging. The larger the volume of soil (i.e., the greater the number of values in each average) the more the individual fluctuations balance out.

The same thing happens in averaging soil properties within a continuous block of soil. The soil properties fluctuate somewhat from point to point, so the larger the block of soil over which the properties are averaged, the more the high and low fluctuations cancel out. The extent of spatial averaging can be measured by calculating the standard deviation among block averages. The more averaging that goes on within a block, the less variability there is from one block average to another.

For this simple case of averaging individual blow count measurements, the rate of decrease of the standard deviation as the number of data averaged in each boring increases can be approximately calculated. From Part IV, the standard deviation of the boring averages ought to decrease by $1/\sqrt{k}$ as the number of N values in each boring, k, increases, assuming that the blow counts are mutually independent (i.e., the correlation coefficient for each pair is

zero). If the blow counts are not independent, that is, they are autocorrelated, the standard deviation should decrease less quickly than $1/\sqrt{k}$. The data show 'wavy' variations about their spatial mean, and therefore the balancing out of spatial variations takes place more slowly.

This decrease in the standard deviation of soil properties averaged over a volume of soil is summarized by a size effect factor, R. For the averaging case, R is defined as the ratio of the variance of the average soil property within a large volume of soil to the variance among test-sized volumes,

$$R = V_m/V_N \ , \tag{49}$$

in which V_m is the variance of the average or mean property among elements. The ratio of variances rather than standard deviations is used because it is more convenient for subsequent error analysis calculations.

The rate at which R decreases with increasing soil volume depends on how erratic the spatial variations are within a soil element. The more erratic they are, that is, the shorter their 'wave length,' the more averaging that takes place within a given volume of soil. That is, the extent of averaging as reflected in R depends on the autocorrelation function of the soil properties.

The simplest (hypothetical) case occurs when a block of soil is thought of as composed of k smaller elements, each one of which has internally uniform soil propertise which are statistically independent of the properties of the other k-1 elements. Let the mean of the individual element properties be m_x and their standard deviation be s_x. In this case the average property within the block is,

$$m_B = (1/k) \Sigma x_i \tag{50}$$

and the standard deviation of the average m_B among blocks is calculated by Eqn. 16 as,

$$s_{m_B} \doteq \sqrt{\sum \left[\frac{dm_B}{dx_i}\right]^2 v_{x_i}} \quad . \tag{51}$$

$$= s_x/k \quad .$$

So, as the number of elements in the block k goes up, the standard deviation among block averages goes down as $1/\sqrt{k}$. This is approximately what happens in Plate 4, in which the SPT values show little vertical autocorrelation.

In any practical case, the soil block is not divided into discrete elements but is a continuum. The 'waviness' of soil property variations within the continuum is described by the autocorrelation function. Knowing the autocorrelation function, the exact shape of the relation of R to soil volume can be calculated in much the same way Eqn. 49 was calculated.

The size effect factor R for spatial averaging of soil properties along a line is shown in Fig. 36. Three common mathematical expressions are often used to model the decay of autocorrelation with separation distance, that is, the autocorrelation function: the exponential-squared, exponential, and power curve. These expressions are chosen as typical of the models used to analytically summarize autocorrelation. The size effect factor R differs among the three models for short lengths of averaging, but approaches an asymptotic value,

$$R \propto \frac{2\delta_o}{L} \tag{52}$$

as L becomes large. The parameter $_o$ is the autocorrelation distance, the distance at which autocorrelation decays to 1/e, in which e is the base of the natural logarithms.

Fig. 37 shows the size effect factor R for spatial averaging over a two dimensional square. Fig. 38 shows R for spatial averaging within a three dimensional cube. Both Figs. 37 and 38 are based on isotropic autocorrelation.

For spatial averaging of soil properties over other shaped surfaces, within other shaped volumes, or for other autocorrelation functions (e.g., anisotropic autocorrelation), the size effect factor R can be easily calculated using numerical simulation. This requires a programmable calculator or a small computer, but is simple. The procedure for calculating R for arbitrary geometries or arbitrary autocorrelation functions is the following:

1. Specify an analytical expression for the autocorrelation function in the desired number of dimensions.

2. Using a random number generator, randomly choose two points within the geometric volume to be averaged over.

3. Calculate the correlation between the soil properties at these two points from the autocorrelation function.

4. Repeat this process many times, at least 100.

5. Sum the correlations obtained in the simulations and divide by the number of simulations (find average correlation coefficient). This is an estimate of the size effect factor R.

6. The numerical precision of R calculated by simulation has a standard deviation equal to the standard deviation of the simulated correlations divided by the square root of the number of repetitions.

Spatial Extremes

The importance of spatial variability on calculated predictions depends not only on the volume of soil influenced but also on the mode of performance. For modes of performance which depend on average soil properties, spatial variability partially averages out, as described above. However, for modes which depend on worst condtions, for example sliding along a discontinuity or internal erosion in a dam, spatial variability is accentuated. In this latter case the size-effect factor may be greater than one, and an alteration may be caused to the mean. These cases are outside the scope of the present report.

Table 2. Frequency Distribution of Test Statistic for Outliers Based on Range (after Dixon, 1953).

Critical values of the test value

$$= \frac{z_n - z_{n-1}}{z_n - z_1}$$

Sample Size	Critical Values	
n	=0.05	=0.01
3	0.941	0.988
4	0.765	0.889
5	0.642	0.780
6	0.560	0.698
7	0.507	0.637

Abstracted from Dixon (1983)

PLATE 3

SUBJECT: Analysis of Noise in SPT Blow Count Data

Site Conditions

The site is underlain by fine dry sand to a depth of 10m. Fifty SPT borings were made across the site and a limited number of laboratory tests were run to correlate blow count with friction angle. The trend of depth-averaged blow counts corrected by Gibbs and Holtz's method is shown below. The mean of the depth averaged SPT blow counts in the upper levels is 25bpf; the standard deviation is 15.5bpf. Laboratory tests on specimens recompacted to the in situ relative density led to an average friction angle of 36.4°, and a standard deviation of 1.1°.

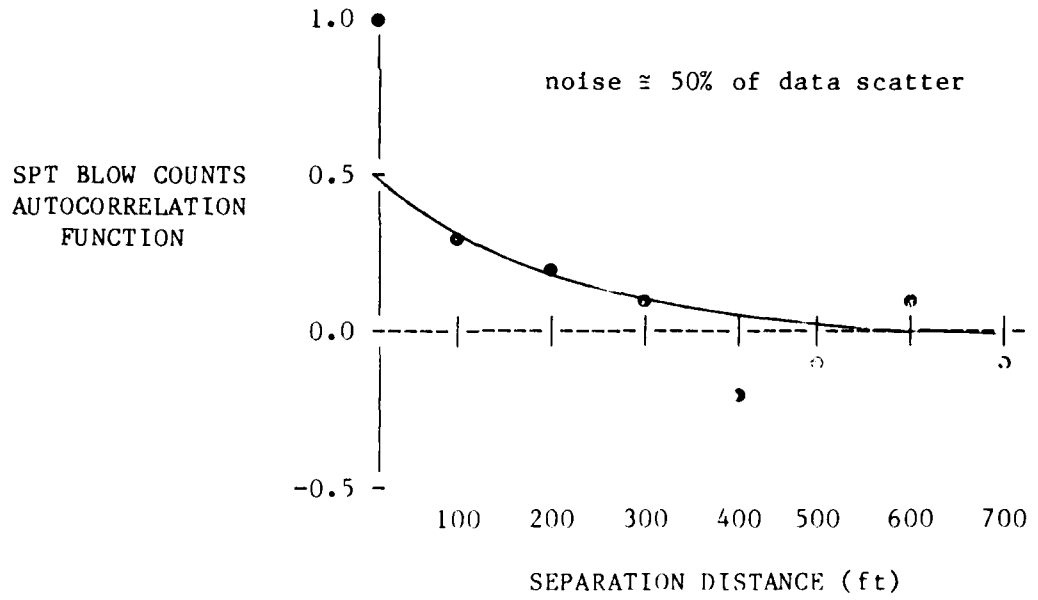

PLATE 4

SUBJECT: Spatial Averaging of SPT Blow Count Data

DEPTH	BORING # 1	2	3	4	5	6
1	2	1	2	8	3	4
2	3	8	5	3	7	4
3	8	6	5	3	7	5
4	6	6	7	0	8	7
5	0	2	5	2	5	0
6	3	2	4	1	9	4
7	3	5	0	0	4	1
8	8	3	0	8	8	7

Average and standard deviation of average of n=1,2, and 8 data:

n = 1 $m_N = 3.3$, $s_m = 2.5$

n = 2 $m_N = 5.7$, $s_m = 2.0$

n = 8 $m_N = 4.2$, $s_m = 0.9$

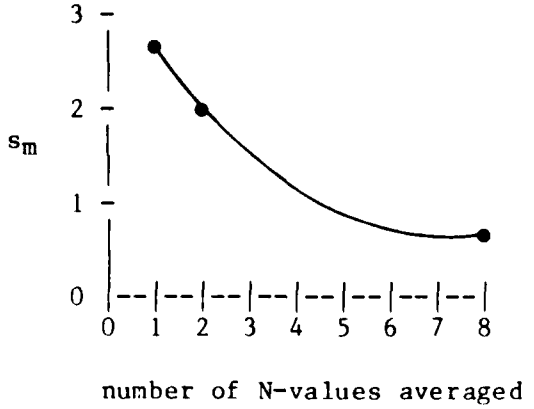

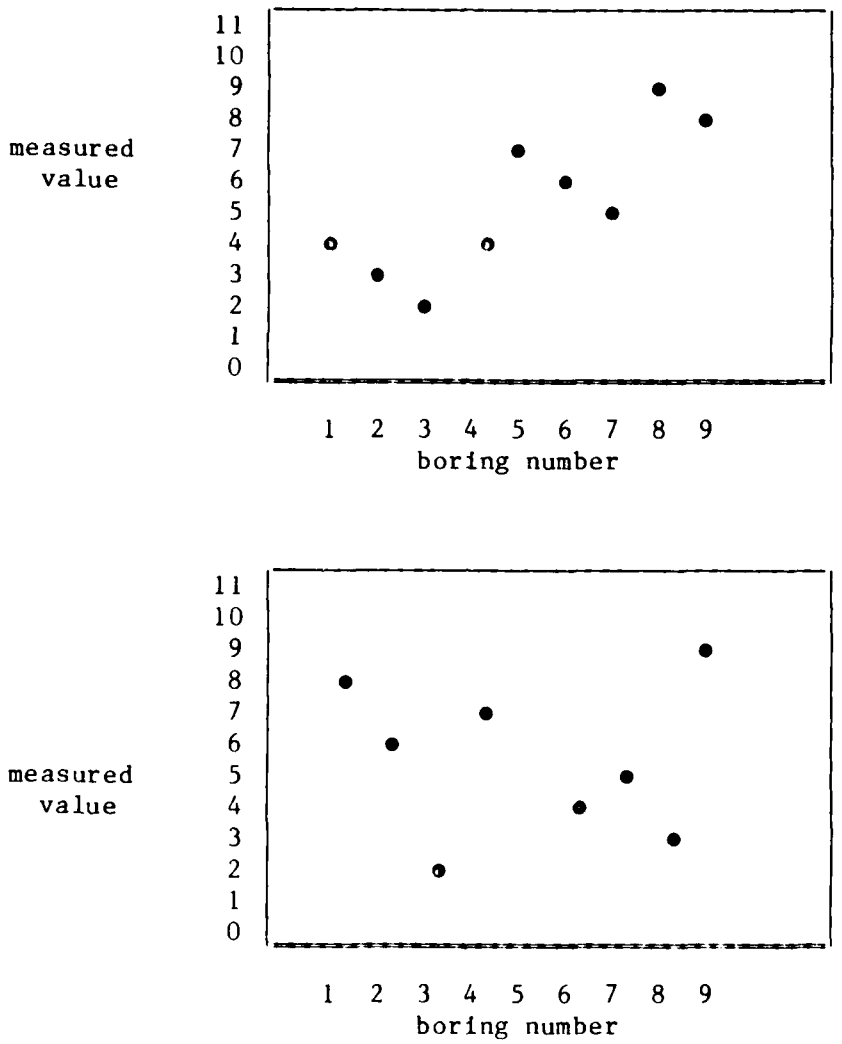

Figure 10 - Spatial Data Displaying: (a) Trend With Location, (b) Erratic Variation With Location.

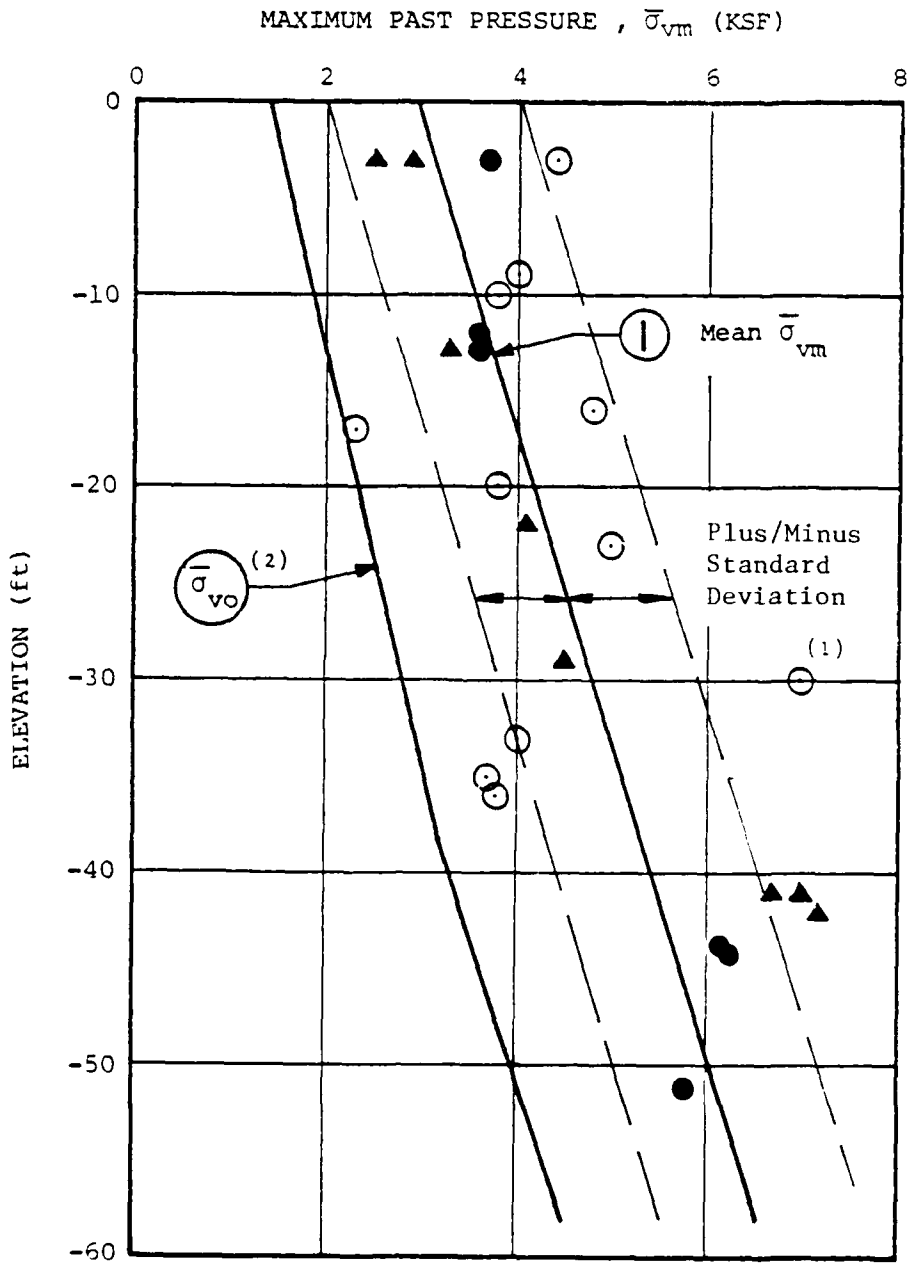

Figure 11. Maximum Past Pressure Data as a Function of Depth. Line marked "1" shows mean with depth. Solid line at left shows in situ effective vertical stress. Symbols refer to different measurement procedures.

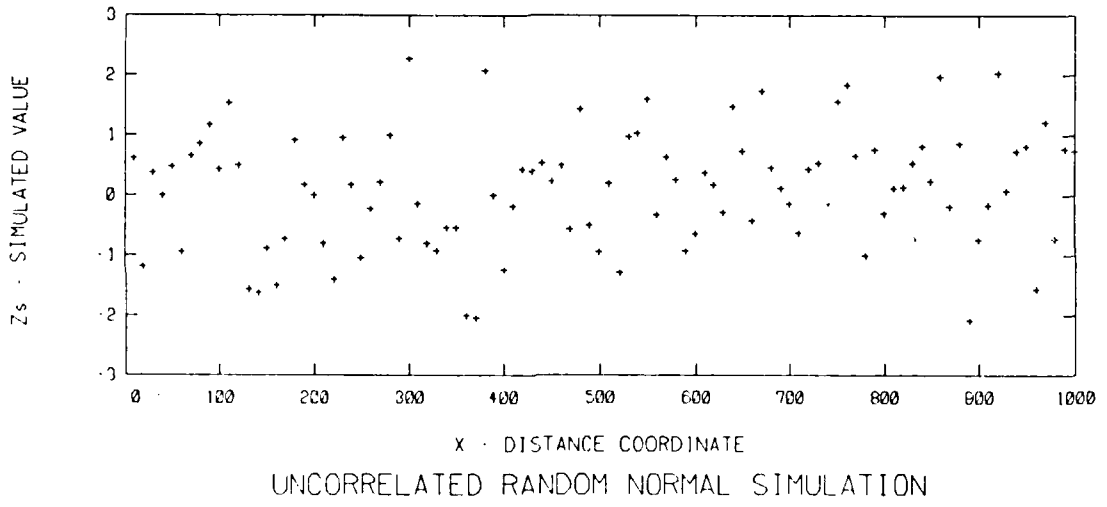

Figure 12a. Artificially Generated Statistically Independent Residuals off Pegression Line.

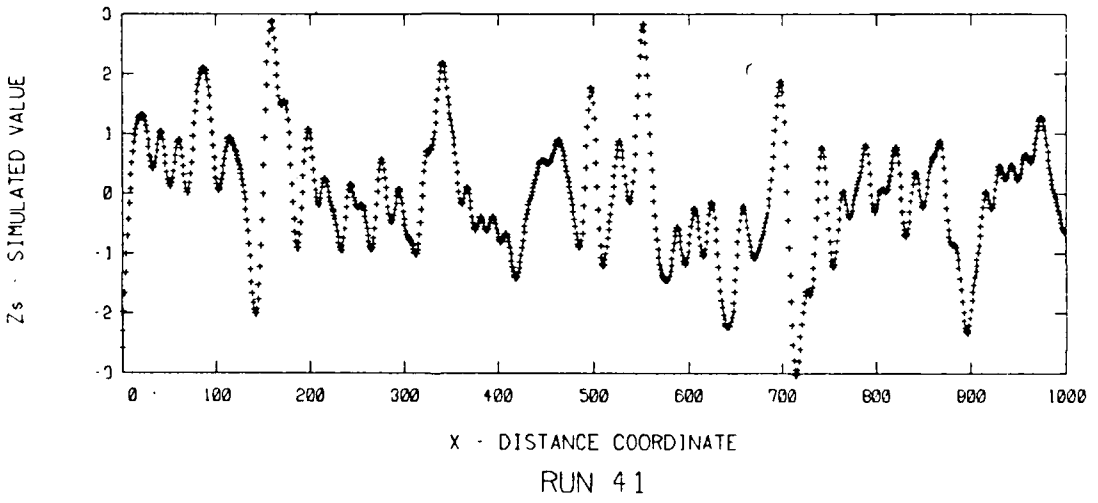

Figure 12b. Dependent Residuals Typical of Actual Soil Data.

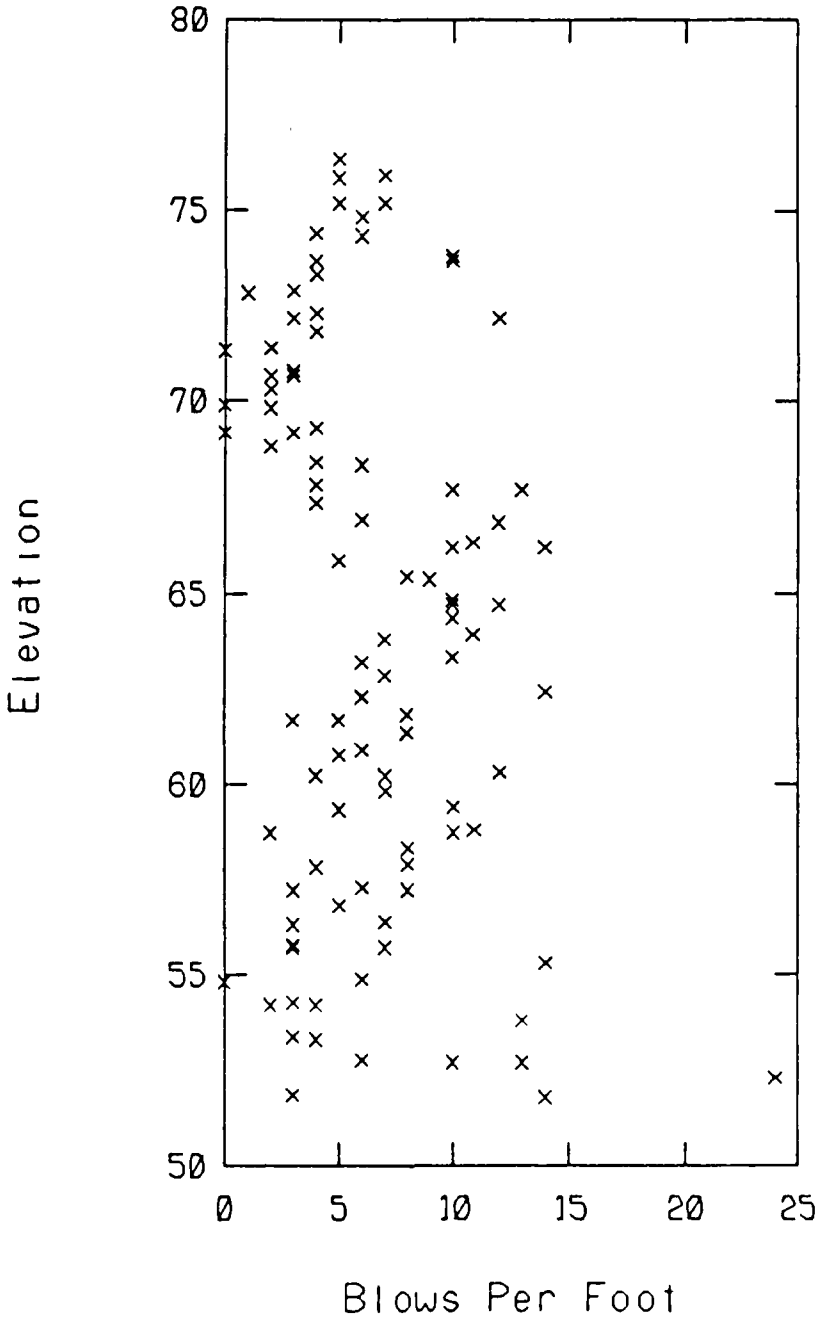

Figure 13. Standard Penetration Test Blow Counts as Function of Depth.

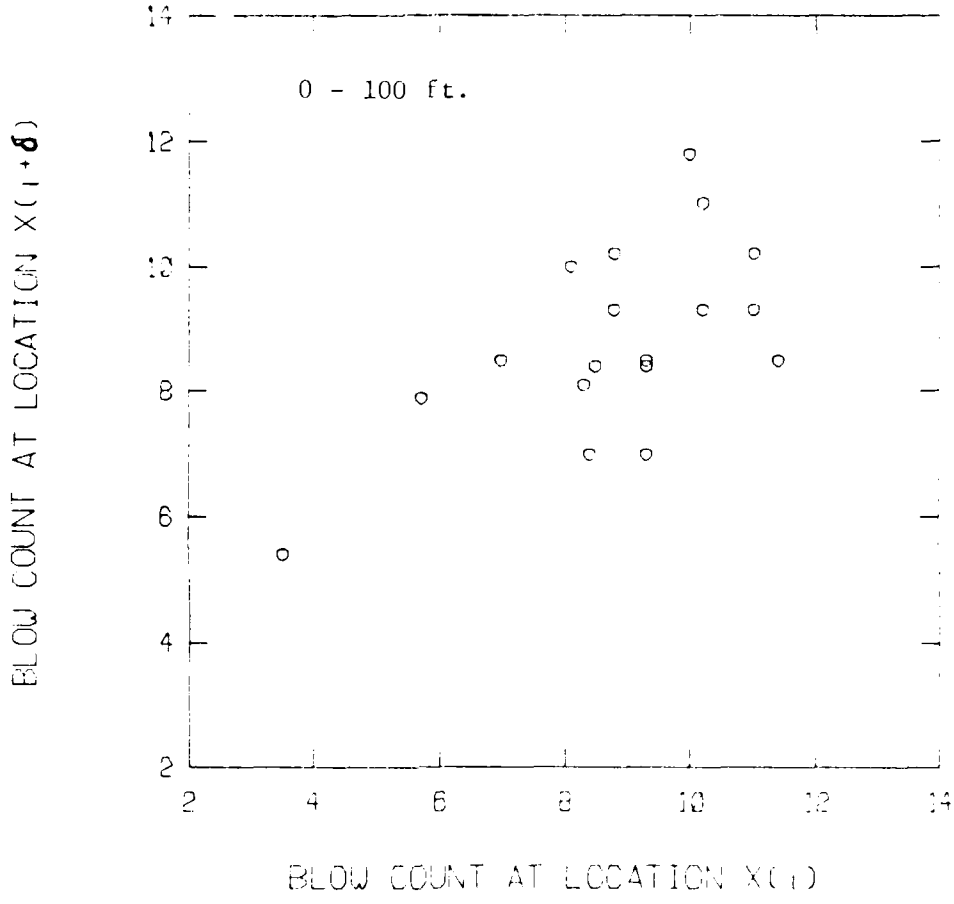

Figure 14a. Scatter Plot of Residuals At Close Spacings.

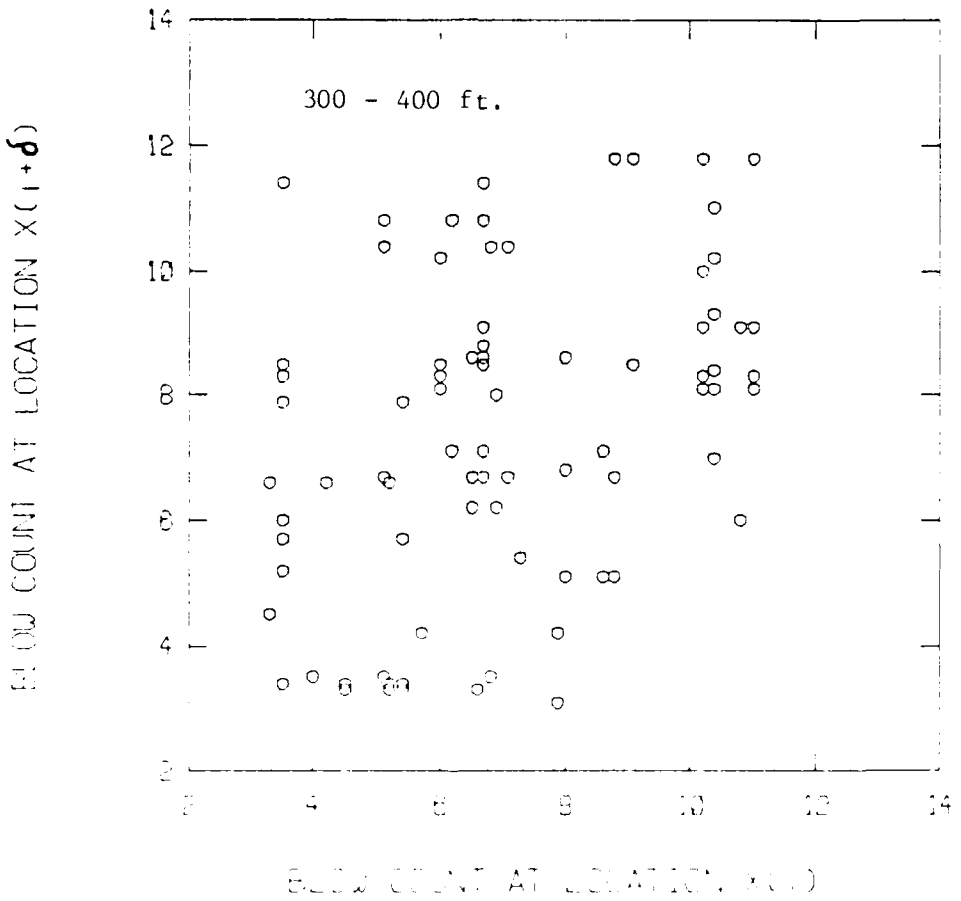

Figure 14b. Scatter Plot of Residuals At Medium Spacings.

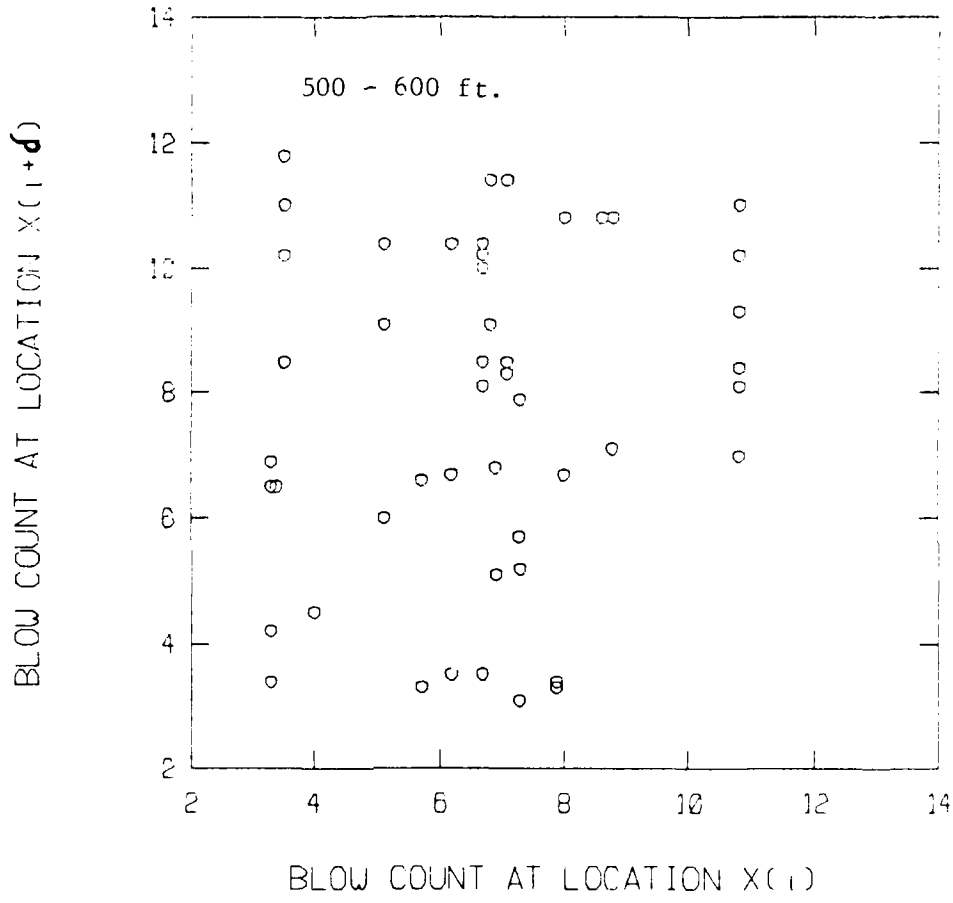

Figure 14c. Scatter Plot of Residuals At Far Spacings.

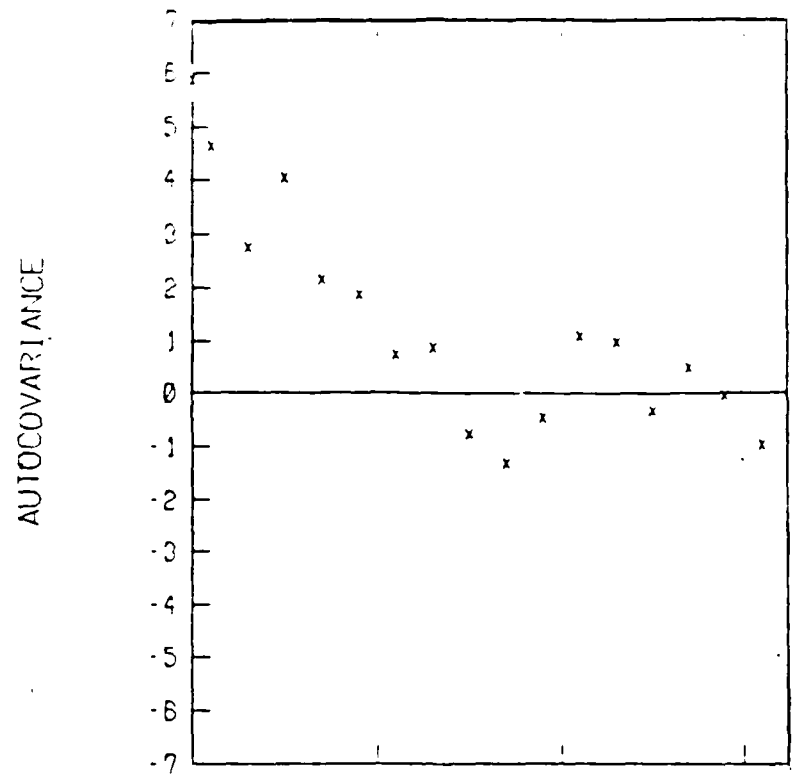

Figure 15. Autocorrelation Function of SPT Data in Figure 13.

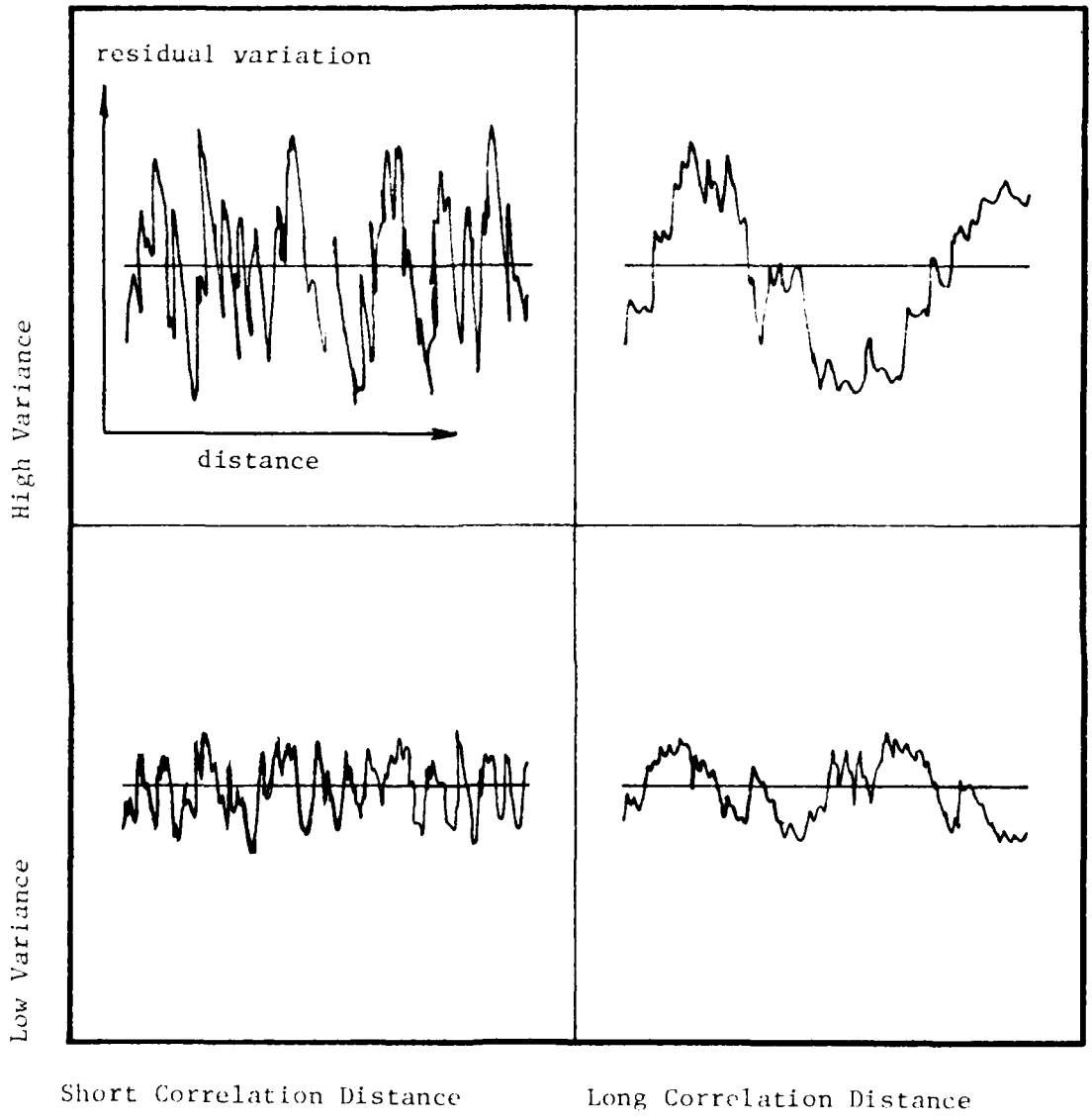

Figure 16. Effect of Variance and Correlation on Variability of Soils Data.

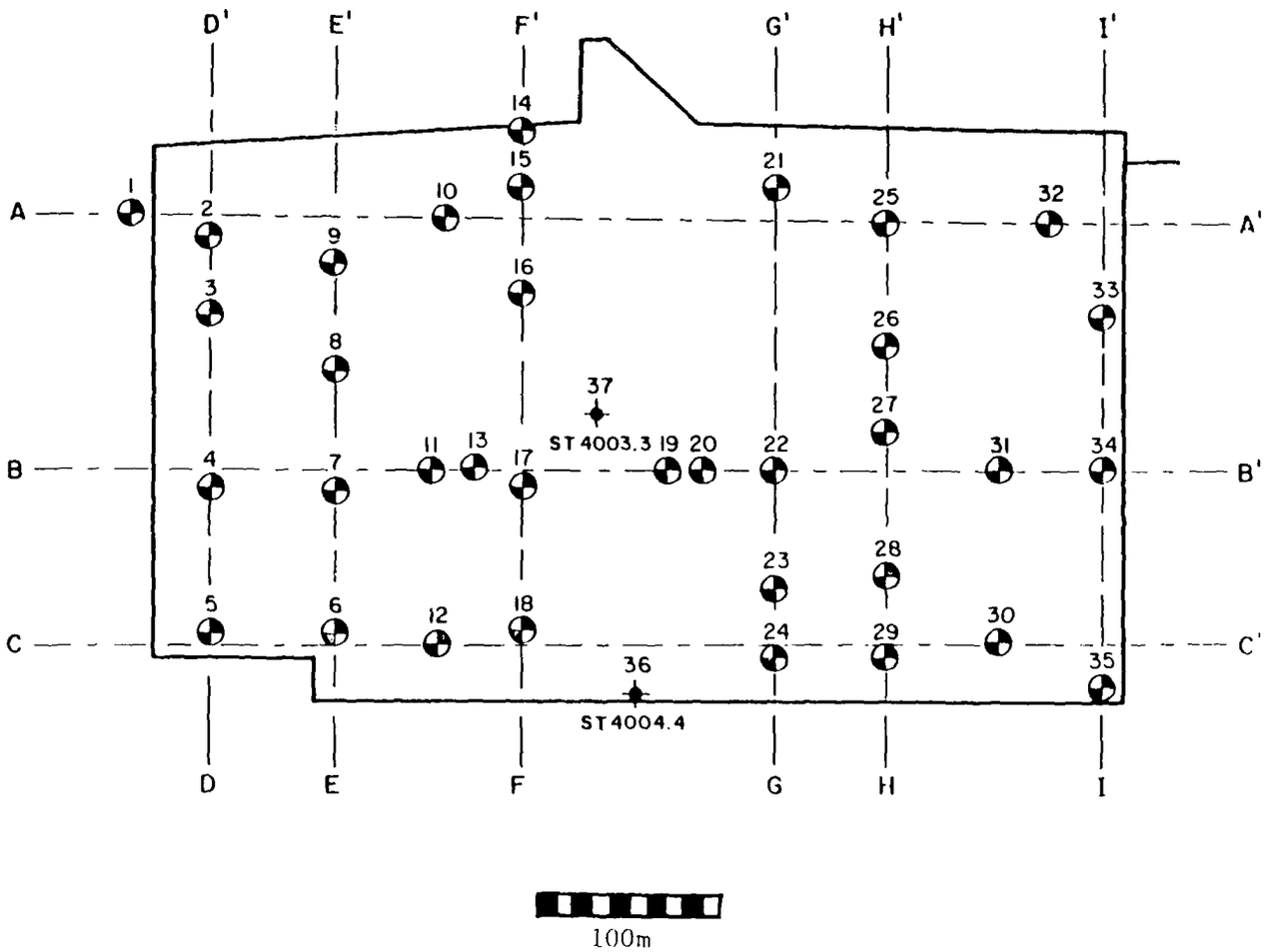

Figure 17. Site Plan for Hydraulic Bay Fill Data.

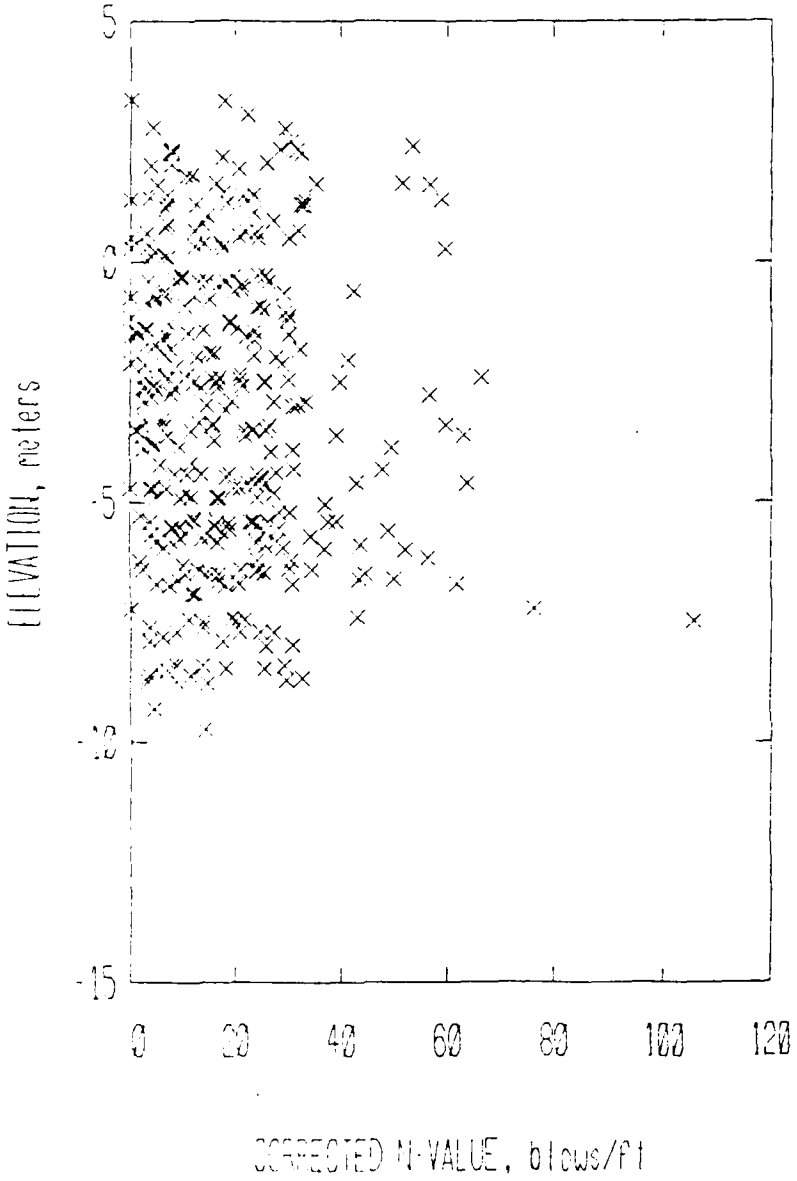

Figure 18. Scatter Plot of SPT Data.

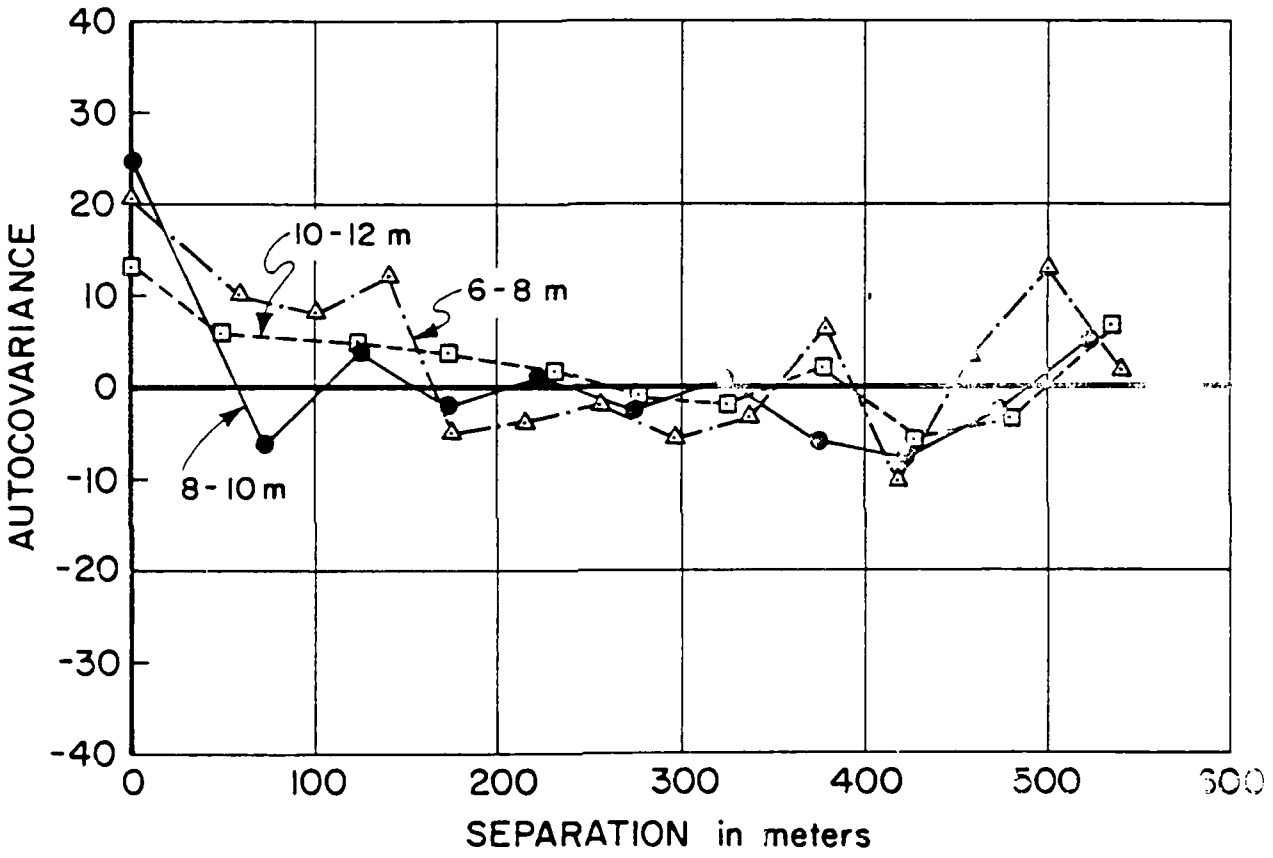

Figure 19. Horizontal Autocovariance Function of SPT Data in Figures 17 and 18.

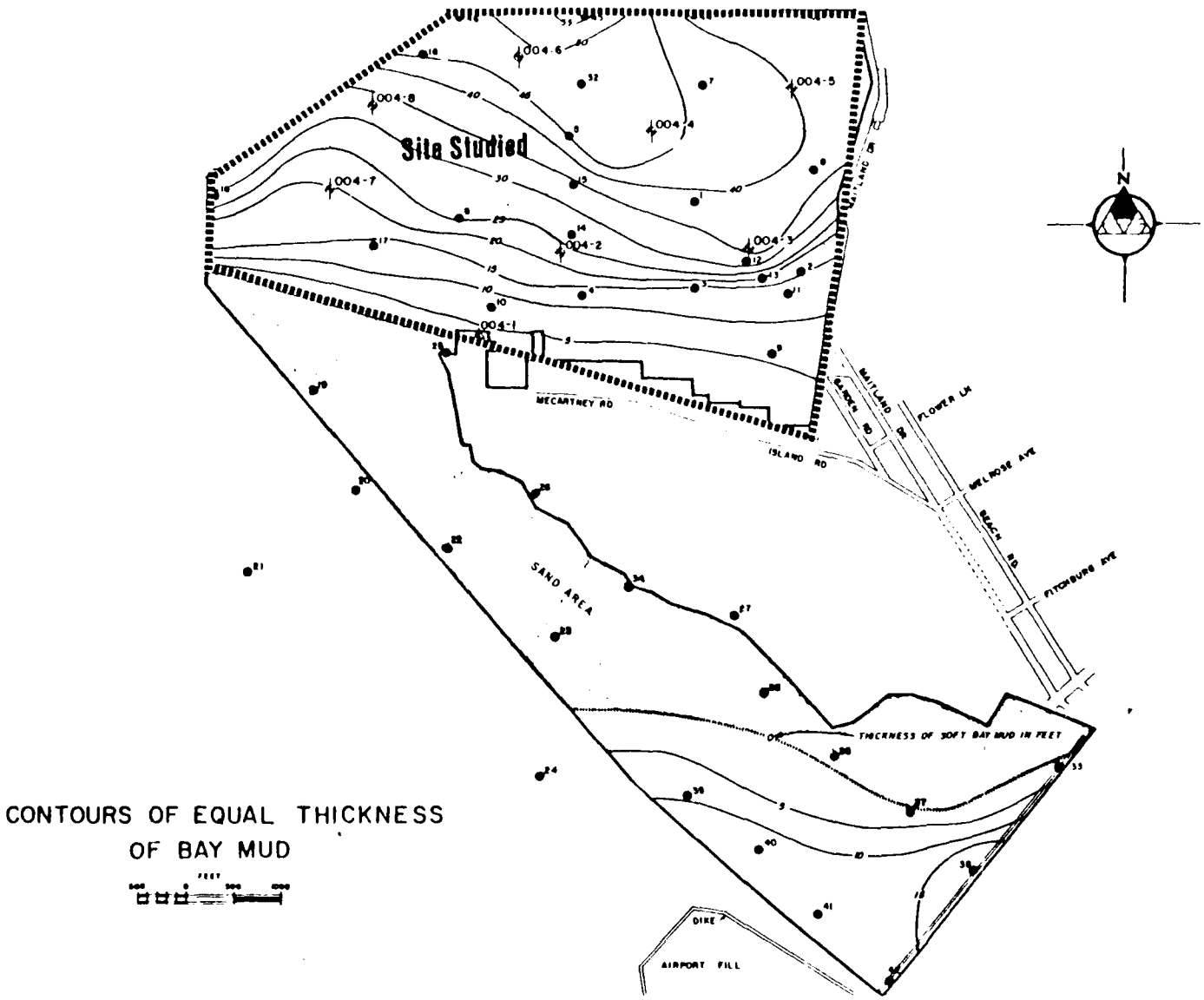

Figure 20. Study Area on SF Bay Mud Analyzed by Javette (1983).

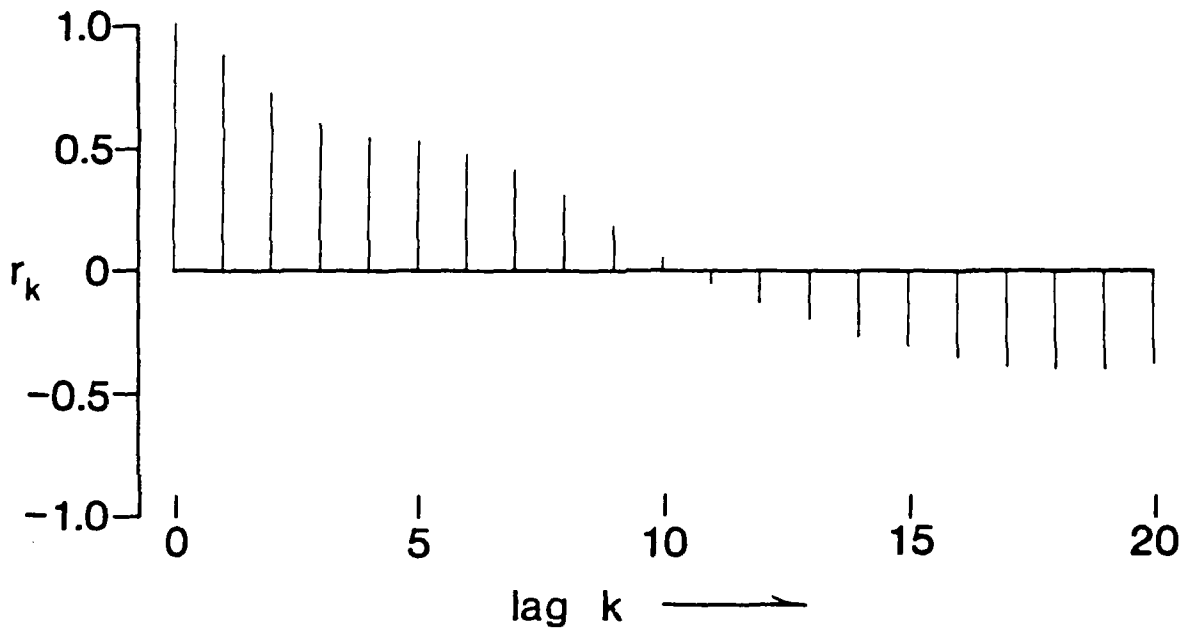

(Lag distance = 0.5")

Figure 21. Autocorrelation Function of Water Content Over Small Interval of San Francisco Bay Mud (after Javette, 1983). Javette uses the symbol r_k for autocorrelation, and expresses distance in lags (i.e., intervals) of 0.5 inch.

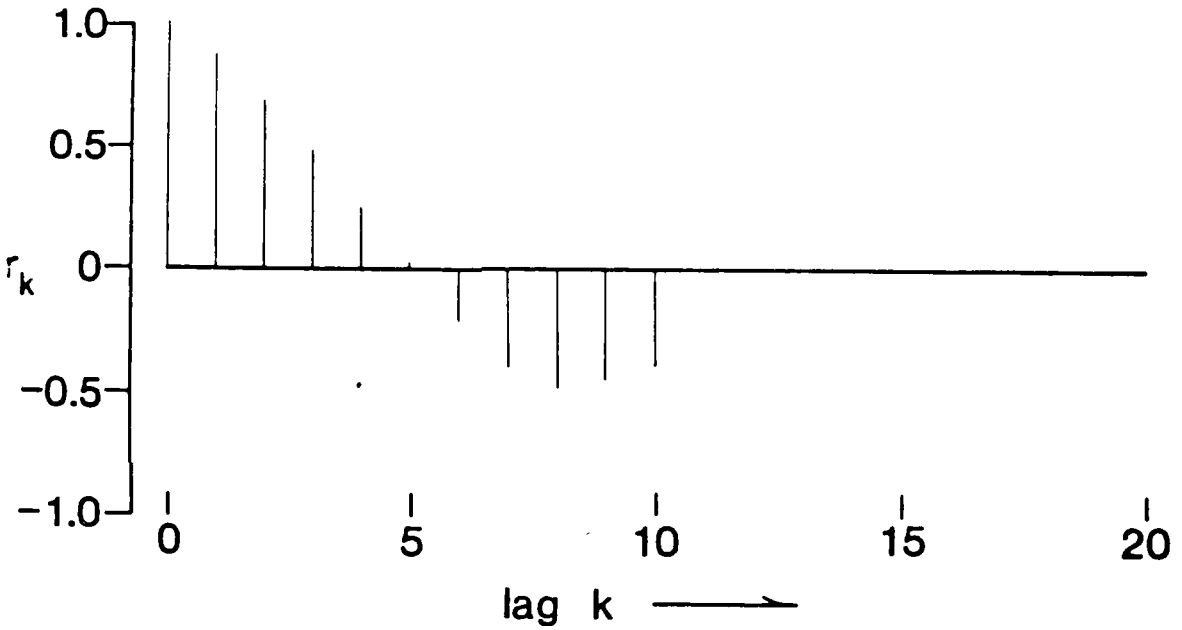

(Lag distance = 25')

Figure 22. Autocorrelation Function of Water Content Over Large Interval of San Francisco Bay Mud (after Javette, 1983). Javette uses the symbol r_k for autocorrelation, and expresses distance in "lags" (i.e., steps), here of 25 ft.

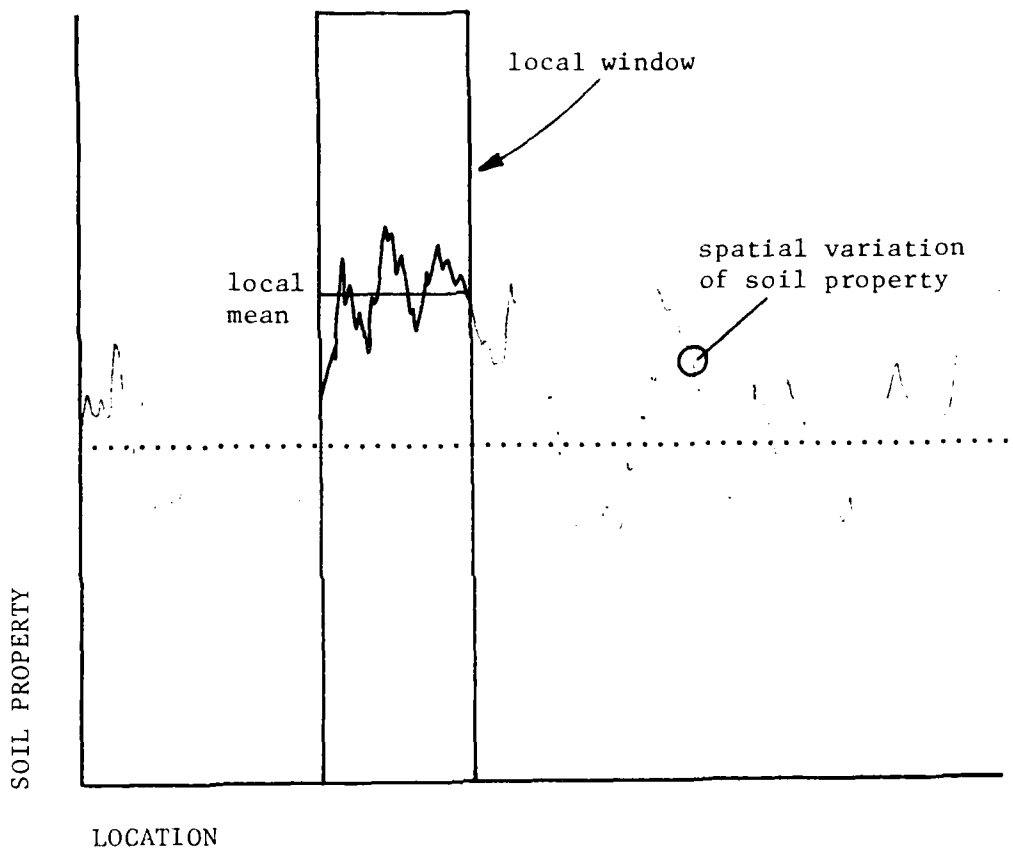

Figure 23. Effect of Scale on Autocorrelation Function.

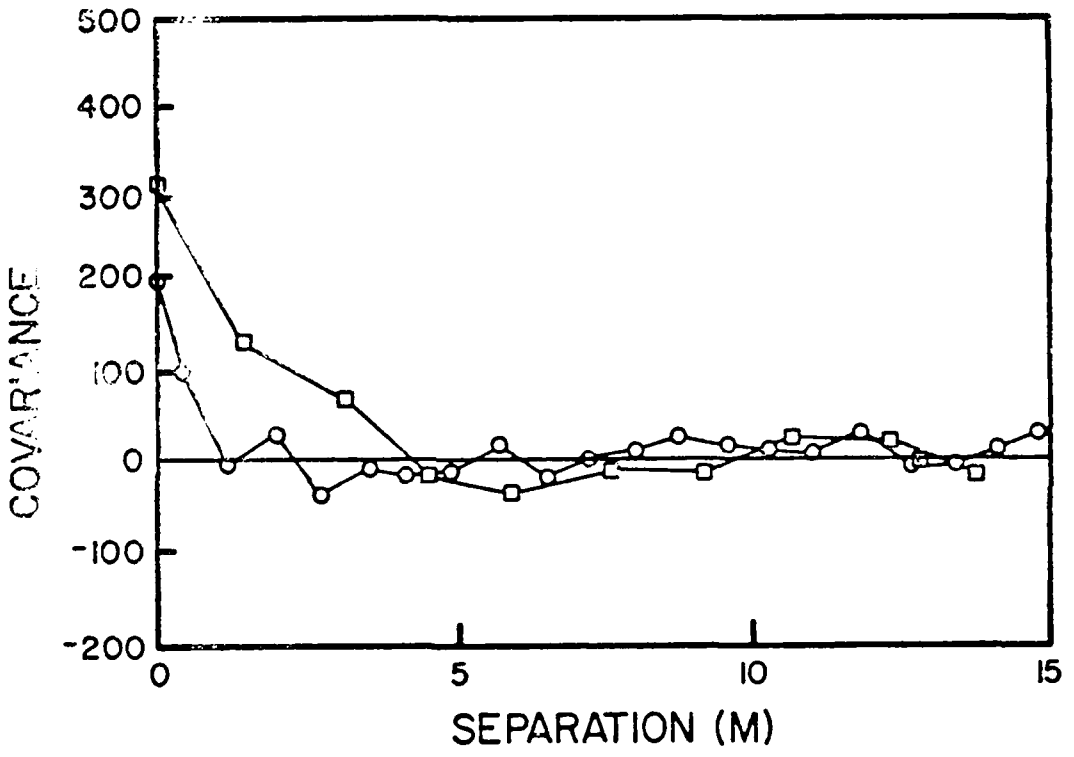

Figure 24. Autocorrelation Function of Rock Joint Density in A Copper Porphyry.

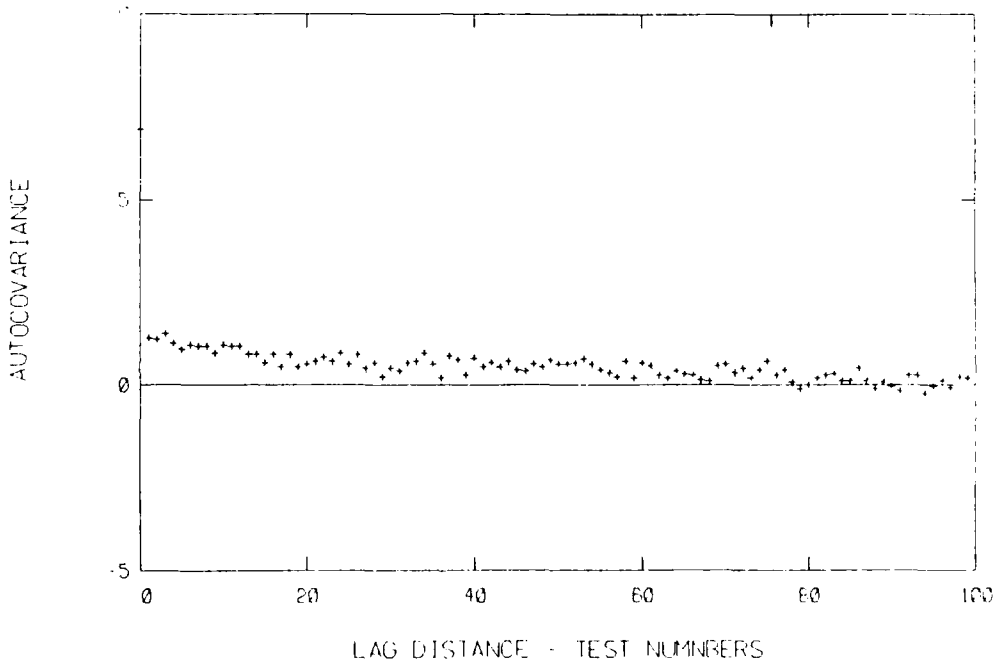

Figure 25. Autocorrelation Function of Compacted Water Content in Clay Core of an Embankment Dam.

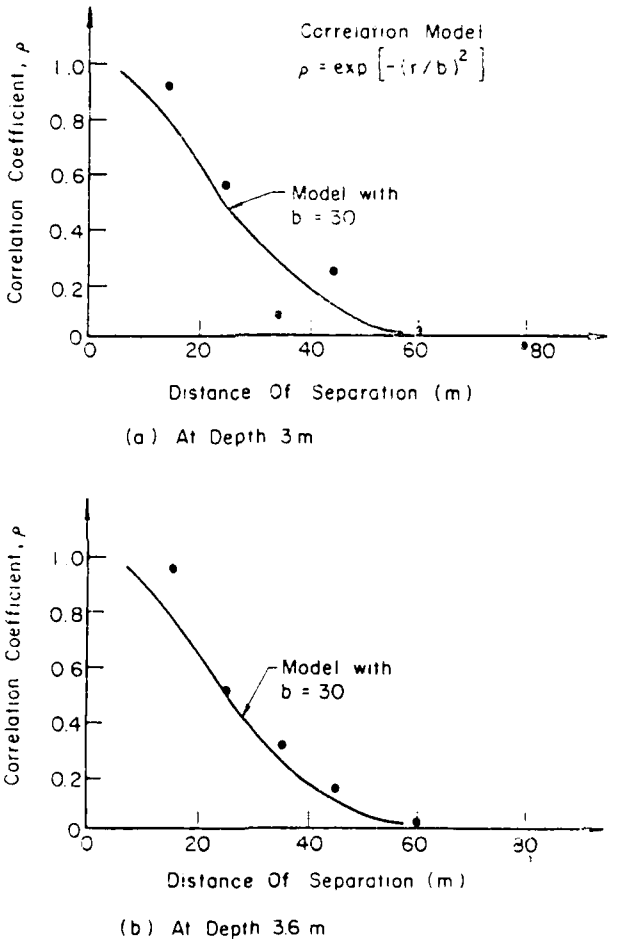

Figure 26. Autocorrelation Function of Cone Penetration Resistance in North Sea Clay (after Tang, 1979).

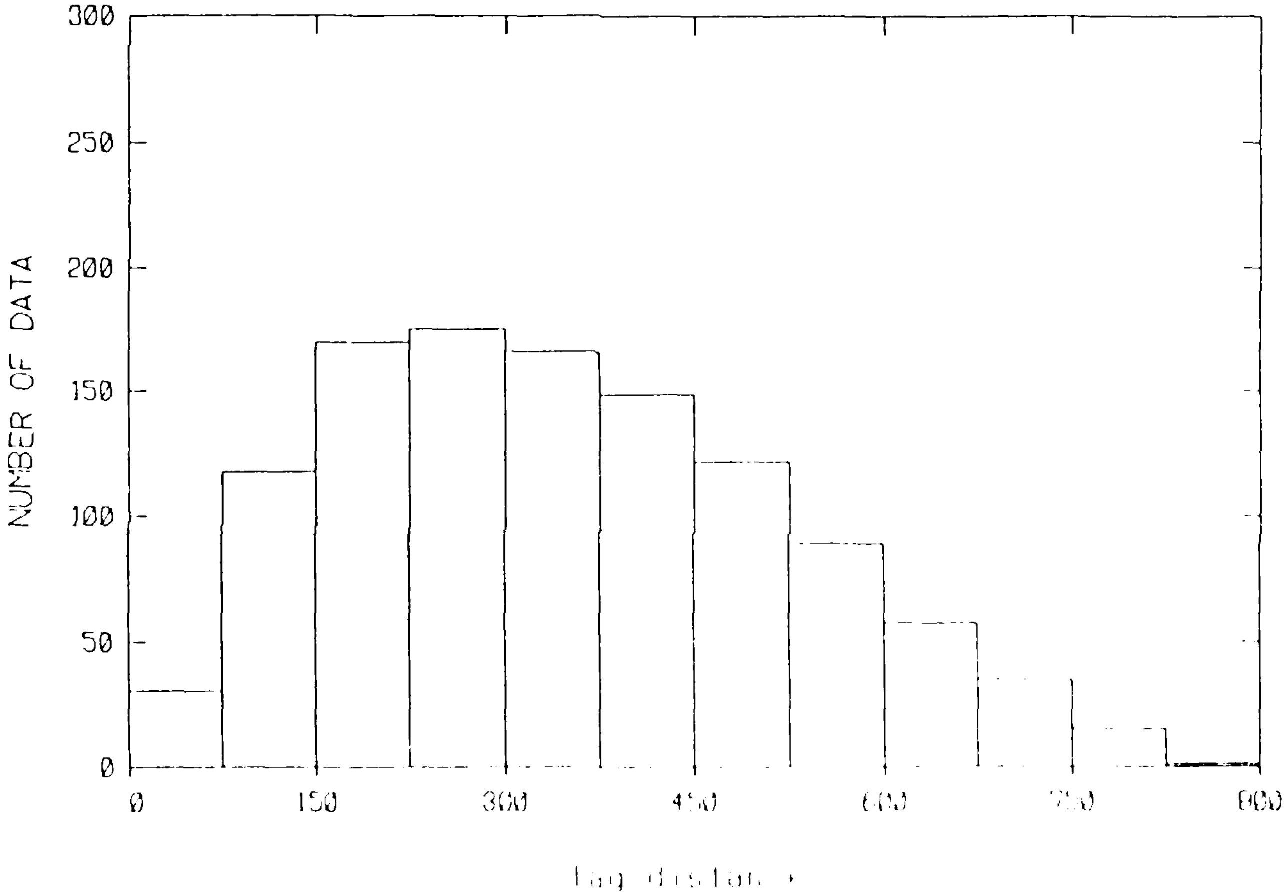

Figure [illegible] Estimation [illegible] for [illegible] Spaced Data: Data pairs are grouped according to separation (lag) distance as shown; covariances or correlations are averaged within each group [illegible] number of pairs [illegible] estimate [illegible] at midpoint of interval.

AD-A186 797 STATISTICAL ANALYSIS OF GEOTECHNICAL DATA(U) NEXUS 2/2
ASSOCIATES WAYLAND MA G BAECHER SEP 87 WES/CR/GL-87-1
DACW39-83-M-0067

UNCLASSIFIED F/G 13/2 NL

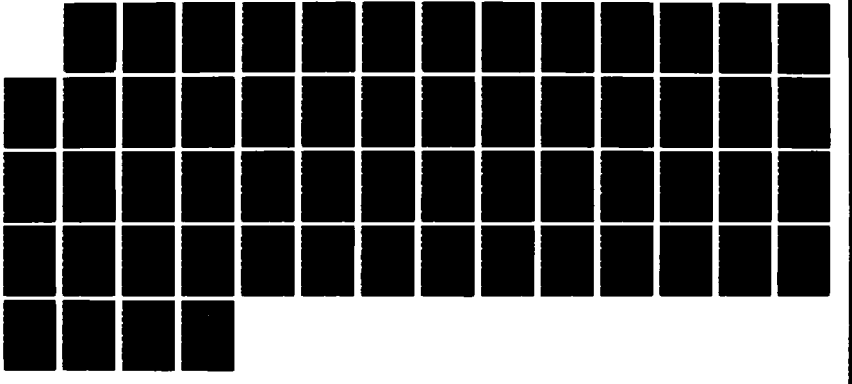

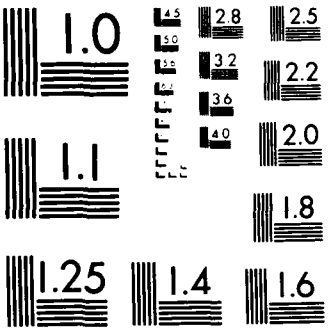

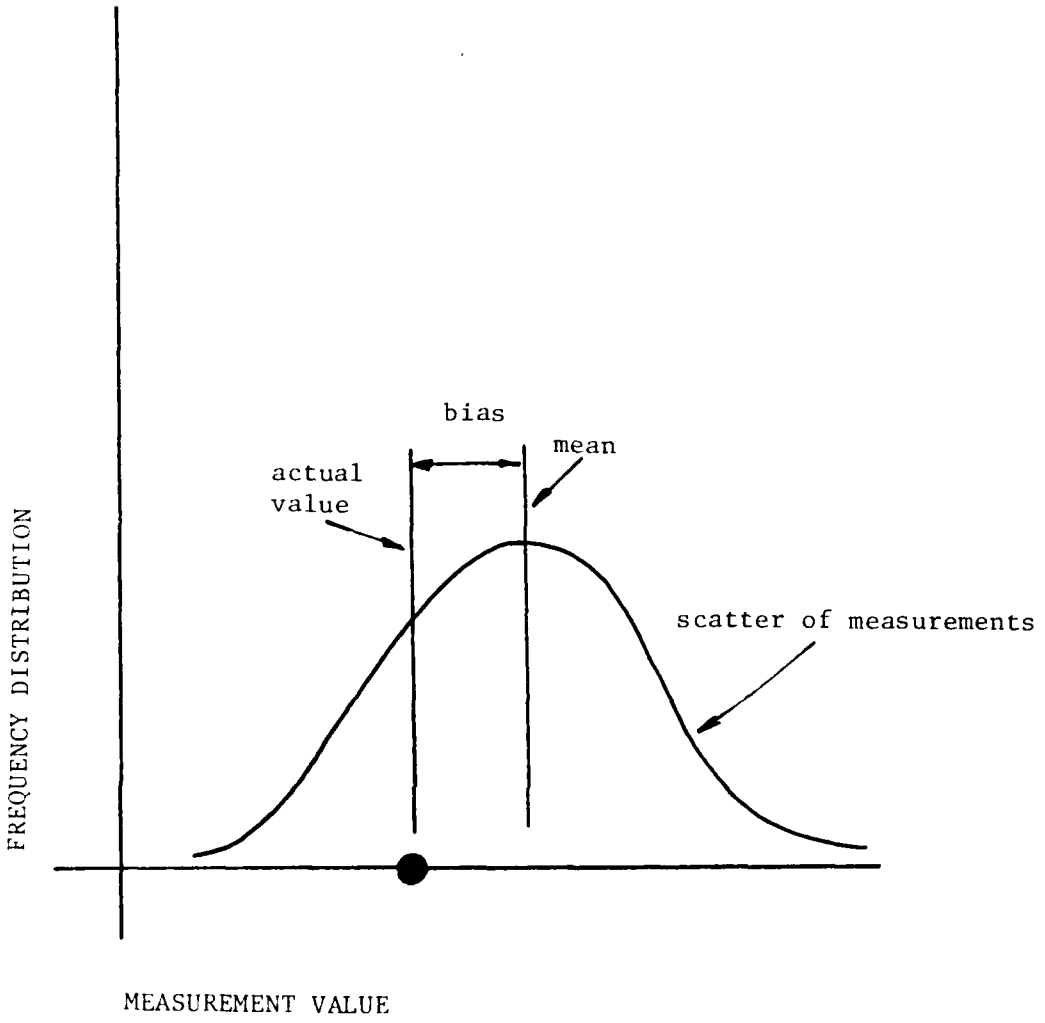

Figure 28. Schematic Representation of Measurement Error.

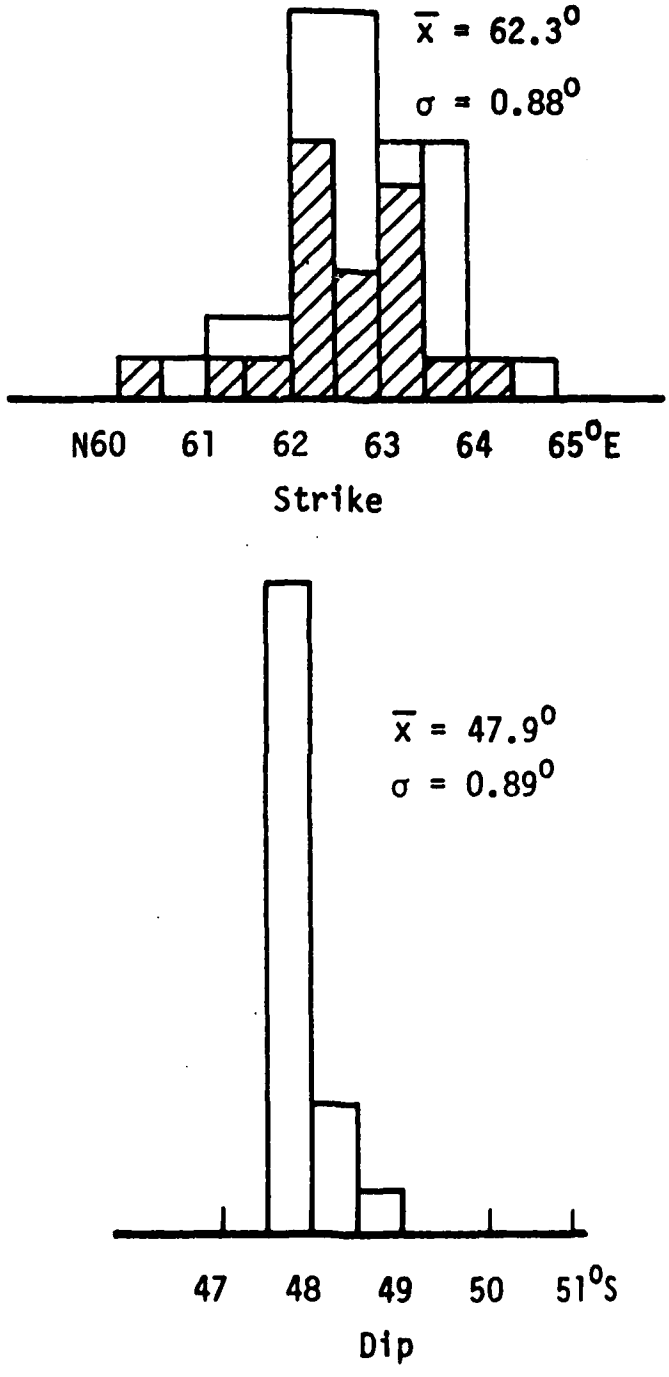

Figure 29. Histogram of Strike and Dip Measurements Made by Different Operators on the Same Rock Joint.

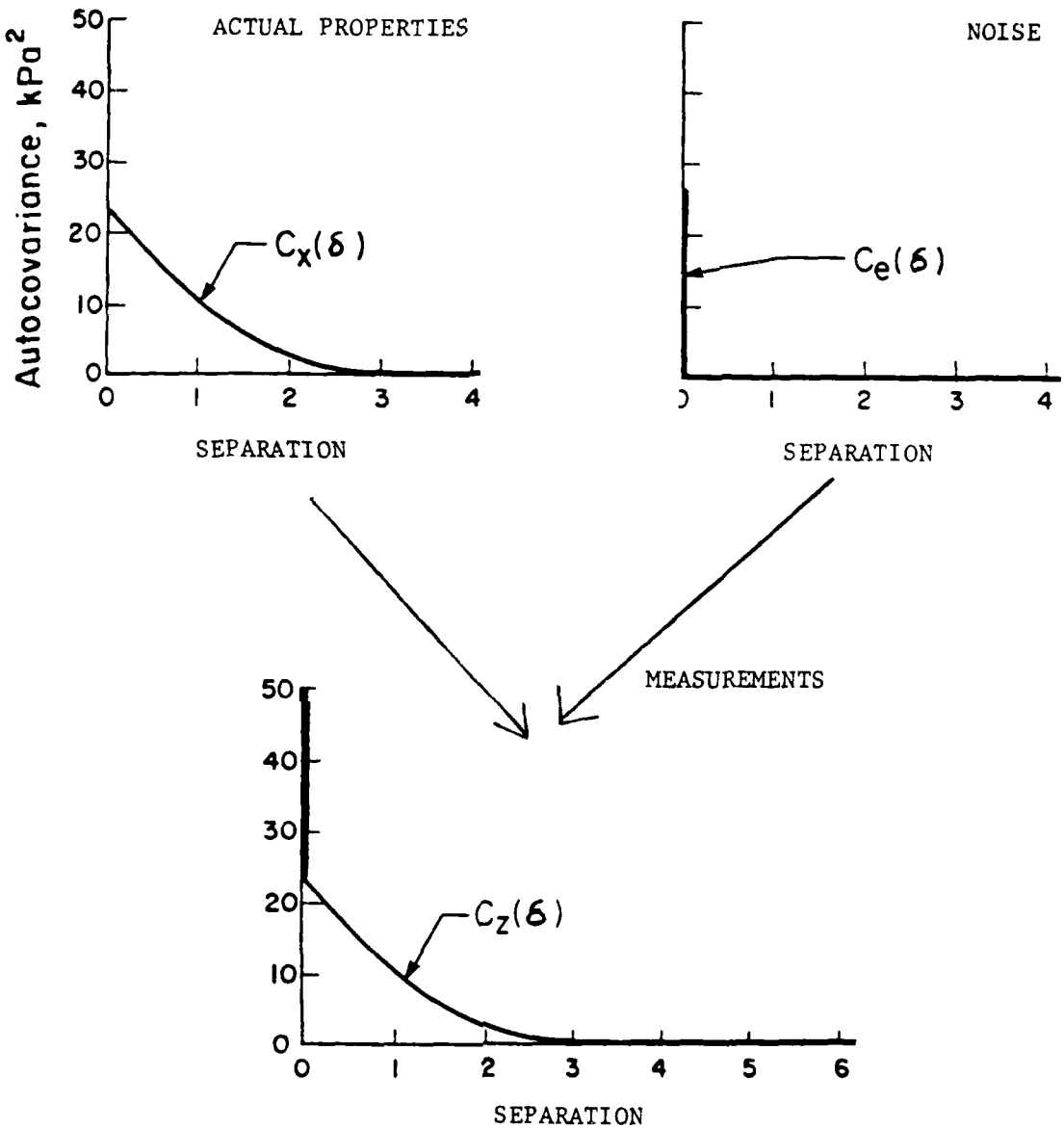

Figure 30. Autocovariance Function is Composed of Spatial Variability and Random Measurement Noise Signatures.

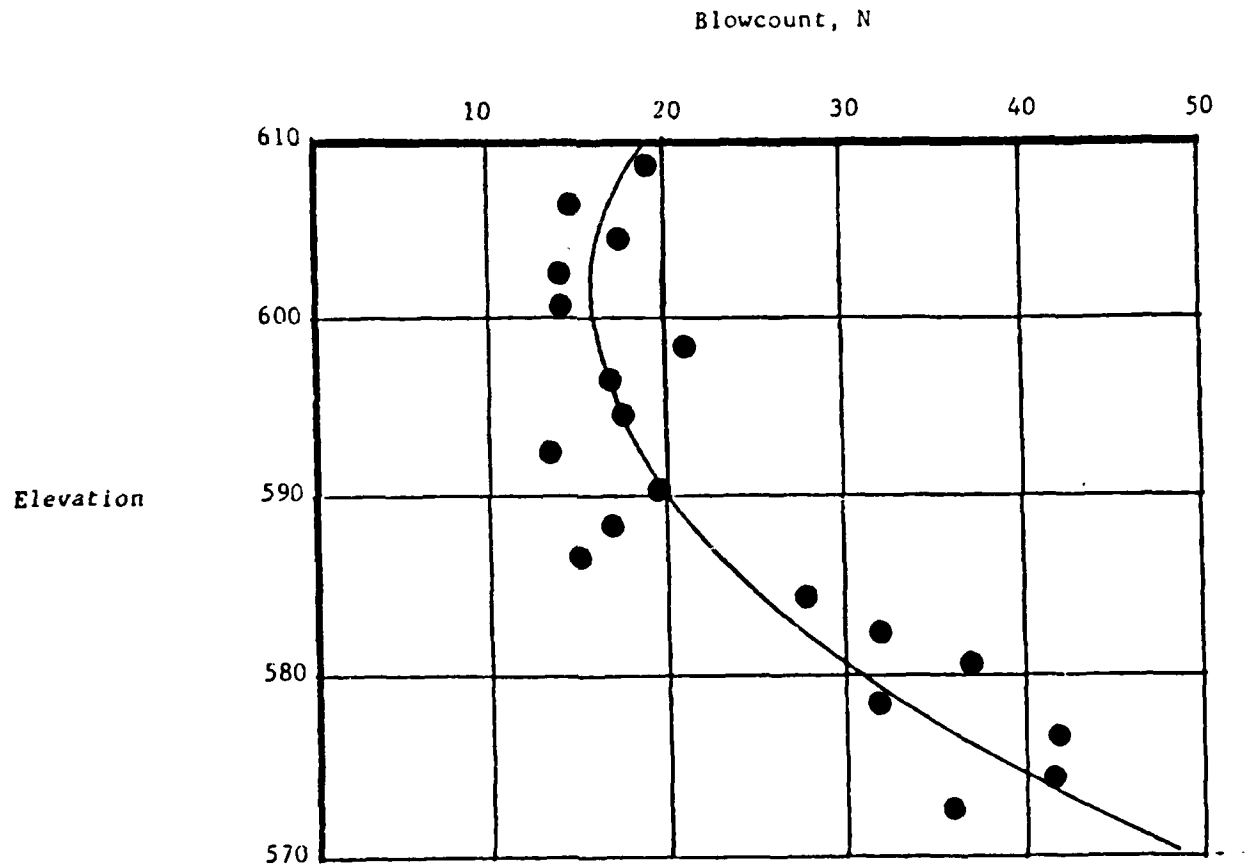

Figure 31a. SPT Blow Count Data in a Dune Sand (after Hilldale, 1971).

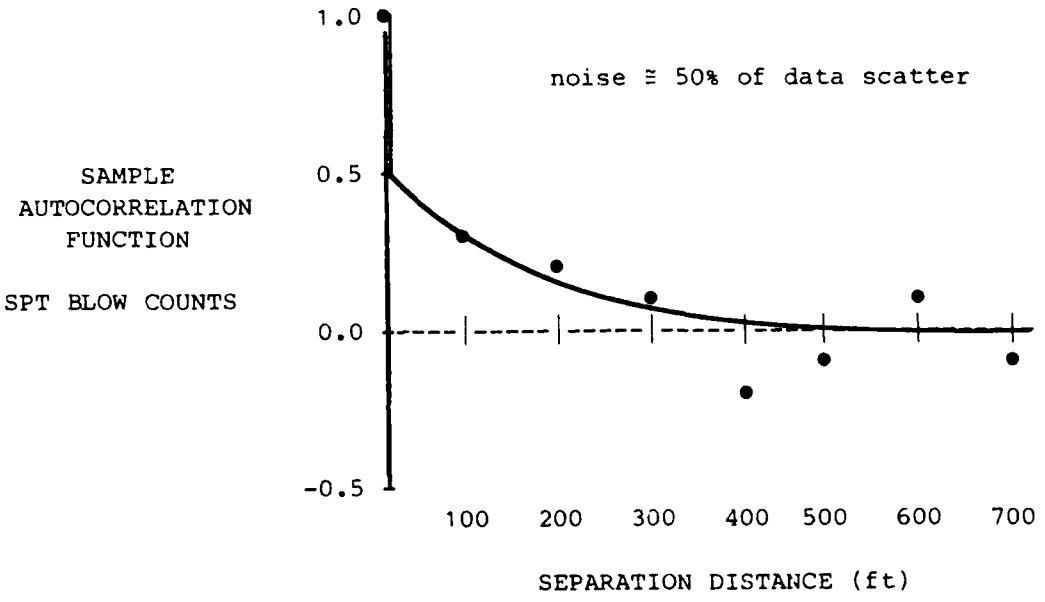

Figure 31b. Autocorrelation of SPT Data in Figure 31a.

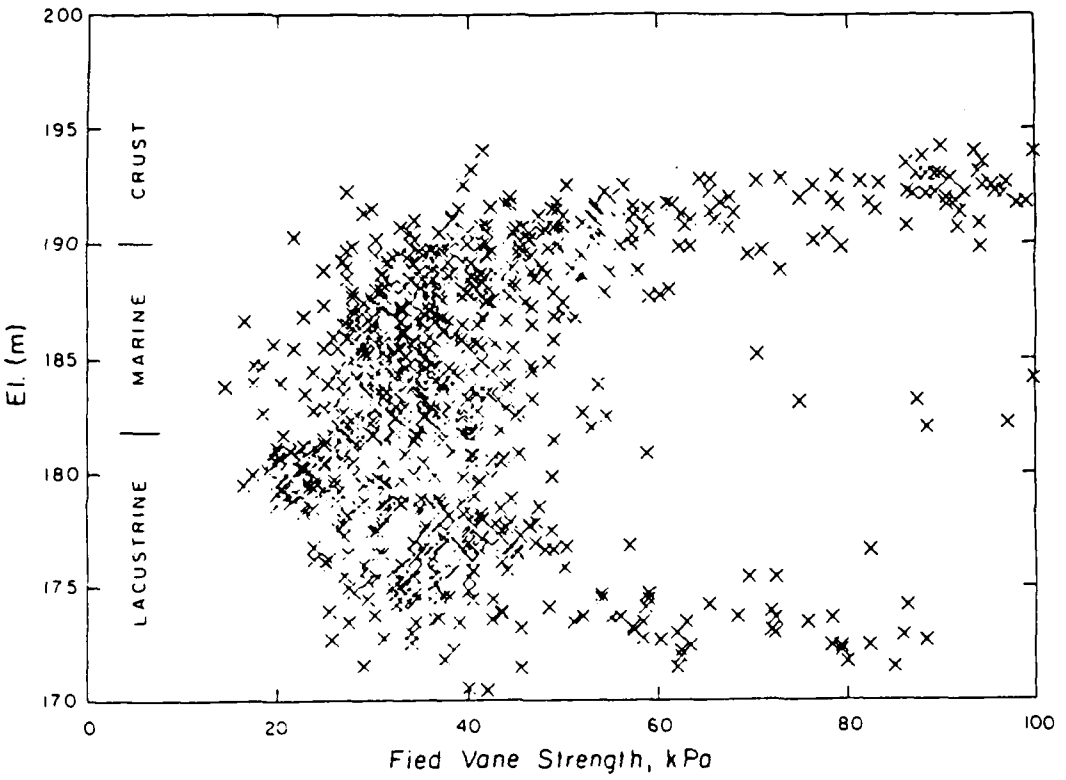

Figure 32. Field Vane Data in a Soft Marine Clay.

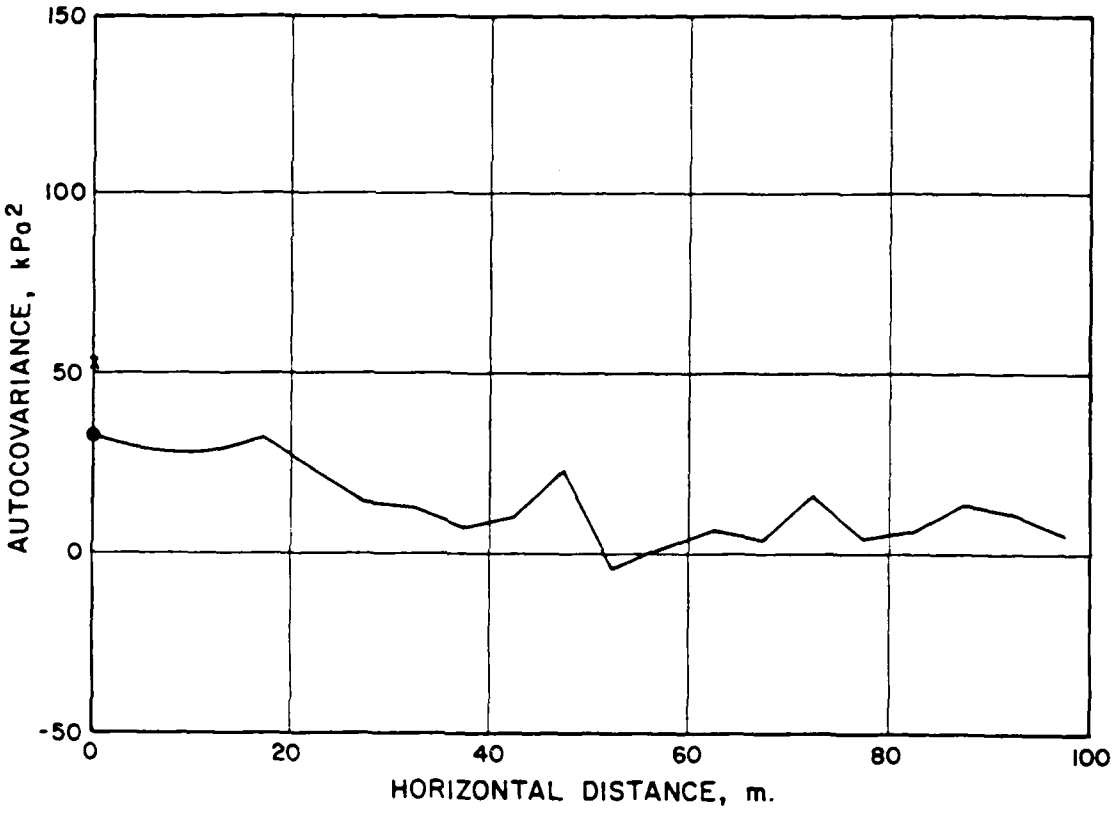

Figure 33a. Horizontal Autocovariance Function for the FV Data of Figure 32.

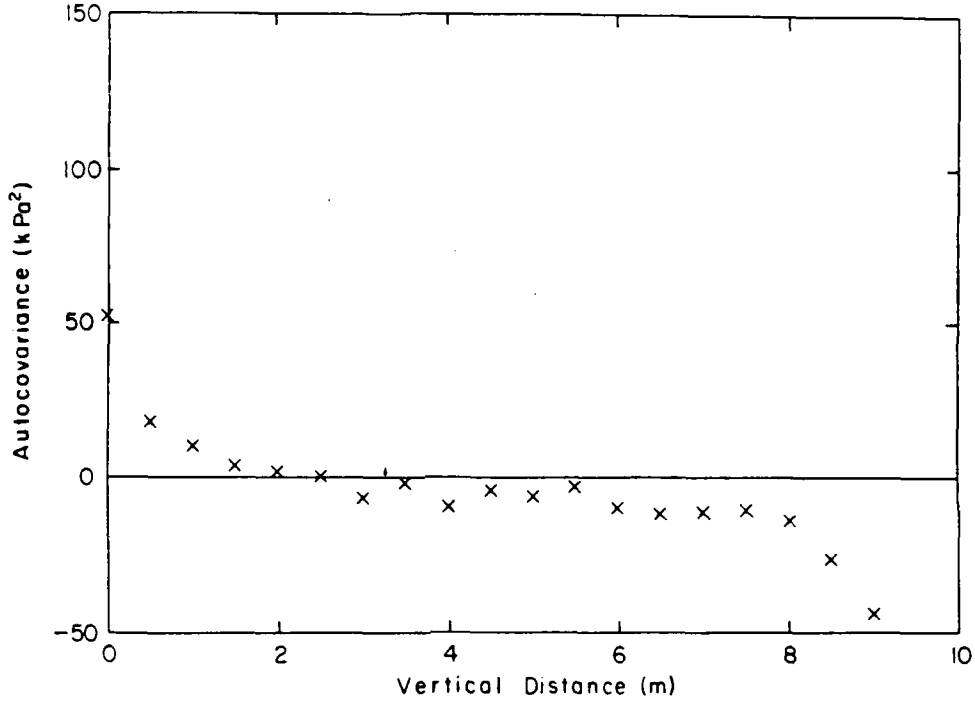

Figure 33b. Vertical Autocovariance Function for the FV Data of Figure 32.

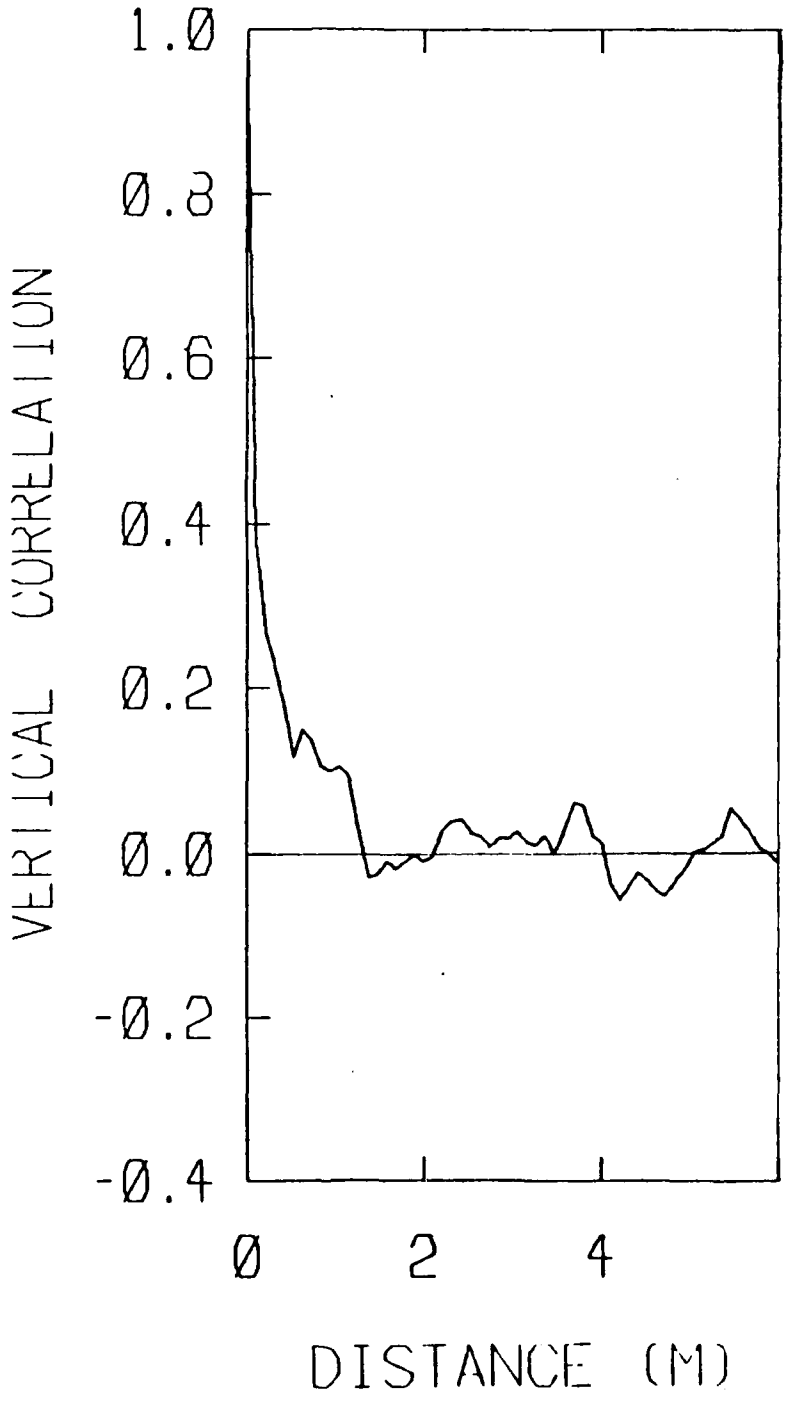

Figure 34. Vertical Autocovariance Function of Cone Penetration Data in a Copper Porphyry Tailings Deposit.

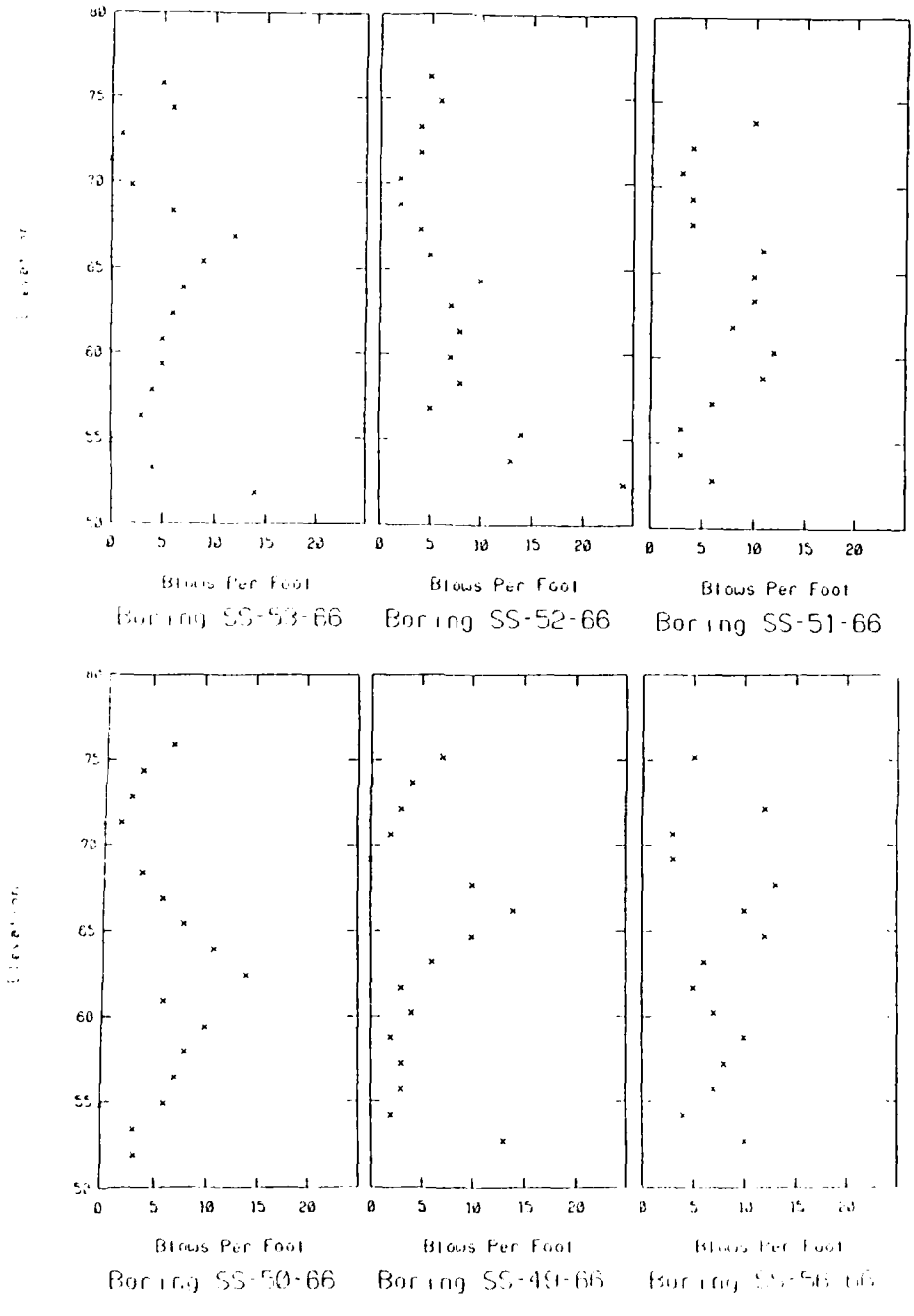

Figure 35. SPT Blow Count Data in a Silty Sand.

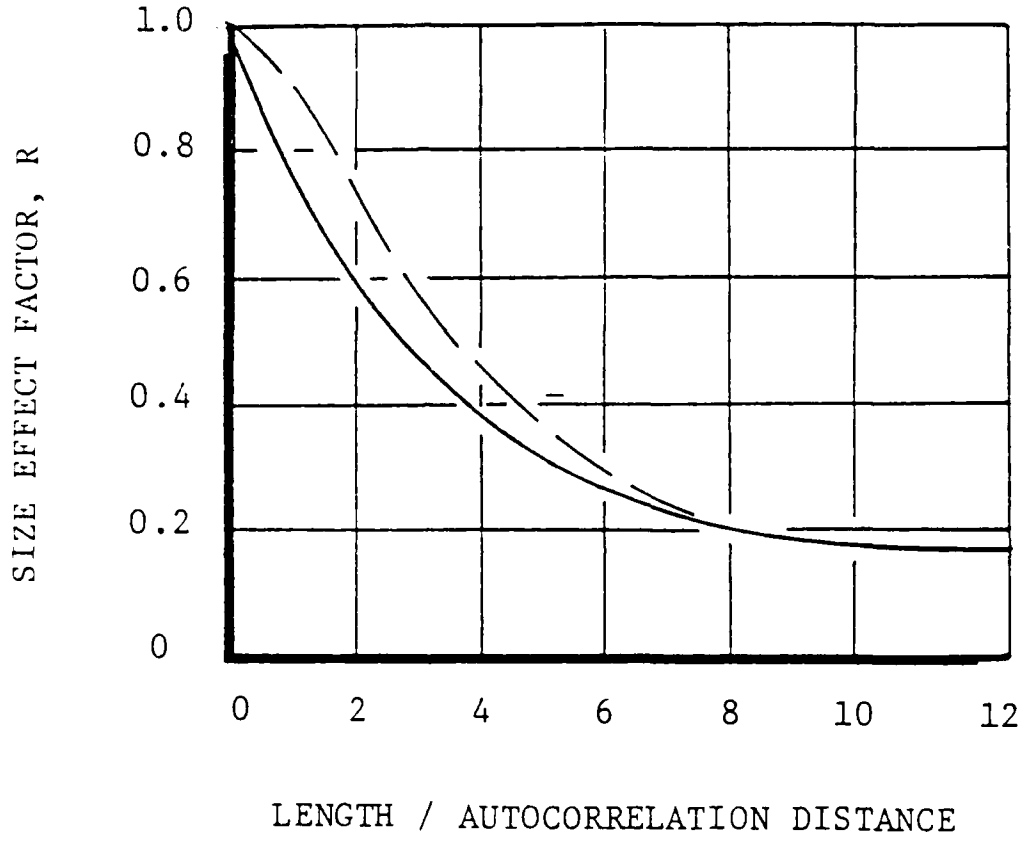

Figure 36. Size Effect Factor for Spatial Averaging Along A Line. Solid line shows R for exponential autocorrelation, dashed line for squared exponential.

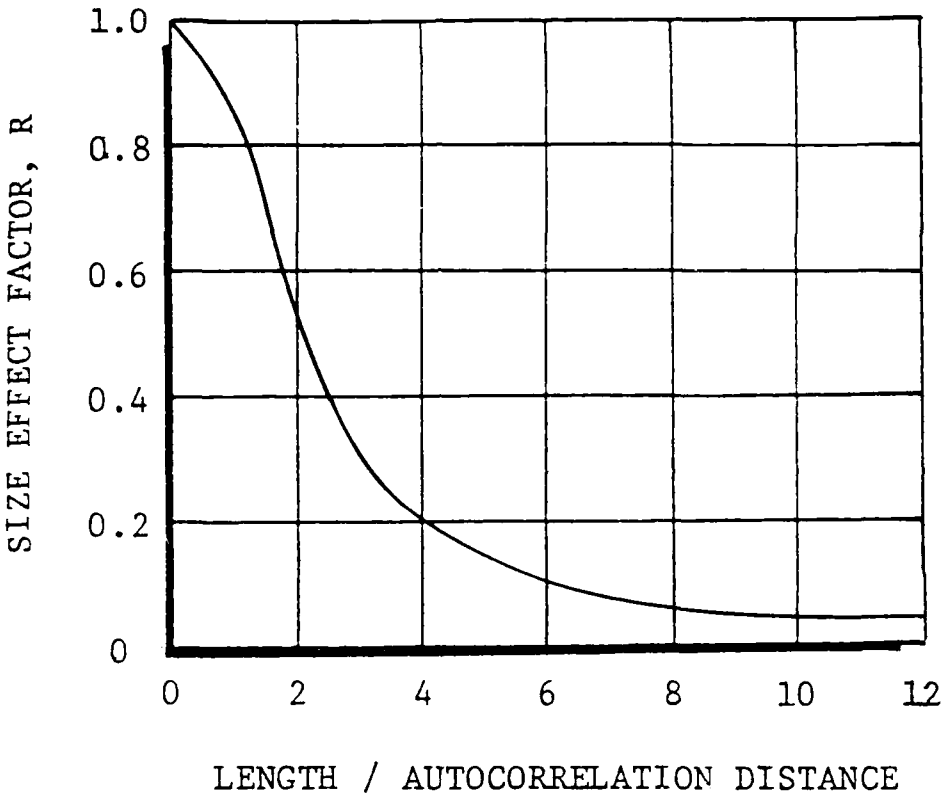

Figure 37. Size Effect Factor for Spatial Averaging Over a Plane. (squared exponential autocovariance function).

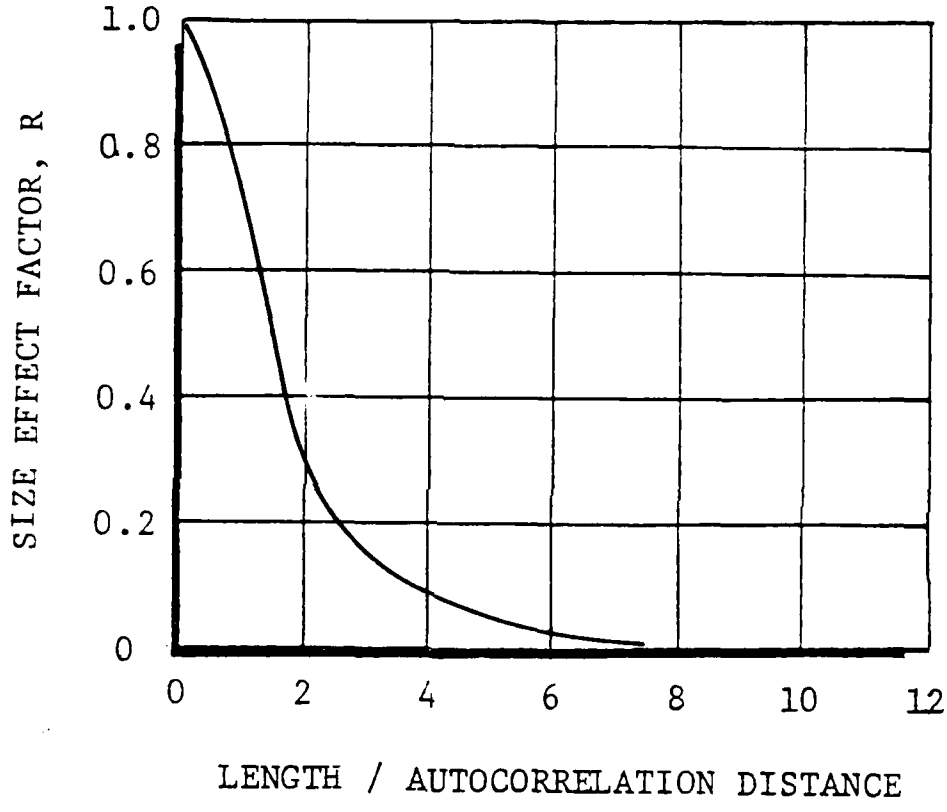

Figure 38. Size Effect Factor for Spatial Averaging Within A 3D Volume (squared exponential autocovariance function).

PART IV: SYSTEMATIC ERRORS

Thus far the analysis of uncertainties has concentrated on data scatter. It was seen that data scatter uncertainties manifest as variability across a site, for example, variability of settlement from one footing to another. Another type of uncertainty is also important: systematic error. Uncertainties due to systematic errors do not manifest as variability across the site, but appear as a difference between the predicted average performance and the average performance that occurs in the field. Systematic errors are biases. Usually they occur because errors are introduced in estimating mean values of soil properties, loads, or other input variables.

Sources and Importance of Systematic Error

The most important sources of systematic error in soil property estimates are measurement bias and statistical error. Measurement bias is caused by inadequacies in the way soil test results are obtained or interpreted. For example, the stress system imposed on a soil specimen during testing often differs from that encountered in a prototype situation. To the extent that strengths or other properties are affected by this difference in stress system, values calculated from test results will be inappropriate for predictions of prototype performance.

Statistical errors are due to limited numbers of tests. Because no two test results are ever the same, variations from one set of results to another cause variations from one sample mean or sample standard deviation to another. These variations go down as the number of measurements in a sample goes up, but they are always present. A sample statistic such as the mean or standard deviation always varies somewhat from the corresponding actual value across a soil deposit.

The importance of drawing a distinction between data scatter uncertainties and systematic errors is that the two affect predictions in different ways. For example, spatial variation affects the fraction of a large project, e.g., a long embankment, that might perform adversely. If spatial variation indicates a 10% likelihood of adverse performance, this means that problems should be expected with 10% of the embankment. On the other hand, systematic error affects the likelihood that the entire project performs adversely. If systematic error indicates a 10% likelihood of adverse performance this means that problems with the whole embankment should be expected in one out of 10 projects. The distinction between data scatter and systematic error is important.

A second difference between spatial variation and systematic error lies in the way they are affected by scale. If a very large volume of soil is considered the uncertainty in average soil conditions may not be greatly affected by spatial variation. Above average elements of soil balance against below average elements. This averaging does not affect systematic errors. They are the same everywhere.

It is often convenient to think of spatial variation as the uncertainty in soil properties caused by variations from spot to spot in a soil deposit. Systematic errors are uncertainties about the value of the mean or trend in soil properties.

Measurement and Model Bias

In testing soils, whether in the field or laboratory, a system of boundary conditions is applied to a specimen and response is measured. From this response and a set of physical assumptions (i.e., a model), soil

properties are calculated. These properties are used with another model to predict performance. Non-random errors are introduced to this process at several points, and it is these which give rise to measurement bias. These non-random errors have systematic and variable parts. The systematic part is said to be a measurement bias. The zero-mean variable part is lumped with measurement noise and therefore can be treated as a random error. As a result, bias does not appear in the data scatter, it is a purely systematic error. Fig. 28 illustrates the distinction between systematic and random errors in measurements.

Causes of Measurement and Model Bias

Among the more common measurement errors in soil properties are (a) inappropriate boundary conditions, (b) inappropriate model assumptions, and (c) sample disturbance. In most cases there is little reason to separate measurement bias from model uncertainty. First, measurements and models are often inseparable, and second, the best way to assess measurement bias is to backcalculate 'correct' parameters by modeling observed failures--thereby combining the effects of errors of measurement and errors of modeling.

Assessing Magnitude of Bias

The direct way to establish measurement bias is by comparing predicted and observed performance. For field vane strengths Bjerrum (1972) compared observed slope performance with predictions based on modified Bishop analysis and backcalculated the correction factor,

$$= \frac{c_u \text{ for } F=1 \text{ at failure}}{c_u \text{ measured with FV}} \qquad (53)$$

in which c_u = undrained strength and F = factor of safety. The correction factor reconciles observed failures with predictions (Fig. 39). This bias factor combines measurement technique and prediction model and is no longer appropriate if a stability model based on other assumptions is used (e.g., a 3D model).

Introducing a measurement/model bias B into Eqn. 38 leads to the statistical model,

$$z = B\,x + e \,, \tag{54}$$

and the summation of variances,

$$V_z \doteq m_B\ V_x + m_x\ V_B + V_e \quad , \tag{55}$$

in which V_B is the uncertainty in the value of the bias correction B, and all parameters are valued at their means. In the special case where field vane measurements were used as input to modified Bishop analysis, B=(1/).

Statistical Error

Sampling Variations

Because a limited number of measurements are made at any depth, about 40 in Fig. 32, their average may be above or below the actual spatial average even if there were no measurement bias. If another set of 40 borings had been made at slightly different locations, the exact test results would have been slightly different from those obtained here, and a slightly different estimate of the average, standard deviation, and other parameters would have resulted. Thus, the average vane strength at any depth as shown in Fig. 40 probably

differs somewhat from the (actual) spatial average that would be obtained from a very large number of measurements. That is, the estimate of the average is somewhat in error. To the extent the estimate is in error, this error is the same everywhere along the axis. It is a systematic error.

Statistical theory allows an assessment to be made of the probable magnitude of error that results from limited numbers of observations. One never knows, before hand, the exact magnitude or direction of this statistical error, but the likely range of magnitudes can be calculated. Typically, statistical error is expressed as a variance or standard deviation on the estimated parameter. For example, the statistical error on the estimate of the average field vane strength at any depth in Fig. 40 would be expressed as a variance on the estimated average, $V_{m_{FV}}$, in which m_{FV} is the estimate of the mean FV strength. The corresponding standard deviation of the estimate is said to be the standard error.

The larger the number of measurements at any depth, the lower one might expect the statistical error to be. In general, the variance of the statistical error decreases approximately in proportion to the reciprocal of the number of observations, n. Doubling the number of tests, therefore, reduces the standard error of a parameter such as the mean or standard deviation by about 1/ 2. The benefit of increased testing displays marginally diminishing returns.

Error in the Mean

From Eqn. 16, the variance of the statistical error of the mean of a population is approximately,

$$V_{m_x} = \frac{V_x}{n} \quad . \tag{56}$$

If repeated samples of n tests from the same soil deposit are made, if each of the tests is statistically independent of all others, and if for each sample the mean is calculated, then the variability of those means would have variance V_x/n.

Settlement of footings on cohesionless soils is often estimated to depend inversely on the average SPT blow count immediately beneath the footing as, for example, through an equation of the form of Eqn. 41. If only one SPT test is taken beneath the footing, the variance of the average N from one footing to another is, obviously, V_N. If more than one test is made and the results averaged, then the variance among the averages decreases, as can be seen in Fig. 41. As the number of tests n increases, this variance reduces as 1/n.

This sampling variance of the estimate of the mean is not the uncertainty of the estimate directly, but the variation one might expect to see in repeated sampling from the same deposit. Nevertheless, under fairly general conditions this variance is close or identical to the so-called 'Bayesian' variance of the parameter which expresses the uncertainty directly.*

Eqn. 56 refers to the case in which measurements are statistically independent of one another. When the measurements are not independent, Eqn. 56

* More precisely, the posterior variance on m_x in a Bayesian sense is V_x/n, if the prior distribution on m_x is uniform and V_x is known. If V_x is unknown and the prior distribution on (m_x, s_x) is noninformative ($1/s_x$), then the marginal posterior variance on m_x is somewhat larger.

must be modified. The most common case in which measurements are dependent occurs when the spacings among the measurements are small, so that auto-correlation comes into effect. From Eqn. 15, the variance of m_x accounting for dependence among the measurement x_i is

$$V_{m_x} = \frac{1}{n^2} \quad C_{x_i,x_j} \tag{57}$$

in which $C_{xi,xj}$ = covariance between the measurements x_i and x_j. The individual covariances can be estimated from the autocovariance function evaluated at the appropriate separation distance. For computer applications a more convenient matrix version of Eqn. 57 is

$$V_{m_x} \quad \frac{1}{n} \; t\underline{C}_x \; \frac{1}{n} \tag{58}$$

in which $1/n$ is a vector of dimension n, each element of which is 1/n, and $\underline{C}_x$ is the covariance matrix of the observations. The ij^{th} element of $\underline{C}_x$ is $C_{xi,xj}$. If the measurements are widely spaced, Eqn. 58 reduces to Eqn. 56. In fact, in most practical applications Eqn. 56 is used unless the measurements are made very close together in space.

Error in the Standard Deviation

The variance of a soil property is usually estimated by the sample variance,

$$s_x = \frac{1}{n-1} \quad (x_i - m_x) \tag{59}$$

This is an unbiased estimate of V_x the soil property variance, and has sampling variability characterized by,

$$V_{s_x} \quad \frac{2\ V_x}{n-1} \tag{60}$$

Eqn. 60 is exact when the data are Normally distributed, but only approximate otherwise. The uncertainty in the standard deviation of x is characterized approximately by the standard deviation.

$$s_{s_x} \quad S_x / \sqrt{2n} \ . \tag{61}$$

Again, Eqn. 61 is exact for Normally distributed x_i, but only approximate otherwise. More detail is provided by Duncan (1974). For most purposes the uncertainty in s_x can be ignored in developing a design profile. For example, the sample variance of the data of Fig. 32 is about (10kPa) with a sample size of n=40 at any elevation. Thus, the standard deviation of s_x from these data is approximately 1.1 kPa.

Error in Regression Coefficients

The estimates of slope and intercept coefficients in regression analysis are mathematically defined functions of the measurements from which they are inferred (i.e., $\underline{x} = x_i, \ldots, x_n$), and thus the statistical error in these estimates can be calculated to a first-order approximation by methods given in Part II,

$$V_a = \frac{V_u \ x_i^2}{n(\ x_i\ ) - (\ x_i)} \quad , \text{ and} \tag{62}$$

$$V_b = \frac{n\ V_u}{n(\ x_i\ ) - (\ x_i)} \quad . \tag{63}$$

in which V_u = the variance of the residuals about the regression line (Eqn. 23).

The location of the regression line represented by the equation,

$$y = a + bx + u \tag{64}$$

is predicted at any point x by inserting the estimates of the regression coefficients a and b . The uncertainty in the location of the line at any value of x is found by first-order approximation to be (Eqn. 15),

$$V_{m_{y|x}} = V_a + V_b (x - m_x) \tag{65}$$

in which $V_{m_{y|x}}$ is read, 'the variance of the mean of y given the value of x.' This is shown in Fig. 43 for the data of Fig. 42. These standard deviation envelopes represent uncertainty of the regression line, that is, of the mean, not of the location of individual measurements which vary about the line. The uncertainty on the residuals about the mean trend is expressed by V_u. Taken together, the standard deviation envelopes expressing the uncertainty on the magnitude of an individual measurement, accounting both for uncertainty on the mean trend and on residual variation about the mean trend, is,

$$V_{y|x} = V_a + V_b(x - m_x) + V_u \quad . \tag{66}$$

This is read, 'the variance of y given the value of x,' and is shown as the outer envelopes in Fig. 43.

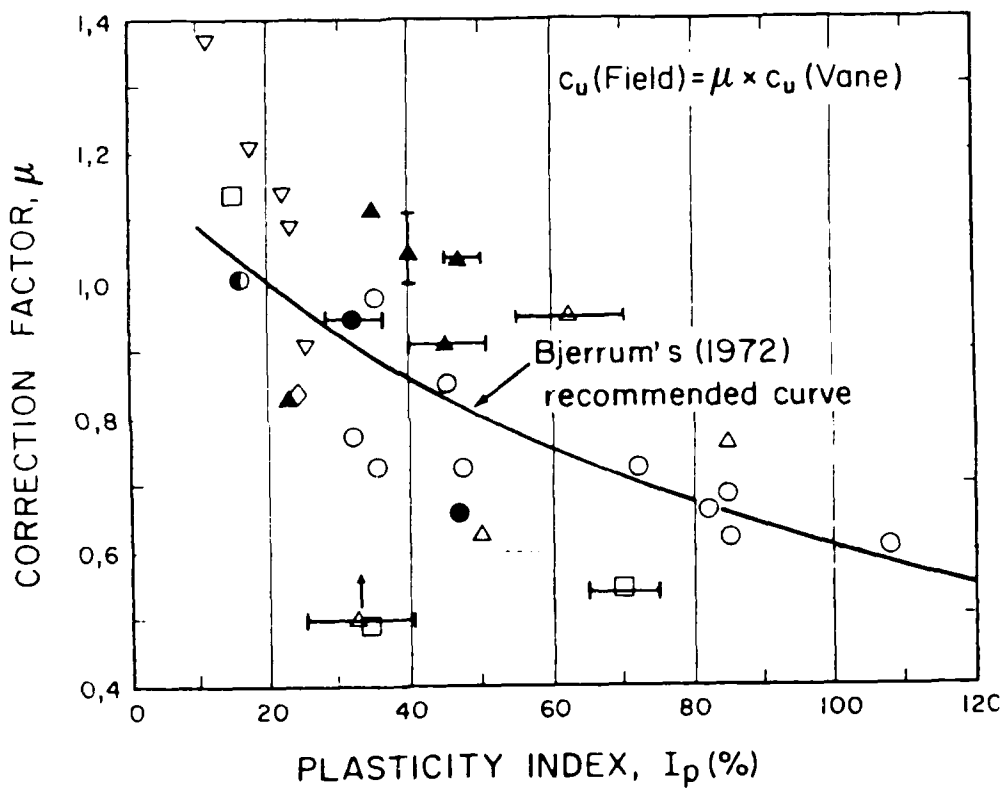

Figure 39. Bjerrum's Correction Factor for Field Vane Strength Measurements in Soft Clay.

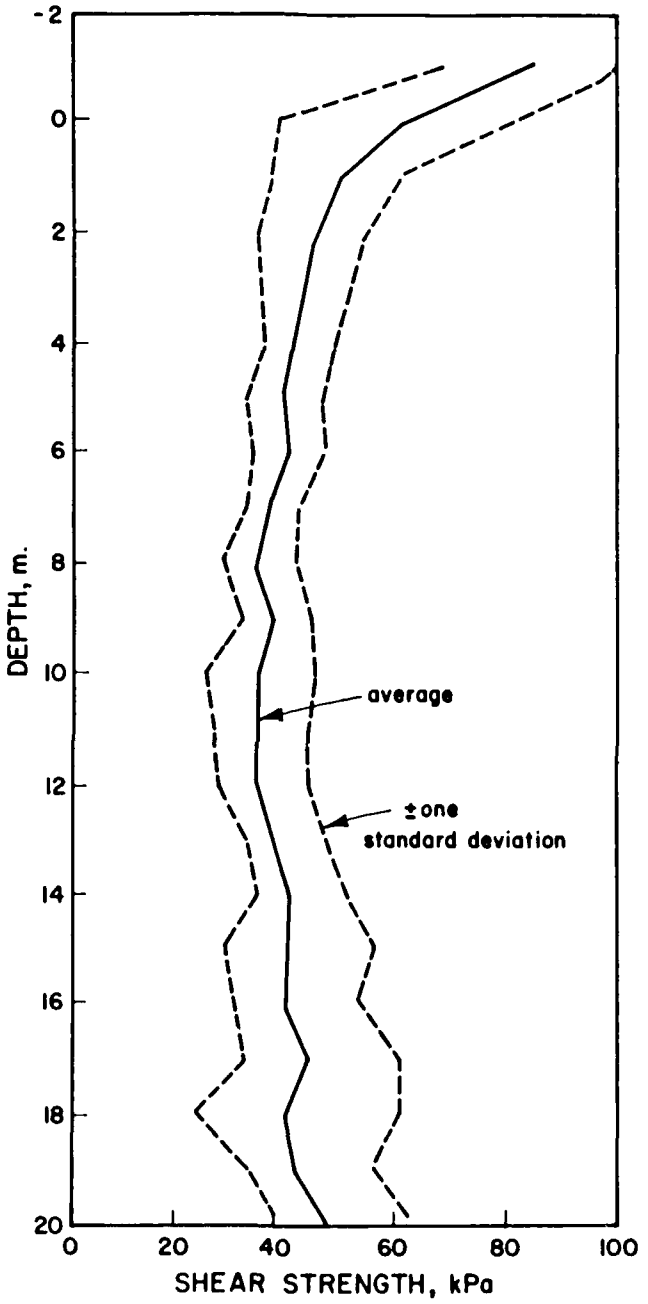

Figure 40. Average Field Vane Strength With Depth for the Data of Figure 32.

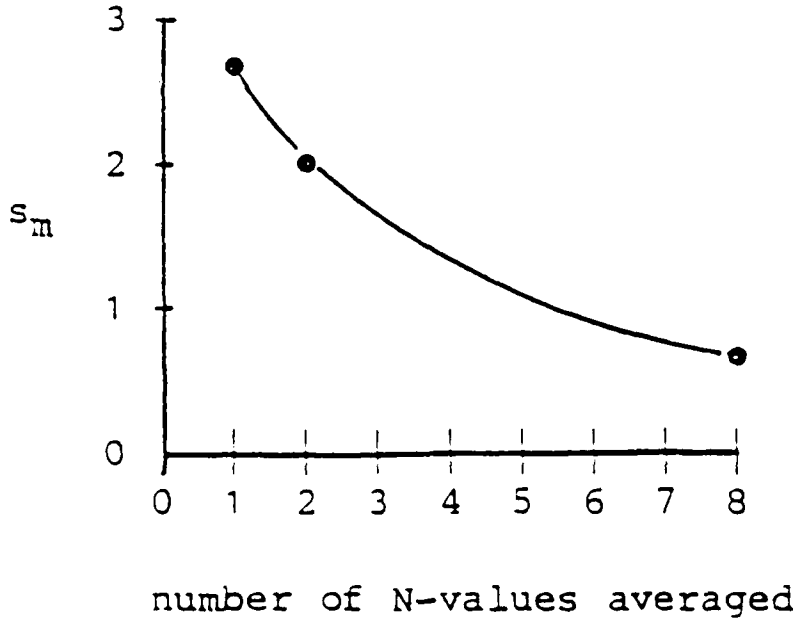

Figure 41. Averaging of Blow Count Data.

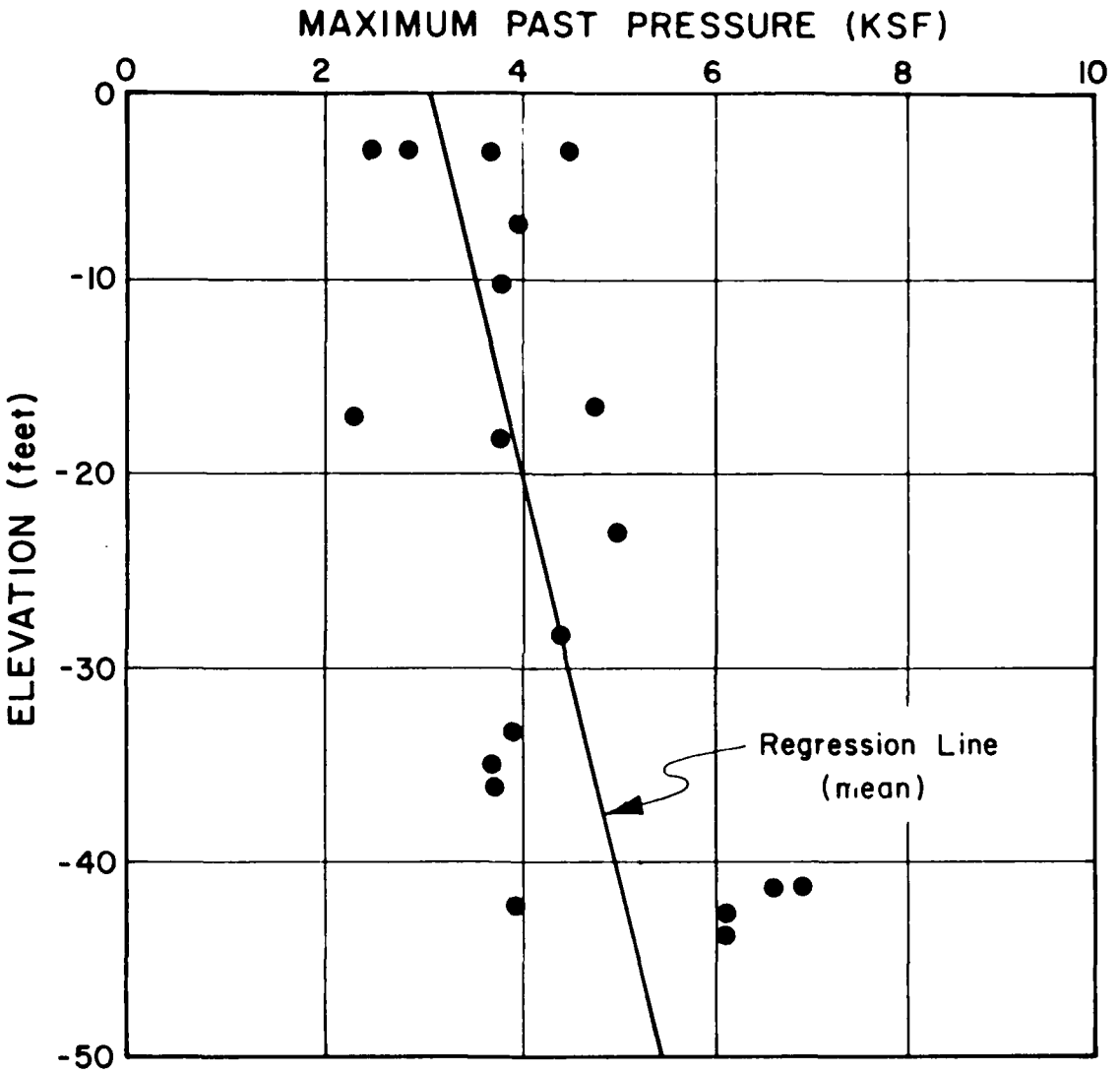

Figure 3. Maximum Past Pressure Data in an Overconsolidated Clay.

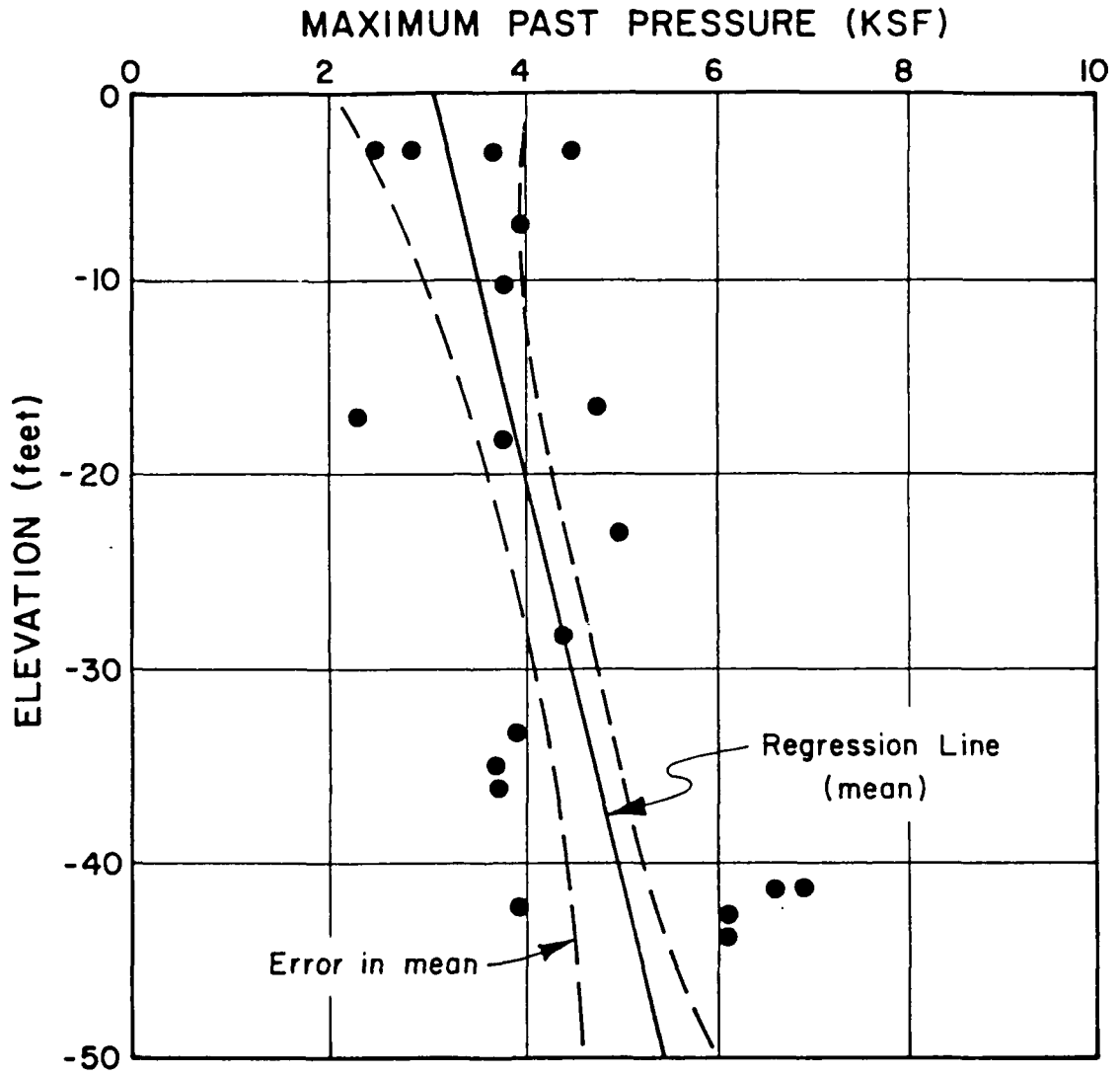

Figure 43. Statistical Error in Maximum Past Pressure For the Data of Figure 41.

PART V: CONSTRUCTING A STATISTICAL SOIL ENGINEERING PROFILE

This final part presents the procedure for combining best estimates of soil properties and uncertainty about those estimates into a statistical soil property profile.

The design profile summarizes available information on the variation of soil properties with depth. Specifically, the design profile gives,

A best estimate of soil properties with depth, and

Uncertainty envelopes about the best estimate.

These envelopes show the magnitudes of two types of uncertainty in the soil property estimates. The first set of envelopes shows spatial variability of soil properties about their mean. The second set shows uncertainty or error in the mean itself. Each set of envelopes shows a +/- one standard deviation interval.

Decomposition of Uncertainty

The methodology presented in this report is based on a decomposition of uncertainty in soil property estimates. In a statistical profile, the sources of uncertainty which have been analyzed and quantified separately are now brought back together.

Uncertainty in soil property estimates have been divided into four components: (i) real (spatial) variability of the soil deposit, (ii) random measurement noise, (iii) statistical estimation error, and (iv) measurement or model bias (Fig. 44). The overall error in an estimate of soil properties at any one point in the soil profile is found by combining the individual contributions of the four sources.

The contributions are mathematically combined by taking advantage of a convenient result from probability theory, that the variances (i.e., the squares of the standard deviations) of the individual contributions are additive (Cf., Eqn. 15),

$$V_x = \begin{vmatrix} V_{\text{data scatter}} & \begin{vmatrix} V_{\text{spatial variation}} \\ + \\ V_{\text{measurement noise}} \end{vmatrix} \\ + & \\ V_{\text{systematic error}} & \begin{vmatrix} V_{\text{statistical error}} \\ + \\ V_{\text{measurement bias}}. \end{vmatrix} \end{vmatrix} \tag{67}$$

$$V_x = V_{\text{spatial variation}} + V_{\text{measurement noise}} + V_{\text{statistical error}} + V_{\text{measurement bias}}. \tag{68}$$

in which V_x = the total uncertainty in an estimate or prediction of soil property x, expressed as a variance.

In separating spatial variability and systematic error, it is easiest to think of spatial variation as scatter about the trend and to think of systematic error as uncertainty on the trend itself. The first envelope reflects soil variability after random measurement error is removed. The second envelope reflects statistical error and measurement bias.

Rearranging Eqn. 66, the variance of a soil property x is related to the variances of data scatter, measurement error and measurement bias by,

$$V_x = \frac{1}{m_B^2}(V_z - V_e) + \Omega_B^2 m_x^2 \qquad (69)$$

The additional uncertainty contributed by statistical error in m_x adds to the right-hand-side (RHS) of Eqn. 69 the term V_{mx} of Eqn. 56. The total variance in point to point values of x is thus,

$$V_x = \frac{V_z - V_e}{B^2} + m_x^2 \Omega_B^2 + \frac{V_z}{n} \qquad (70)$$

The first term on the RHS is the contribution of spatial variation to V_x. The second term is the contribution of uncertainty in measurement bias. The third term is the contribution of statistical error. Taken together, the second and third term are the systematic error in x, or the error on the mean value. The first term is the additional uncertainty due to variation of the soil from one location to another.

Note that the contribution of random measurement error V_e appears only in its effect on statistical error. Thus, in specific instances--e.g., if V_B is small and n is large--the variance in x, V_x, can be much less than the data scatter variance V_z.

Simple Soil Profile: Field Vane Data

This example illustrates the construction of a design profile for the case in which in situ test results are used directly to estimate soil properties.

Site Conditions

The facility was a long water retaining embankment constructed on approximately 20m of soft marine and lacustrine clays. Field vane data were collected at every 1m of depth in 27 borings (Fig. 32), and were scattered. The scatter in the data varied with depth, but had a coefficient of variation ranging from 18 to 45%.

Horizontal and vertical autocovariance functions for the Marine clay are shown in Figs. 33a and 33b. Extrapolations to the origin indicate that about 40% of the data scatter variance in the marine clay can be attributed to noise, however, little of the scatter in the lacustrine clay appears to be noise. This difference may be due to small scale variability of the marine clay rather than measurement error, or may be due to other differences between the two clays, as e.g., in plasticity index or sensitivity. The resulting separation of data scatter expressed as coefficients of variation is given in Table 3.

Systematic Error

Systematic uncertainty on the mean strength derives from two sources, statistical error due to limited numbers of tests, and measurement bias due to differences between the field vane strength and the actual strength mobilized in embankment failures. Statistical error can be calculated approximately as Eqn. 56, which assumes the tests to be independent. Given the separation of the tests is larger than the autocovariance distances, this assumption seemed satisfactory.

Field vane correction factors, , were used to account for measurement bias. These were estimated starting from Bjerrum's chart, Fig. 43, and back calculating strengths from local dyke failures. Uncertainty in the correction

factors were estimated by judgement and inspection as shown in Table 3. Due to a lack of laboratory strength and consolidation data at depth a site specific μ was not developed for the lacustrine clay.

Statistical Soil Engineering Profile

The resulting statistical soil engineering profile is shown in Fig. 45. The best estimate undrained strength with depth is the mean undrained strength. The inner envelopes show $\pm$ one standard deviation due to spatial variation. The total uncertainty in the value of undrained strength at any point, expressed as a variance is found by adding the variance due to error on the mean to the variance due to spatial variation. A standard deviation envelope on the total uncertainty in estimating soil properties at a point is found, correspondingly, by taking the square root of the sum of the squared standard deviation envelope on error in the mean and spatial variation.

In Part III, a size effect factor R was introduced to account for the averaging out of spatial variation in a large volume of soil. For design use this size effect factor R is applied to the spatial variability part of the soil property uncertainty. The uncertainty in average soil properties in such a volume of soil is found by reducing the spatial variance contribution by the factor R, and adding this to the variance in the mean. This has been done for the profile of Fig. 45 to obtain Fig. 46. This figure shows the best estimate (mean) profile with $\pm$ one standard deviation envelope appropriate to different size failure surfaces through the clay for the purpose of limit equilibrium stability analysis. These envelopes are obtained as,

$$s_{\substack{\text{average soil}\\ \text{property along}\\ \text{failure surfaces}}} = \sqrt{R\, s^2_{\substack{\text{spatial}\\ \text{variability}}} + s^2_{\text{mean}}} \quad . \qquad (71)$$

In design, the statistical soil engineering profile of Fig. 46 is the starting point for error analysis, as described below.

Simple Soil Profile: SPT Data

The second example illustrates a case similar to the first, except that the site lies on silty-sand alluvium which was characterized by standard penetration testing.

Site Conditions and Data Scatter

The facility was a low water-retaining rockfill embankment associatd with a large multiple-use water resource project. The foundation profile consisted of approximately 25 feet of alluvium in which a large number of borings were made (Fig. 47). The horizontal sample autocorrelation function for the SPT data, shown in Fig. 48, indicated little measurement noise. The supposition was that lack of significant noise in the data was due to the looseness of the soil and the low average blow count. The data scatter varied somewhat with depth, giving a coefficient of variation of about 32%.

Systematic Error

Because the SPT data are used directly, that is, they are not translated into a fundamental soil property such as strength or deformability, no measurement bias term was used in developing a statistical soil property profile. The profile is expressed directly as SPT results. The statistical

error in the estimate of the mean SPT blow count at any depth interval was calcuated a per Eqn. 56. This is shown in Plate 5.

Statistical Soil Engineering Profile

The resulting statistical soil engineering profile is shown in Fig. 49. This profile was constructed according to Eqn. 70. The vertical bar in each case shows mean water elevation plus or minus one standard deviation of spatial and temporal variability.

Derived Soil Profiles

The foregoing case illustrates the construction of a design profile for calculations directly relating field measurements to model parameters. Not all situations are direct in this way. Many involve profiles derived from field measurements, as for example, when using normalized soil properties (e.g., the SHANSEP approach of Ladd and Foott, 1974). Such a derived soil profile was used in analyzing an ore stockpile on soft Gulf of Mexico Clay.

Site Conditions

The facility was an industrial plant sited along a barge canal on 15 m of normally consolidated clay. Ores for processing are shipped up the canal and stockpiled next to a dock. Strength data for the site taken by field vane testing are scattered, as are maximum past pressure measurements (Fig. 50). This leads to uncertainty in factors of safety against strength instability. The uncertainty on factor of safety, in turn, leads to uncertainty on how high the stockpile

can be built before strength increases from consolidation are required to provide strength stability.

Normalized Soil Properties (SHANSEP)

The field vane data are too few and too widely spaced and too scattered to confidently estimate soil properties. Therefore, the decision was made to base stability predictions on normalized soil properties, and to determine the calibrating constants from measurements made in the laboratory.

The SHANSEP procedure was adopted which relates undrained strength c_u to in situ stress through the equation,

$$\frac{c_u}{\sigma'_{vo}} = k\,[\sigma'_{vm}/\sigma'_{vo}]^q \quad , \tag{72}$$

in which σ'_{vo} = effective vertical stress, σ'_{vm} = maximum past pressure, and

$$k = [\,c_u/\sigma'_{vm}\,]_{\text{normally consolidated}} \quad . \tag{73}$$

k is the undrained strength ratio for normally consolidated clay. The parameters k and q are considered material constants, and $[\sigma'_{vm}/\sigma'_{vo}]$ = OCR is the over-consolidation ratio.

Applying Eqn. 19,

$$\sigma^2_{c_u} \doteq \sigma^2_k + m^2_q \sigma^2_{\sigma'_{vm}} + \ln^2(\sigma'_{vm}/\sigma'_{vo})\,\sigma^2_q \tag{74}$$

providing a linear composition of the uncertainties on each of the three soil parameters, k,q, and σ'_{vm}.

Soil Data

One dimensional consolidation tests were made on specimens recovered in piston samples at the site. Maximum past pressure estimates σ_{vm}' from these tests are shown in Fig. 11. The trend of σ_{vm}' with depth was approximated by fitting a regression line to the data using Eqns. 20, 21, and 22. The least squares fit is shown in Fig. 11. The data scatter about the regression line was estimated using Eqn. 23 to be s_x=1ksf.

Laboratory direct simple shear tests were performed to determine the soil parameters k and q for the undrained strength model of Eqn. 72. The results of these tests are shown in Fig. 51. From the test results and judgemental interpretation the best estimates and standard deviations of q and k were concluded to be

$$\begin{aligned} m_q &= 0.86 \qquad s_q = 0.03 \\ m_k &= 0.21 \qquad s_k = 0.22 \end{aligned} \tag{75}$$

Because the measurements of q and k were made with care in the laboratory, and because too few data were available to establish the structure of spatial variation in an autocorrelation function, measurement noise was assumed to be zero. That is, the assumption was made that V_e=0 for the soil parameter estimate q and k. This assumption is conservative in that uncertainty is over estimated, but the extent of conservatism was thought to be small. Because of limited data on σ_{vm}', the same assumption that V_e=0 was made for estimates of maximum past pressure.

Systematic Errors

Statistical errors in q and k were estimated from Eqn. 56. There is slight correlation in the estimates of q and k, because q is measured by the increase of normalized strength c_u/σ' with OCR, starting from k at OCR=1.0. This correlation turned out to be small and was neglected. Statistical error in the trend of σ_{vm}' with depth was estimated from the regression analysis using Eqn. 65. Plus/minus one standard deviation envelope on the mean of σ_{vm}' with depth are shown in Fig. 11. Measurement and model bias errors were estimated subjectively, based on experience with the SHANSEP procedure and on the quality of the laboratory testing program.

Statistical Soil Engineering Profile

The resulting statistical soil engineering profile is shown in Fig. 52. The best estimate of undrained strength with depth is the mean. The inner envelopes show plus or minus one standard deviaton of error on the best estimate or mean. The outer envelopes show plus or minus one standard deviation of the spatial variation in undrained strength about the mean trend. The statistical profile was developed from Eqn. 74 by separately estimating spatial and systematic components for each of the three terms on the RHS, corresponding respectively to uncertainties in k, σ_{vm}', and q (Plate 6). The three spatial contributions were added to get the total spatial variability, and the three systematic terms were added to get the total systematic error. In essence, Eqn. 74 and the division of uncertainty into component types provides an accounting format for keeping track of where uncertainties or errors originate and how they logically combine.

In this project too few data were available to confidently assess autocorrelation functions from field data. As a result, the size effect summarized by the factor R could not be precisely quantified. Therefore, the final statistical profile shows only the limiting cases of spatial averaging: the case of very small failure surfaces for which R=1.0, and the case of very large failure surfaces for which R→0. If a subsequent error analysis shows that this range of uncertiantiy is too large to be dealt with in design, then more data would have to be gathered.

Error Analysis

The end result of the statistical data analysis presented in this report is a statistical soil profile summarizing data scatter and estimates of systematic error. The design profile gives a best estimate of soil properties with depth and two sets of standard deviation envelopes, one on the mean and one on spatial variation.

The next step is to incorporate this statistical characterization of soil property information in design calculations. That is, to use means, standard deviations, and correlations of soil properties as the input to geotechnical modeling. The result of that modeling is a best estimate or mean prediction of engineering performance, accompanied by a standard deviation on the prediction. The techniques for accomplishing this are presented in the companion report, "Error analysis for geotechnical engineering," (Contract Report GL-87-3).

Table 3

Summary of Parameter Estimates for Error Analysis of End-of-Construction Stability Analyses for An Embankment on Soft Clay.

Field Vane Statistics

m_z	Marine	Lacustrine
Mean, kPa	34.5	31.2
Data Scatter, θ_z	0.236	0.272
Spatial Variability, θ_x	0.183	0.272
Measurement Noise, θ_e	0.149	0.000
Systematic Error		
Statistical, θ_{mx}	0.030	0.045
Correction factor, θ_μ	0.075	0.15
TOTAL Bias, $\theta_{mx+\mu}$	0.08	0.16
TOTAL $\theta_{x,TOTAL}$	0.20	0.29

Table 4

Soil Profile Uncertainties for Error Analysis

Variable	Expected Value	Variance		
		Spatial	Systematic	TOTAL
depth of crust	4m	0.96	0.036	1.0
depth to till	18.5m	0.0	1.0	1.0
fill density	20 kN/m^3	1.0	1.0	2.0

SUBJECT: Statistical Soil Engineering Profile for SPT Data

DESIGN PROFILE:

(1) DATA SCATTER: SPT

Station	4+00--13+00	17+00--24+50	25+00--32+00
mean (bpf)	4.8	6.9	8.9
standard deviation	2.9	2.8	4.4
coefficient of variation	0.60	0.41	0.49
Measurement Noise (From Figures 4.6, 4.7)	--	--	--
Spatial Variability $\sqrt{V[x]} = \sqrt{(V[z]-V[e])}$	2.9	2.8	4.4

(2) SYSTEMATIC ERROR

Station	4+00--13+00	17+00--24+50	25+00--32+00
number measurements* per depth interval	14	11	20
Statistical Error $\sqrt{V[m_x]} = \sqrt{V[z]/n}$	0.78	0.84	0.98
Model Bias	n/a	n/a	n/a
Total Systematic Error	0.78	0.84	0.98

* (varies with depth, numbers are representative)

(3) DESIGN PROFILE

(Shown as Figure 49)

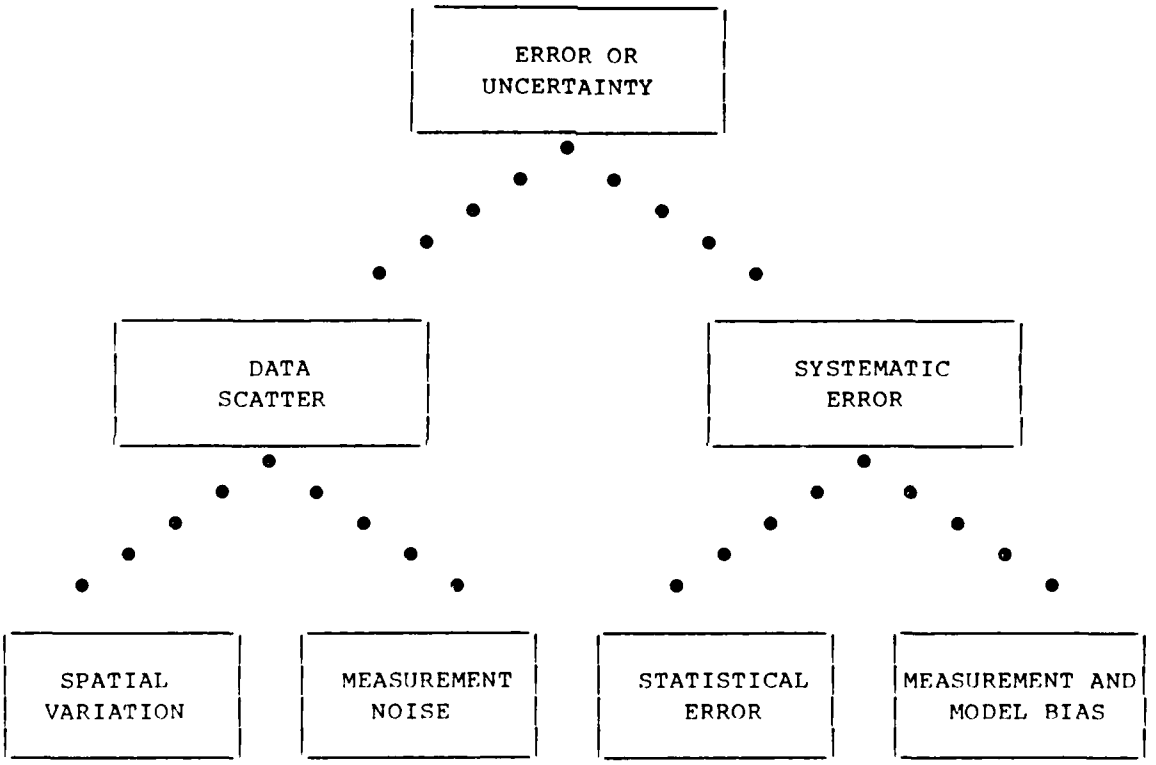

Figure 44. Sources of Error or Uncertainty in Soil Property Estimates.

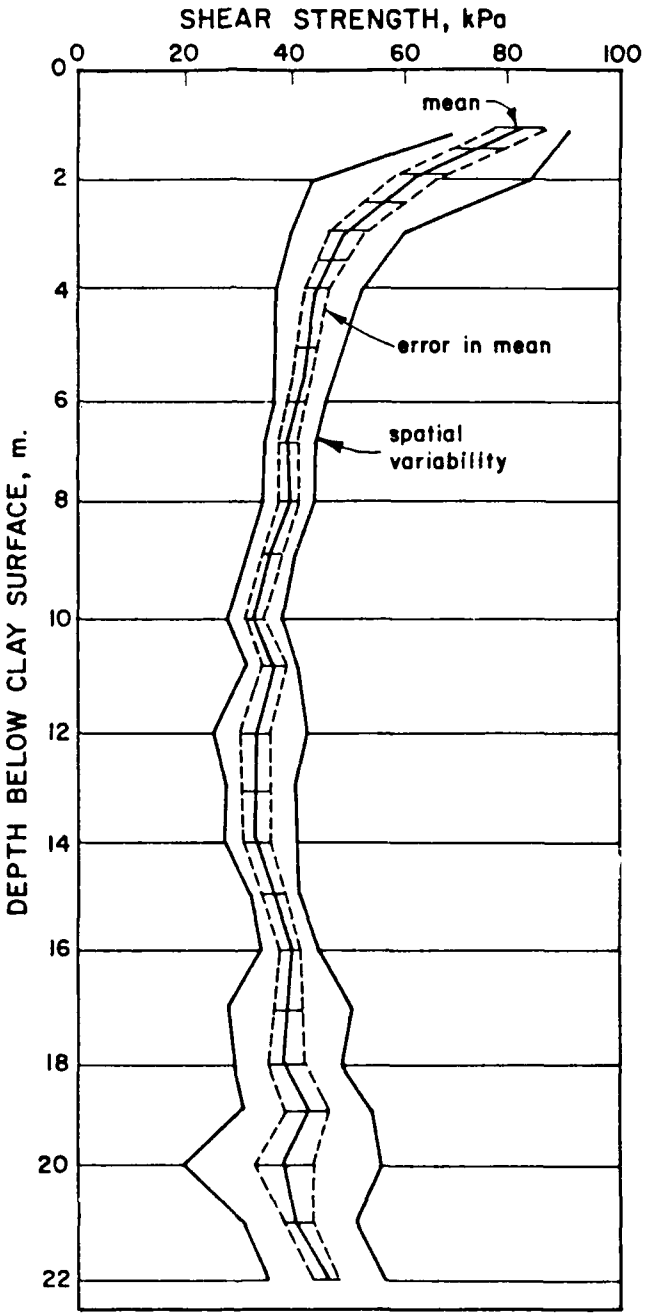

Figure 45. Design Profile for Undrained Strength From the Data of Figure 32.

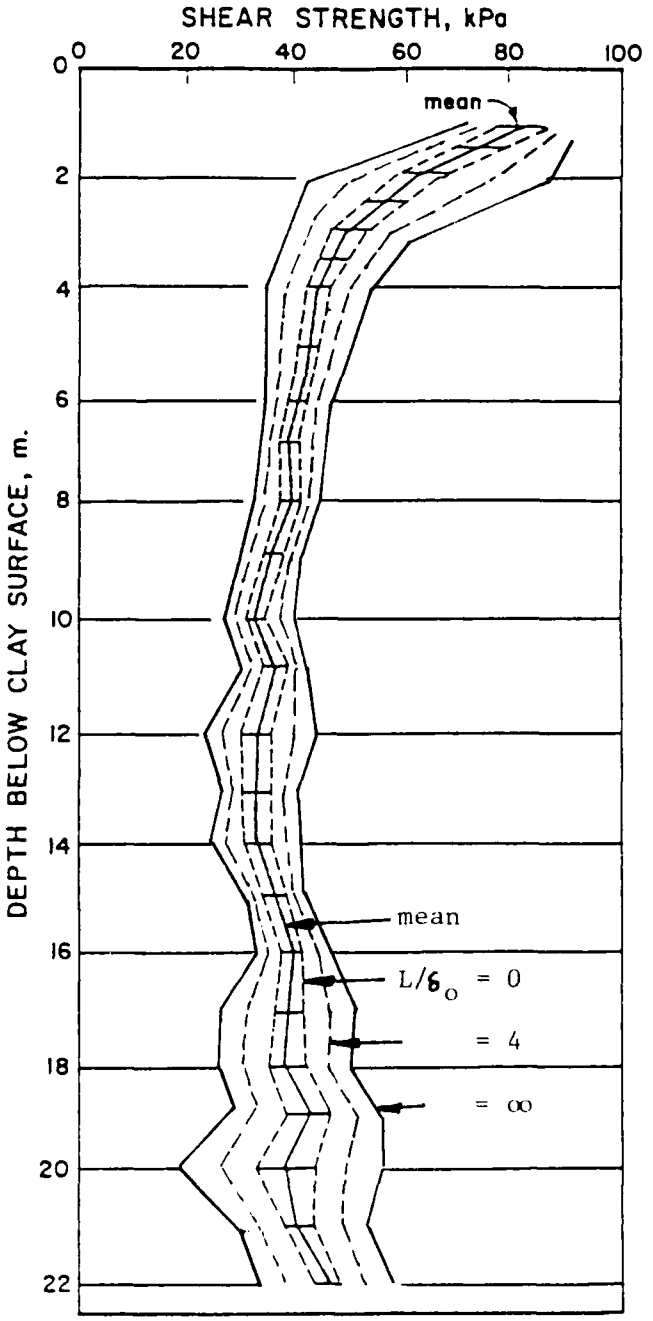

Figure 46. Design Profile for Undrained Strength Showing the Effect of Spatial Averaging on Standard Deviation Envelopes. The normalized parameter L/δ_o is the length over which soil properties are averaged relative to the autocorrelation distance.

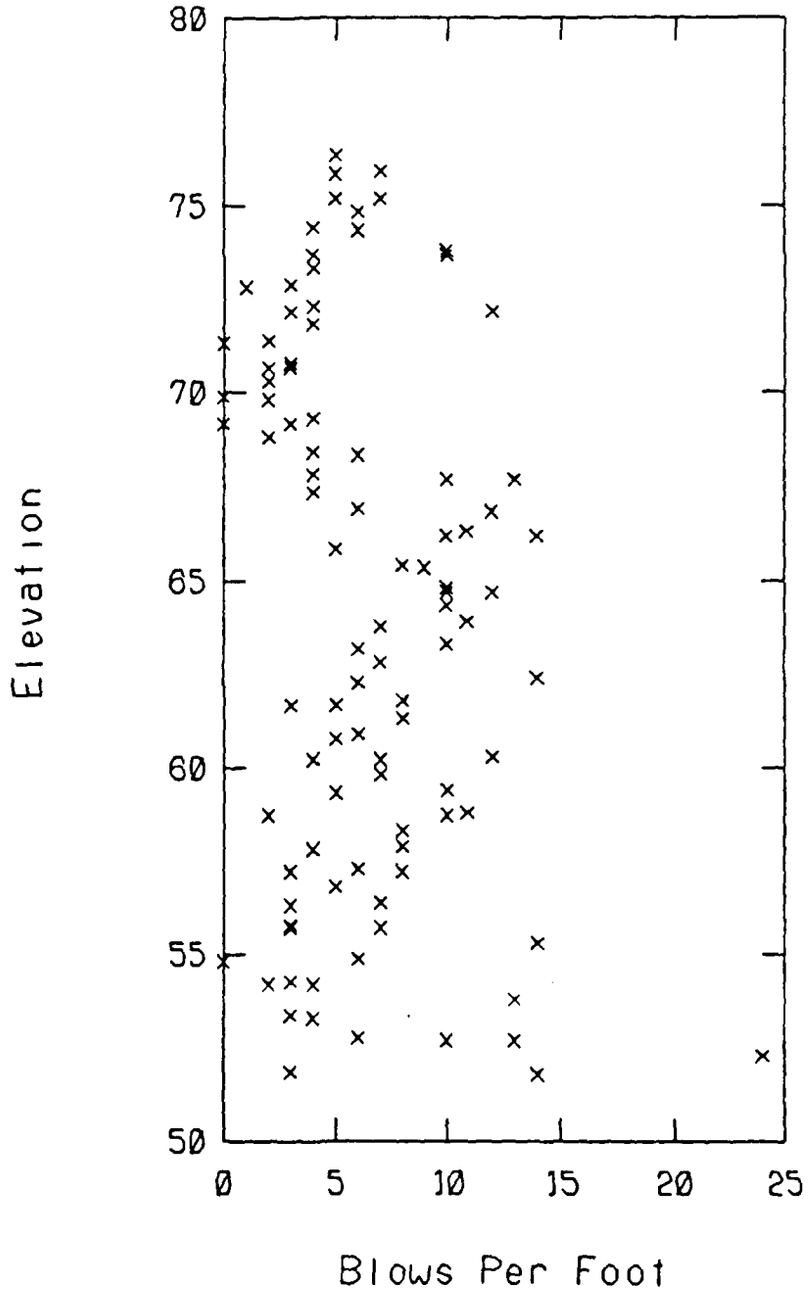

Figure 47. SPT Blow Count Data
Showing Typical Measurements from
One Section of Embankment Foundation

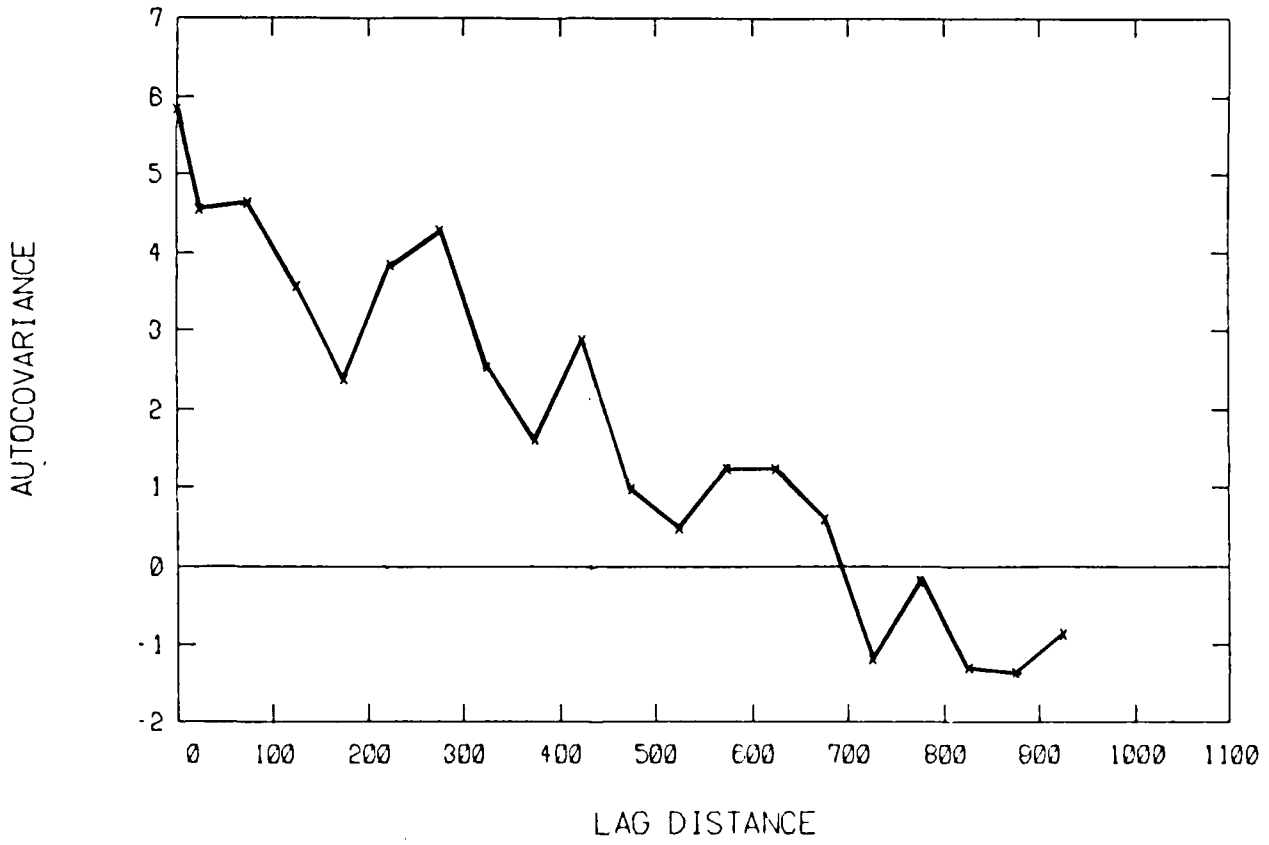

Figure 48. Horizontal Autocorrelation Function for the SPT data of Fig. 47.

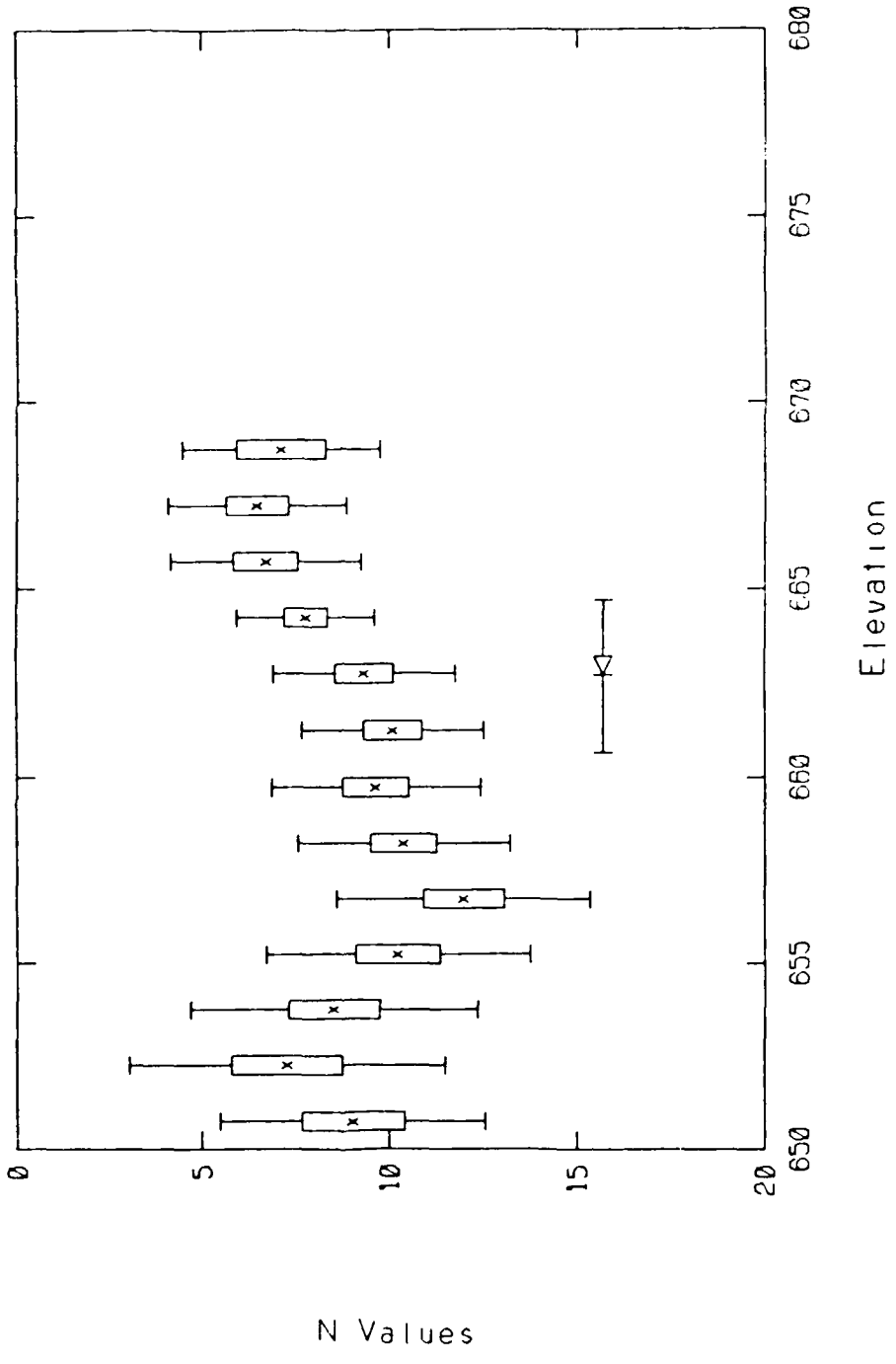

Figure 49. Statistical Soil Engineering Profile Showing Typical Results for One Section of Embankment.

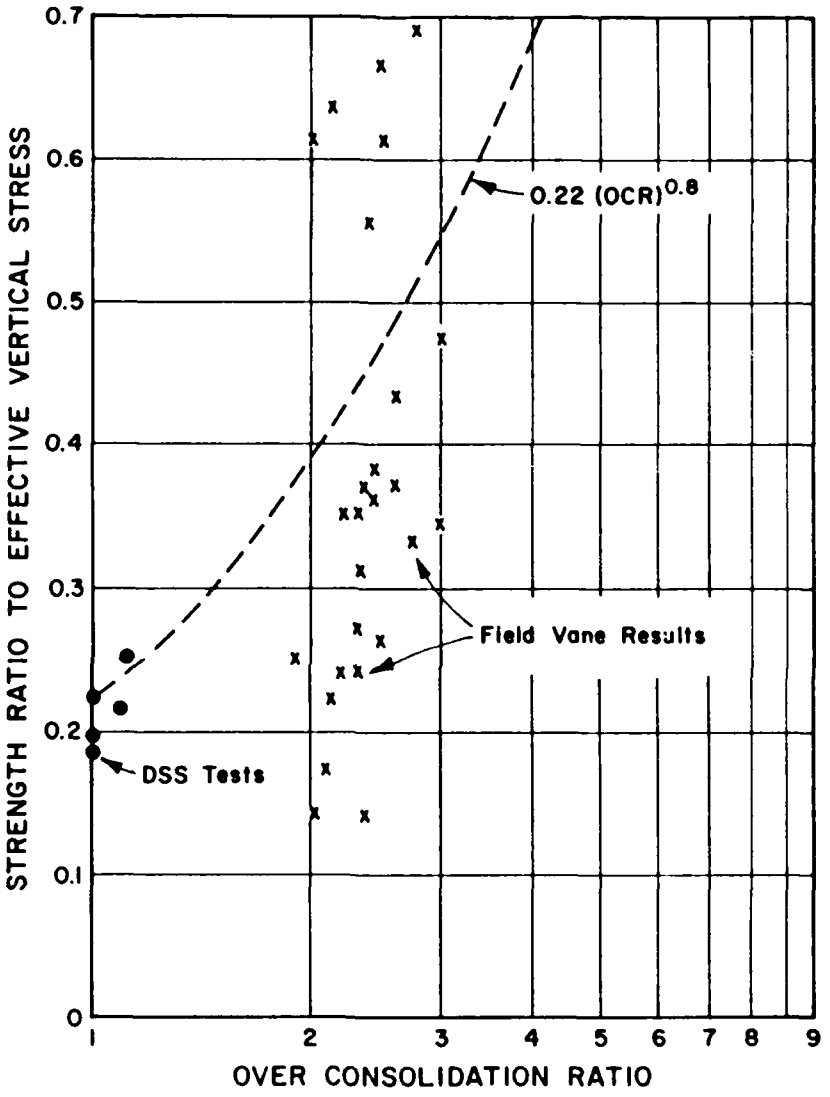

Figure 50. In Situ Undrained Strength Data for a Site on Gulf of Mexico Clay.

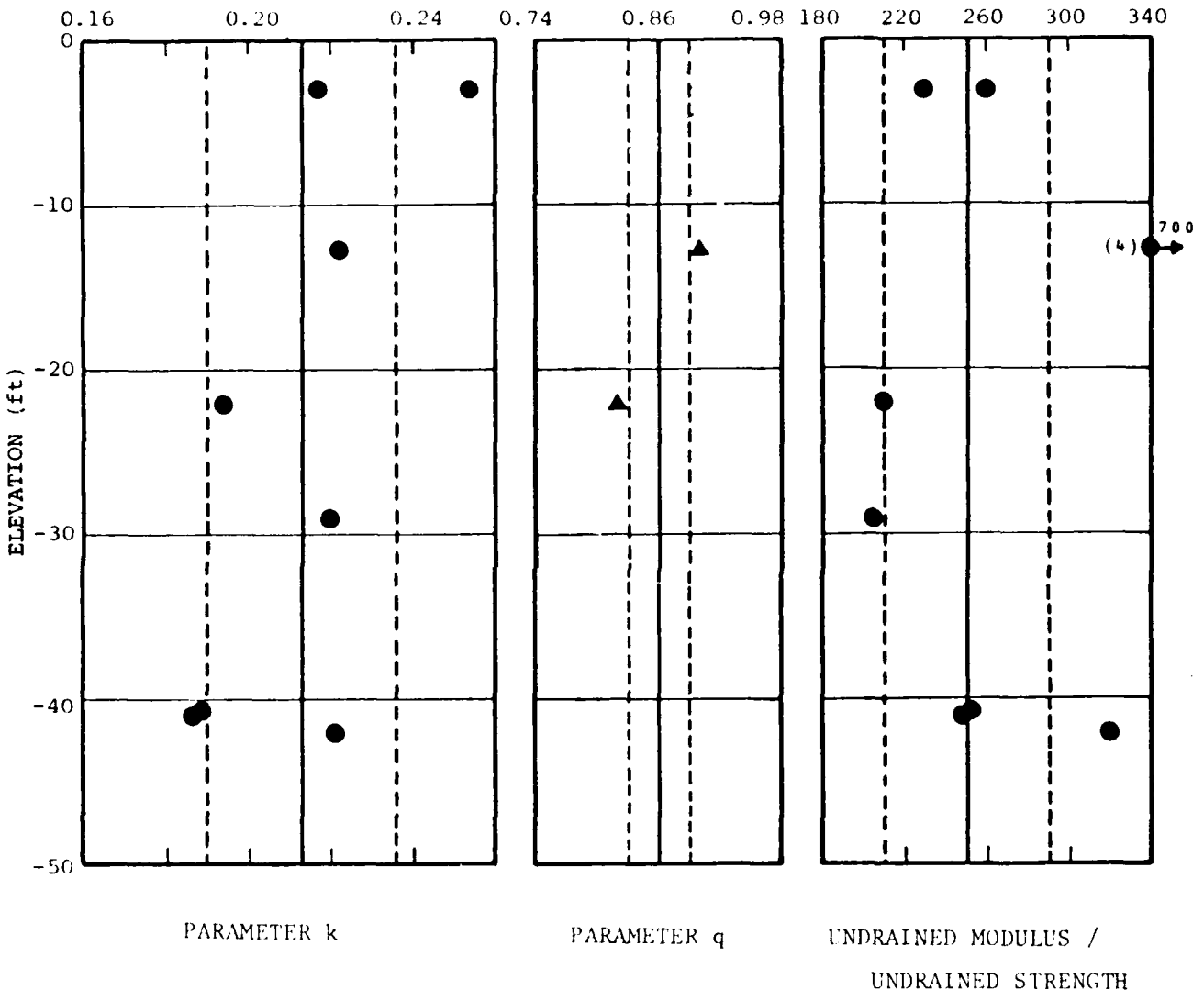

Figure 51. Laboratory Test Results to Determine SHANSEP Strength Parameters. From Noiray, 1982.

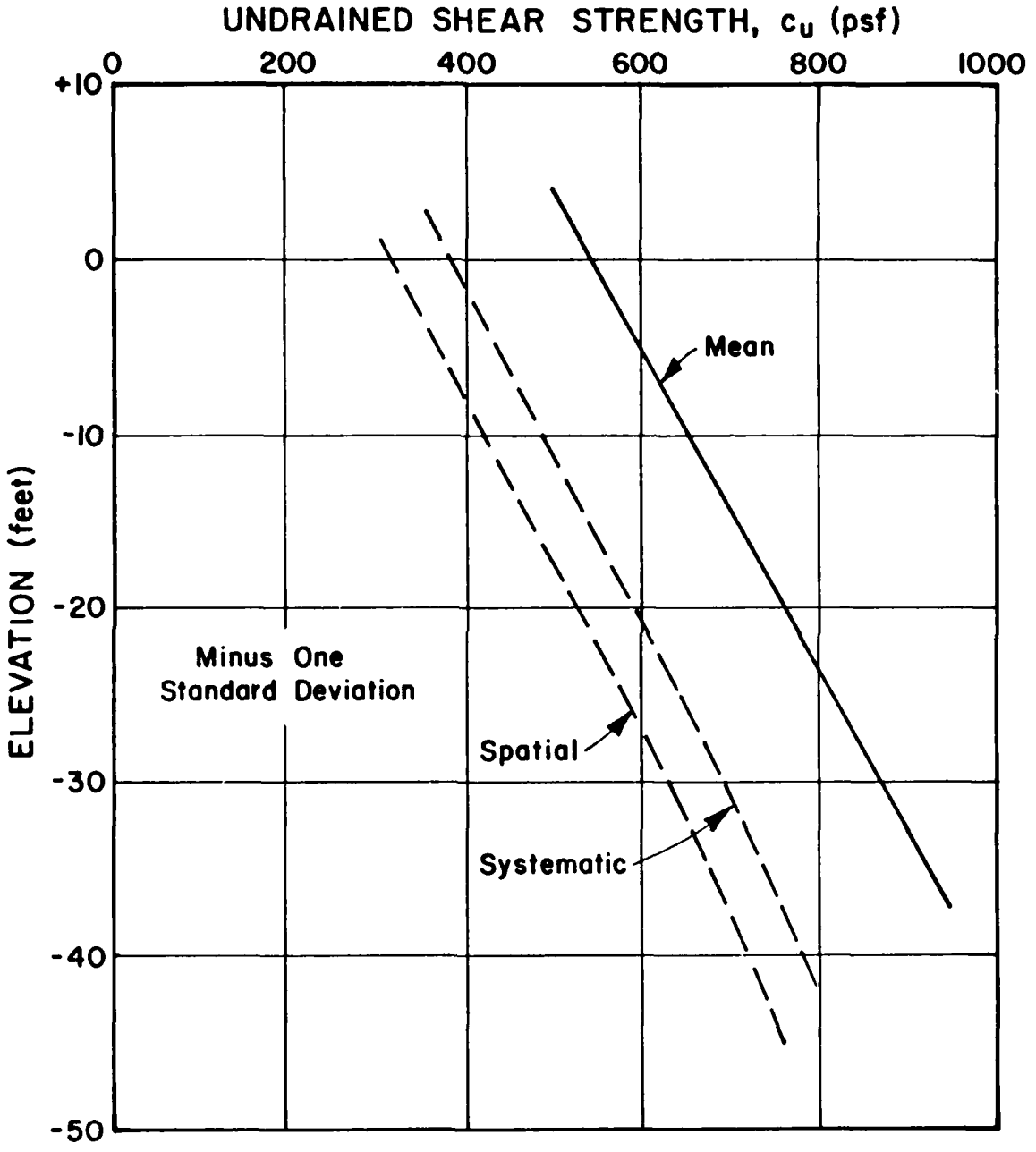

Figure 52. Statistical Soil Engineering Profile for Derived Soil Properties Using SHANSEP Procedure.

REFERENCES

Baecher, G.B., W.A. Marr, J.S. Lin, and J. Consla (1983). "Critical parameters for mine tailings embankments, " Report to the U.S. Bureau of Mines under contract J0215028.

Benjamin, J.R. and C.A. Cornell (1970). Probability, Statistics, and Decision for Civil Engineers. McGraw-Hill Book Company, New York.

Bjerrum, L. (1972). "Embankments on soft ground," Proc. ASCE Specialty Conference On Earth and Earth Supported Structures, v. 2, pp. 111-159.

Chatillon, G. (1984). "The balloon rules for a rough estimate of the correlation coefficient," The American Statistican, v.38(1): 58-60.

DeGroot, D. (1985). "Maximum likelihood estimation of spatially correlated soil properties," thesis submitted to MIT in partial fulfillment of the requirements for the degree Master of Science.

Dixon, W.J. (1953). "Processing data for outliers," Biometrics, V. 9: 74, ff

Duncan, A.J. (1974). Quality control and industrial statistics (4th Ed.). Richard D. Irwin, Inc., Homewood, Illinois, 1047.

Hilldale-Cuningham, C. (1971). "A probabilistic approach to estimating differential settlement," Thesis submitted to the Massachusetts Institute of Technology in partial fulfillment of the requiremetns for the degree Master of Science in Civil Engineering/

Javette, D.F. (1983). "A simple statistical approach to differential settlement on clay," Thesis submitted the University of California at Berkeley in partial fulfillment of the requirements for the degree Doctor of Philosophy in Civil Engineering.

Johnson, J. (1960). Econometric Methods. McGraw-Hill Book Co., NY.

Kavazajian, E. (1982). "Applications of probabilistic methods to geotechnical practice," in USAE-WES Workshop on Probabilistic Methods in Geotechnical Engineering.

Ladd, C.C. and R. Foott (1974). "New design procudure for stability of soft clays," Journal of the Geotechnical Engineering Division, ASCE, v. 100(GT7): 763-86.

Lambe, T.W. and R.V. Whitman (1969). Soil Mechanics. John Wiley and Sons, NY.

Matheron, G. (1971). "The theory of regionalized variables and its application," Cah. Cent. Morphol. Math., 5.

Noiray, L. (1982). "Predicted and measured performance of a soft clay foundation under stage loading," Thesis submitted to the Massachusetts Institute of Technology in partial fulfillment of the requiremetns for the degree Master of Science in Civil Engineering.

Shilling, M.F. (1984). "Some remarks on quick estimation of the correlation coefficient," The American Statistican, v.38(4): 330-331.

Snedecor, G.W. and W.G. Cochran (1980). Statistical Methods (7^{th} Ed.). The Iowa State University Press.

Spikula, D. (1983). "Statistical estimation of soil properties, an application," Thesis submitted to the Massachusetts Institute of Technology in partial fulfillment of the requiremetns for the degree Master of Science in Civil Engineering.

Sturges, H.A. (1926). "The choice of a class interval," Journal of the American Statistical Association, v. 21: 65-66.

Tang W.H. (1979). "Probabilistic evaluation of penetration resistances," Journal of the Geotechnical Engineering Division, ASCE, v.105(GT10): 1173-1191.

APPENDIX A: STATISTICAL CONSIDERATIONS IN ESTIMATING AUTOCOVARIANCE

ESTIMATION OF AUTOCOVARIANCE FUNCTIONS

This appendix briefly discusses alternative statistical approaches to estimating autocovariance functions from soil data. Detailed presentation of mathematical procedures and statistical properties of the techniques are presented in Spikula (1983) and DeGroot (1985).

Three techniques are commonly used to estimate autocovariance functions in the analysis of site characterization data: the moment estimator, the BLUE minimization estimator, and the maximum likelihood estimator. These have different strengths and weaknesses, and may lead to slightly differing results.

Moment estimator

The moment estimator uses the autocovariance function calculated directly from the observed measurements as an estimator of the autocovariance of the underlying spatial process:

$$C_z(\delta) = \left(\frac{1}{n_\delta - 1}\right) \sum (z_i - m_z)(z_{i+\delta} - m_z) \qquad \text{(A1)}$$

in which n_δ = the number of data pairs at separation distance δ.

BLUE minimization estimator

The BLUE minimization uses the autocorrelation function that minimizes the squared error between estimated and observed soil properties at the measurement points as an estimate of the autocovariance of the underlying spatial process. That is, soil properties are estimated at each of the observed points by removing that measurement from the data base and using the remaining (n-1) data to estimate it using a best linear unbiased estimation (BLUE) technique

(Spikula, 1983). That autocovariance function which minimizes the variance of the error between observed and predicted measurements is taken as the estimate. This is a parametric model in that the mathematical shape of the autocovariance function must be specified.

Maximum Likelihood Estimator

The maximum likelihood estimator uses the autocorrelation function that maximizes the conditional probability of the measurements actually made (i.e., the 'likelihood') as the estimator of the autocovariance of the underlying spatial process,

$$C_z(r) \text{ s.t.: } \min_{C_z(r)} L[z_1, \ldots, z_n] = \min_{C_z(r)} MN(\underline{\beta x}, \underline{\underline{C}}_z) \qquad (A.2)$$

in which $L[\underline{z}]$ = the likelihood or conditional probability of the vector of data $\underline{z}$, MN() = the multiNormal probability density function, $\underline{\beta}$ = a vector of regression coefficients for the mean trend of the data, $\underline{\underline{x}}$ = the matrix of location coefficients each row of which is $\langle 1, x_i, x_i^2, x_i^3, \ldots, x_i^k \rangle$ where k is the order of the regression surface, and $\underline{\underline{C}}_z$ = the covariance matrix of the observations calculated via the autocovariance function (DeGroot, 1985). This is also a parametric model.

Comparison of Estimation Techniques

The moment estimator technique is by far the most commonly used approach in present (1985) practice, but it has statistical limitations. The advantages of the moment approach are that it is mathematically and conceptually easy to use, and that it requires relatively modest computations. The disadvantages are that it is statistically biased and inefficient, and it is difficult to use when data are not sampled on uniform grids.

The BLUE estimator technique has not been widely used in geotechnical engineering, but it is common in mining engineering and 'geostatistics.' Its principal advantages are that it is more flexible than the moment estimator in making use of non-uniformly sampled data, and it requires less intuitive input. Its principal disadvantages are that it is computationally intensive and its statistical properties are poorly studied.

The maximum likelihood estimator is not widely used in either geotechnical engineering or mining, but it is increasingly common in other areas of statistical data processing (e.g., in time series analysis and signal processing). Its major advantage is that its statistical properties are well known and desirable (e.g., it is asymptotically unbiased and efficient), and it easily accommodates non-uniformly sampled data. Its major disadvantage is that the computational algorithms required to use the method are complicated, although not intensive of computer time. This disadvantage can be overcome using packaged programs.

Packaged computer programs are available for each of the three methods of estimating autocorrelation functions. Most can be tailored to run on present microcomputers.

APPENDIX B: SYMBOL LIST

a,b = regression coefficients
a_i = constant
B = measurement bias correction coefficient
b = footing width
C_f = cost of failure
C_R = risk cost
$C_x(\delta)$ = autocovariance function for separation distance δ
$C_{x,y}$ = covariance of x and y
$\underline{C}_x$ = covariance matrix
$CR_{\varepsilon c}$ = virgin compression ratio
$CR_{\varepsilon r}$ = recompression ratio
c_u = undrained strength
d = embedment depth of footing
D,d = geometric properties of scatter graph
e = random measurement error
f_i = cumulative frequency of observation i
E = elastic modulus
F = factor of safety
FV = field vane
$\underline{G}$ = matrix of derivatives with ij^{th} element dy_i/dx_j
g(x) = deterministic function of x
H = horizontal load
H,h = geometric properties of scatter graph
H_i = stratum thickness
h = SHANSEP strength parameter
i = dilation angle
k = counter number
m_x = mean of x
n = number of measurements
L = length
L[z] = likelihood of z
m_v = vertical compression coefficient
N = SPT blow count
N_γ = bearing capacity factor
OCR = overconsolidation ratio
P_{BC} = probability of bearing capacity failure
P_f = probability of failure
P_ρ = probability of excessive settlement
Pr{.} = probability of
q = SHANSEP strength parameter
q = applied footing stress
q_{vo} = design stress
q_v = bearing capacity
r_{xy} = correlation coefficient of xy
r_o = autocorrelation distance, $C_.(r_o)=1/e$
R = size effect factor
$R_x(\delta)$ = autocorrelation function over separation distance δ
s_x = standard deviation of x

APPENDIX B: SYMBOL LIST
(continued)

t = Student's t statistic
t_i = trend
u = residual variation about regression line
V = vertical load
V_x = variance of x
w_x = range of x
x = soil property
$\underline{x}$ = vector of data $x_1,\ldots,x_n$
x_i, = i^{th} measurement of property x, or x at location i
x_{max} = largest value of x
xmin = smallest value of x
$x_{0.25}$ = 25th fractile of x
$x_{0.5}$ = 50th fractile of x
$x_{0.75}$ = 75th fractile of x
y = predicted performance variable
y_o = design specification on variable y
z = measured soil property, depth

α = critical probability level
β = reliability index
$\underline{\beta}$ = vector of regression coefficients
γ = soil density
δ = separation distance
δ_o = autocorrelation distance
ε = strain
η = point of expansion in Taylor's series
θ = slope angle
μ = Bjerrum's FV correction factor
ν = degrees of freedom
ρ = settlement
σ = stress
σ_{vm}' = maximum past pressure
σ_{vo}' = effective vertical stress
σ_{vf}' = final consolidation stress
ϕ' = effective stress friction angle
Ω_x = coefficient of variation
ω = outlier test statistic

END

FEB.

1988

DTIC